

Fakultät für Medizin

Institut für Medizinische Mikrobiologie, Immunologie und Hygiene

Isolation of minimally manipulated regulatory T cells for adoptive T cell therapy

Fabian Mohr

Vollständiger Abdruck der von der Fakultät für Medizin der Technischen Universität München zur Erlangung des akademischen Grades eines

Doktors der Naturwissenschaften

genehmigten Dissertation.

Vorsitzende:

Prof. Dr. Ulrike Protzer

Prüfer der Dissertation:

1. Prof. Dr. Dirk Busch
2. Prof. Dr. Aphrodite Kapurniotu

Die Dissertation wurde am 01.08.2018 bei der Fakultät für Medizin der Technischen Universität München eingereicht und durch die Fakultät für Medizin am 10.03.2020 angenommen.

1. Content

1.	Content	3
2.	List of Figures	6
3.	List of tables	7
4.	Abstract	8
5.	Introduction	9
5.1.	Hematopoietic Stem Cell Transplantation.....	9
5.2.	GvHD the main adverse effect of HSCT	10
5.2.1.	GvHD in mice and implications for treatment in men	12
5.2.2.	Phases of acute GvHD induction	14
5.2.3.	Treatment of GvHD	14
5.2.4.	Immunomodulatory cell therapies to treat GvHD	17
5.2.5.	Tregs as therapeutic agent to treat GvHD	17
5.2.7.	First-in-man trials using Treg therapy to treat GvHD.....	20
5.3.	Antibody-mediated effects on cells.....	22
5.4.	Streptamer technology.....	25
6.	Aim.....	27
7.	Results	28
7.1.	Enrichment of Tregs freed from staining reagents	28
7.1.1.	Characterization of existing and newly generated Fab multimer reagents	28
7.1.2.	Measuring Koff rates of Fab Monomers from the cell surface	32
7.1.3.	Development of a double Fab multimer staining	37
7.1.4.	Comparison of FACS isolated mAb or Fab multimer stained Tregs	38
7.2.	<i>In vivo</i> Engraftment	40
7.2.1.	Transfer into wt C57BL/6 mice	40
7.2.2.	Co-transfer of mAb and Fab Multimer sorted cells into wt C57BL/6 mice	41
7.2.3.	Co-transfer of “untouched” Tregs and “isolated reagent freed” Tregs	44
7.2.4.	Why do Fab multimer-sorted Treg cells engraft better	46

7.2.5.	The role of the complement system in the depletion of mAb labeled Tregs	47
7.2.6.	Antibody-dependent cell-mediated cytotoxicity	51
7.2.7.	Fab removed to Fab non-removed	54
7.3.	Functionality of Fab Multimer isolated Tregs	58
7.3.1.	<i>In vitro</i> functionality.....	58
7.3.2.	<i>In vivo</i> functionality of Fab Multimer isolated Tregs	59
7.4.	Enrichment of Treg subpopulations using Fab multimers.....	61
7.4.1.	Enrichment for three markers of murine Tregs using Fab multimers	62
7.4.2.	In vivo growth of CD62L high and low Fab, multimer sorted cells	63
8.	Discussion	65
8.1.	Choosing the right Fab Monomers	65
8.2.	Defining the of the Fab Monomers using a flow-based k_{off} rate assay	67
8.3.	Development of a double multimer staining	69
8.4.	<i>In vivo</i> engraftment.....	70
8.5.	Improved Functionality of isolation reagent freed cells.....	73
8.7.	Human application	75
9.	Summary	77
10.	Acknowledgement.....	78
11.	Material and Methods.....	79
11.1.	Plastic	79
11.2.	Fab Streptamers & plasmids	79
11.3.	Antibodies	80
11.4.	Buffer	81
11.5.	Solutions and chemicals.....	83
11.6.	Software	84
11.7.	Organisms	84
11.8.	Enzymes	84
11.9.	Machines	84

12.	Methods	86
12.1.	Production of electrical competent E.coli JM83	86
12.2.	Mutagenesis PCR	86
12.3.	Periplasmic Fab- expression.....	87
12.4.	Preparation of mouse organs – spleen & lymph nodes	89
12.5.	IL-2 stimulation assay	89
12.6.	SDS-PAGE and analysis	90
12.6.2.	Silver staining.....	91
12.6.3.	Western blot analysis	91
12.6.3.1.	Semi-dry - blot	91
12.7.	Suppression assay.....	92
12.9.	Cell staining.....	93
12.9.1.	CFSE staining.....	93
12.9.2.	Fluorescence-activated cell analysis	93
12.9.3.	Fluorescence-activated cell sorting	94
12.11.	Removal of Fab-multimers from the cell surface using D-biotin	95
14.	List of abbreviations.....	97
15.	Table of literature	99

2. List of Figures

Figure 1 acute GvHD The initiation and maintenance of acute graft-versus-host disease.	11
Figure 2 Mechanisms of Treg suppression	18
Figure 3 Antibody mediated effects on cells.....	23
Figure 4 Illustration of the basic principle of reversible Fab-multimers.....	26
Figure 5 Test staining for newly generated Fab monomers.. ..	29
Figure 6 Prolonging staining time	29
Figure 7 Reversibility test of CD4 and CD25 Fab staining:	30
Figure 8 Dye coupling to the α CD4 Fab Monomer.	32
Figure 9 Analysis of flow off rate data.	33
Figure 10 Comparison of half-lives of OregonGreen488 or Alexa488	34
Figure 11 Comparison of microscopic and flow-based koff rate.	35
Figure 12 Off-rate of human α CD4 Fabs human PBMCs.....	35
Figure 13 Isolation of regulatory T cells freed from staining reagents	37
Figure 14 Reversibility of the Fab Multimer double staining:.....	37
Figure 15 Treg cells after sorting Comparison of Fab Multimer and mAb Tregs	39
Figure 16 Transfer of differentially sorted Tregs <i>in vivo</i>	40
Figure 17 Co-transfer into wt C56BL/6 mice model and setup.	41
Figure 18 Co-Transfer of differentially sorted Tregs <i>in vivo</i>	42
Figure 19 Co-transfer into C57BL/6 mice phenotype of recovered cells	43
Figure 20 Co-Transfer of GFP sorted and Fab Multimer sorted Tregs.....	44
Figure 21 Co-Transfer of GFP sorted and Fab Multimer sorted Tregs.....	45
Figure 22 Engraftment of Tregs into Rag2 ^{-/-} cyc ^{-/-} mice.	46
Figure 23 <i>in vitro</i> deposition of C3 on the cell surface of Tregs	47
Figure 24 Transfer of Fab multimer- and mAb-sorted Tregs into C3 ^{-/-} mice	50
Figure 25 Transfer of Fab Multimer- and mAb-sorted Tregs into Fc γ R ^{-/-} mice	51
Figure 26 Early recovery of transferred Tregs 1hour after transfer	52
Figure 27 Schematic experimental setup:	54
Figure 28 Sorting strategy for lable free and Fc-free labeled cells.	54
Figure 29 Removal of Fab multimers from the cell surface is important	55
Figure 30 intracellular IL2 signaling.....	56
Figure 31 <i>In vitro</i> proliferation of r Fab and nr Fab sorted Tregs.....	56
Figure 32 <i>In vitro</i> Treg suppression Assay:	58
Figure 33 GvHD therapy using isolation reagent freed Tregs A-C)	60

Figure 34 Representative FACS blots depicting single living lymphocytes.....	62
Figure 35 cumulative enrichment data using enrichment columns	63
Figure 36 Sorting Gates for CD62L ^{high} and low,	63
Figure 37 <i>in vivo</i> engraftment and growth of CD62L subpopulations.....	64
Figure 38 Isolation of regulatory T cells using Fab Multimer double staining.....	69
Figure 39 Influence of blood D-Biotin on Multimer stability:.....	73

3. List of tables

Table 1 CD25 mutants.....	31
Table 2 half-life of surface-bound α CD4 Fab and backbones	35
Table 3 Relative affinity of human α CD4 mutant Fab Monomers	36
Table 4 α CD62L Fab mutants	61

4. Abstract

The transfer of T cells, either freshly isolated, *in vitro* expanded or further modified, represents a promising therapeutic approach not only to fight malignancies or infectious diseases but also to dampen misdirected immune responses, like autoimmune diseases, graft versus host disease or chronic inflammatory syndromes. Clinical isolation of highly pure regulatory T cell (Treg) populations is still challenging, and labeling reagents can influence their viability and functionality, potentially altering the potency of isolated Treg cell products. The reversible Fab Multimer-based Treg purification, established during this thesis, can prevent label-induced interferences, occurring during conventional antibody isolation, *in vitro*, and *in vivo*. A substantial increase in engraftment efficacy of Treg grafts in C57BL/6 wildtype mice was observed when the cells were freed from isolation reagents. This difference in engraftment efficacy was mediated by Fc- γ -receptor- as well as IL-2 receptor-dependent mechanisms. In a preclinical model for acute GvHD, it was revealed that these 'label-freed' Treg grafts are protective at substantially lower cell numbers as compared to conventional non-reversible isolated grafts, leading to a significantly improved survival of mice treated with minimally manipulated Tregs. These findings might have significant clinical relevance for future Treg-based cell therapies.

5. Introduction

5.1. Hematopoietic Stem Cell Transplantation

Hematopoietic Stem Cells (HSC) are the best-characterized adult tissue stem cells and are one of the few cell types used in the clinical routine for cell therapy (Müller & Henschler, 2016). HSC Transplantation (HSCT) is an organ replacement therapy in which multipotent hematopoietic stem cells, which are derived from bone marrow (BM), peripheral blood, or umbilical cord blood of healthy donors, are transferred into patients to be used for the management of a range of malignant and non-malignant diseases of the hematopoietic system and for the treatment of immunodeficiencies (Boieri M, Shah P, Dressel R, 2016; Müller & Henschler, 2016). The patient's diseased hematopoietic system is eradicated by myeloablative radiotherapy and chemotherapy. Afterwards, donor stem cells are infused and can replenish the hematopoietic niche possibly curing the patient of its disease. Barnes et al. first described successful HSCT in 1956 and 1957 using an animal model demonstrating that HSCT can be used to eradicate recipient tumor cells in mice (Barnes & Loutit, 1957; Barnes DW, Corp MJ, Loutit JF, 1956). However, early studies already observed that some animals died of a secondary "wasting disease" consisting of diarrhea, weight loss, skin inflammation, and liver disease, after having cleared the leukemic cells (Barnes, Loutit, & Micklem, 1962). These symptoms are still a potential side effect of HSCT and were later on termed Graft versus Host Disease (GvHD). In 1962, Thomas et al. demonstrated the first leukemia cure by HSCT in men (Thomas & Ferrebee, 1962), but similar to the findings in mice; this patient died from complications caused by GvHD. Nevertheless, no residual leukemia cells were found, making evident that allotransplantation could be curative for hematologic malignancies if GvHD could be overcome. Three years later the first case of successful long-term engraftment without GvHD after allogeneic HSCT was reported by Mathé et al., shedding hope on the applicability of HSCT in the treatment of cancer patients (Mathé, Amiel, Schwarzenberg, Catran, & Schneider, 1965). The identification of individual Human Leukocyte Antigens (HLA) in humans allowing for donor and recipient HLA matching (van Rood, 1968) led to a new clinical trial by the Thomas group. They reported 100 transplantations with 13 patients surviving without disease 1–4.5 years after HSCT (Thomas et al., 1977), showing the power of the immune system to eradicate cancer. Application of allogeneic HSCT in the course of acute leukemia led to a cure rate of 50% in AML patients transplanted in first remission (Thomas et al., 1979). The extension of the donor pool from only including related donors to also including unrelated HLA matched donors (Hansen et al., 1980) made a broad clinical application of HSCT possible. Despite the early encountered adverse effects of HSCT, has proven to be very valuable in therapeutic usage

in men, often as the only curative option for many hematological malignancies (Morales-Tirado, Luszczek, van der Merwe, & Pillai, 2011).

Since its establishment in clinical routine, it has been shown that HSCT is not only a replacement of the diseased organ but additionally, that donor immune cells kill remaining cancer cells. This effect was termed Graft-versus-tumor effect (GvT) (F. Baron, 2005; Frédéric Baron et al., 2005; Kolb, 2008). As immune cells are the primary mediators of this effect, GvT can be boosted by additionally infusing donor lymphocytes (DLI) into the patient (Porter & Levine, 2006). GvT can occur in allogeneic HSCT despite the HLA matching, as mismatches in minor histocompatibility antigens can be detected by immune cells. These minor differences can as well as mismatches in the major histocompatibility antigens lead to the induction of GvHD, which remains the major cause of morbidity after HSCT and is still a big hurdle for broader applications of HSCT (Pasquini, Wang, Horowitz, & Gale, 2010).

5.2. GvHD the main adverse effect of HSCT

GvHD is a tissue damage disease occurring in recipients of allogeneic transplanted tissue as a result of the activity of immunocompetent donor lymphocytes that recognize the tissue of the recipient as foreign. GvHD has been described in the first successful HSCTs (Barnes et al., 1962) and classically defined by Billingham in 1966 (Billingham, 1966). While the transplant-related mortality has decreased due to better supportive care, enhanced treatment of severe infections, and improved conditioning protocols that lowered the toxicity (Henig & Zuckerman, 2014), GvHD has been and still is the primary cause of morbidity and mortality after allogeneic stem cell transplantation. Approximately 15% of HSC transplant recipients succumbing to it after transplantation (Pasquini et al., 2010). Further, the incidence of GvHD stayed at this constant high level for the last years although aggressive immunosuppressive therapies are used after transplantation, as well as allele-level Human Leukocyte Antigen (HLA) matching between donor and recipient (Pasquini et al., 2010). Though HSCT is the only curative option for a variety of hematological diseases, the enormous adverse effect of GvHD still limits the applicability of HSCT, much research is conducted on the reduction and management of GvHD after HSCT (Blazar, Murphy, & Abedi, 2012; Edinger & Hoffmann, 2011; Wood, Bushell, & Hester, 2012). As GvHD is a multi-factorial disease, the treatment of GvHD can be quite complicated and requires in-depth mechanistic studies to delineate the involvement of the different compartments of the immune system. A great deal of knowledge on the pathophysiology of aGvHD is derived from animal models.

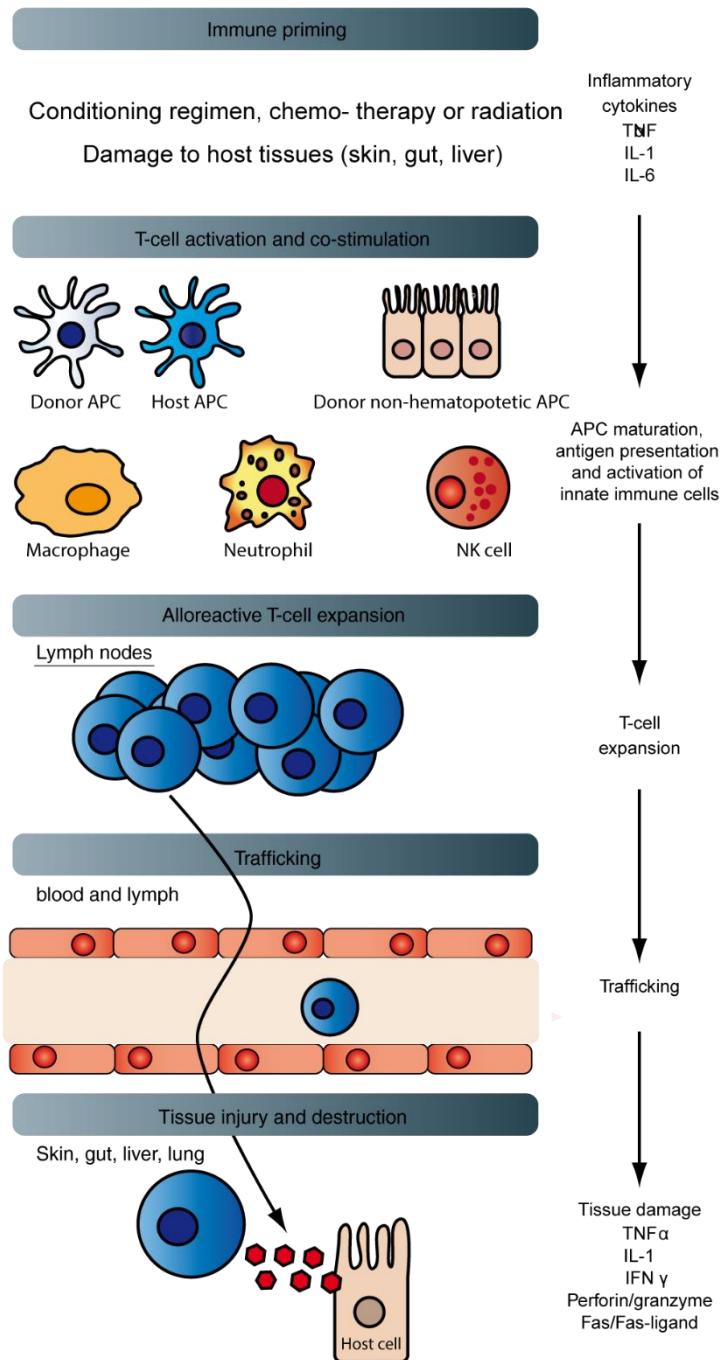


Figure 1 acute GvHD. The initiation and maintenance of acute graft-versus-host disease (GVHD) has been conceptualized into several phases: 1) Immune Priming phase: Activation and priming antigen-presenting cells (APCs), via tissue destruction, and increases APC function. Additionally, the release of gut bacteria, pathogen-associated molecular patterns (PAMPs) and chemokines during the conditioning phase can also lead to the activation of innate immune cells that participate in direct tissue damage and contribute to the cytokine storm. Host hematopoietic APCs probably have the most important role in the initiation of GVHD, but this may depend on the model; the potential role of donor APCs and host non-hematopoietic APCs should not be ignored. 2) Antigen presentation to and co-stimulation of T cells. Cytokines produced during the priming phase further promote antigen presentation and the recruitment of effector T cells and innate immune cells, which further augment the pro-inflammatory cytokine milieu. 3) T cell expansion and 4) Trafficking to organs of T cells, were 5) Finally, the effector T cells, natural killer (NK) cells, macrophages and pro-inflammatory cytokines (such as tumor necrosis factor (TNF)) result in end-organ damage, which is clinically recognized as acute GVHD in the skin, lungs, gut and liver. Figure modified from Schroeder & DiPersio, 2011

5.2.1. GvHD in mice and implications for treatment in men

Clinical routine shows that GvHD can develop in two different forms that differ in pathogenesis, symptoms, and organ involvement. Acute GvHD (aGvHD) affects up to 50% of alloHSCT patients and accounts for 15% of post-transplantation mortality (Pasquini et al., 2010; Qian, Wu, & Shen, 2013). Typical target tissues for aGvHD are the gastrointestinal tract, skin, and liver, but other atypical tissues include kidneys, salivary glands, oral epithelium, and thymus (McDonald, 2016; Toubai, Sun, & Reddy, 2008; Weisdorf, 2007). Acute GvHD classically develops during the first 100 days after transplantation, but late forms of 'aGvHD' have also been described. Chronic GvHD (cGvHD) develops later, and it occurs in ~50% of long-term survivors (Thepot et al., 2010). Chronic GvHD is associated with significant morbidity and mortality and is still the leading cause of death in long-term survivors of HSCT (Boieri, Shah, Dressel, & Inngjerdingen, 2016). The organs involved are mainly skin, mouth, eye, and liver, and less frequently the gastrointestinal tract and lung. The pathogenesis of cGvHD is not understood, and the manifestations resemble an autoimmune disease characterized by autoantibody production, chronic inflammation, and collagen deposition in target tissues (Boieri et al., 2016). New studies showed that the two classical forms of GvHD, aGvHD, and cGvHD, should be distinguished based on the constellation of symptoms, not the time point of occurrence, making treatment of disease more effective (Filipovich et al., 2005). Several mouse models have been established to resemble various forms of GvHD. Here I focus on models and treatment of acute GvHD, as the project later on also focused on that topic. Most models use the transfer of T cell depleted bone marrow into irradiated mice and then supplement varying numbers and phenotypes of donor lymphocytes to induce GvHD, thereby closely resembling the situation in human patients in a controlled manner. Cumulative data from several mouse models showed that four factors are decisive for the outcome of GvHD.

The first factor influencing the severity of GvHD is the type and dose of T cell subsets infused into recipient mice (Schroeder & DiPersio, 2011). Another determining factor is the dose of irradiation, as it determines the degree of tissue damage and the subsequent cytokine storm (Schroeder & DiPersio, 2011). In humans, the conditioning regimen used has also shown to be a critical factor in GvHD (Alyea et al., 2006; Blazar et al., 2012; Weisdorf, 2007). Environmental pathogens are the third crucial factor in GvHD pathogenesis (Nestel, Price, Seemayer, & Lapp, 1992). Not only pathogens but also commensals, such as the gut flora have an essential role. Thus, manipulation of the gut flora to make it less prone for GvHD induction might be a favorable treatment option. Data from mouse studies already showed decreased morbidity and mortality of animals following the administration of probiotic bacteria (Gerbitz

et al., 2012). The fourth key player of GvHD is the genetic difference between donor and recipient. Next, to the early identified induction of aGvHD by the mismatch of MHC (Barnes et al., 1962; van Rood, 1968), it was observed that aGvHD could occur even in MHC matched transplantation setting (Goulmy et al., 1996). In these transplantation settings, minor histocompatibility antigens (MiHA) were found to induce GvHD. MiHAs are polymorphic genes presented via MHC molecules as processed peptides and are not negatively selected in the donor thymus due to lack of expression. An example of the MiHA-mismatched transplant models is the transfer of cells from B10.D2 (H2^d) into BALB/c or DBA/2 (H2^d) mice, showing, similar to the human, less morbidity than MHC-mismatched models which nevertheless lead to lethal aGvHD (Korngold & Sprent, 1987). MiHA-mismatched models have given valuable insights in the biology of MiHA induced sickness. Donor T cells can target minor histocompatibility antigens and T cell receptors with high affinity to recipient MiHAs can exist within the donor T cell repertoire (Goulmy et al., 1996; Larsen et al., 2010). Respective T cell clones can become activated in an inflammatory environment as caused by pre-transplant regimens and may thereby induce aGvHD.

As at least partly MHC-mismatched transplantations frequently occur in the clinic as well, several mouse models using an MHC-mismatch were developed. In this setting, myeloablative irradiation before transplantation is always necessary when using immunocompetent recipient mice. Most of the MHC-mismatched models are dependent on both CD8⁺ and CD4⁺ T cells to induce pathology, but depending on the health status of the recipient mice, the dominant T cell subset varies even in the same transplantation setting (Schroeder & DiPersio, 2011). A ubiquitous model of aGvHD includes the transplantation of bone marrow and lymphocytes from C57BL/6 (H2^b) donors into irradiated BALB/c (H2^d) recipient mice (Schroeder & DiPersio, 2011). Models of acute GvHD helped to delineate some of the processes during disease induction and disease progression. It could be shown that recipient APCs play a significant role in disease induction (Shlomchik et al., 1999) and that even non-hematopoietic APCs of the recipient are sufficient to induce lethal experimental aGvHD (Koyama et al., 2012). These data clearly show that even if the recipient's professional APCs are mostly destroyed by the conditioning regimen, and if the graft itself does not contain professional APCs, the recipient can still develop aGvHD. To test whether some of the mechanisms found in 'pure' mouse models can be translated to human cells, xenogenic transplant models have been developed. In these models, human T cells are used to induce aGvHD in recipient mice. These very artificial animal models require strong immune suppression to prohibit graft rejection, as Nk cells and

other innate immune cells to battle the human immune cells. Several other immune-deficient mouse strains were used in the meantime with a NOD/SCID common γ chain^{-/-} (NSG mice), showing aGvHD like symptoms after transfer of human PBMCs (Schroeder & DiPersio, 2011).

5.2.2. Phases of acute GvHD induction

Data from mouse experiments and experience gained in the treatment of patients led to a multi-phase model of aGvHD induction. In the immune priming phase, antigen-presenting cells (APCs) are activated and primed by tissue destruction and subsequent inflammation caused by the conditioning regimen. Additionally, gut bacteria are released into the bloodstream through the conditioning regime, leading to even more enhanced levels of pathogen-associated molecular patterns (PAMPs) and chemokines. Already the conditioning can lead to the activation of innate immune cells that elicit direct tissue damage and contribute to the cytokine storm. In the second phase of aGvHD, the APCs present antigen and co-stimulation to T cells. Cytokines produced during the priming phase promote antigen presentation and the recruitment of effector T cells and innate immune cells, further augmenting the pro-inflammatory cytokine milieu. The third phase is defined as T cell expansion phase, followed by the trafficking to organs and end-organ damage by effector T cells, natural killer (NK) cells, macrophages and pro-inflammatory cytokines. The organ is clinically recognized as acute GvHD in the skin, lung, gut, and liver. The resulting tissue damage, if left untreated, will further amplify the process to more severe stages of GvHD pathology, which are increasingly difficult to control. Clinical GvHD is scored based on the severity of the manifested symptoms with a grading system first introduced by Glucksberg and colleagues in 1974 ranging from grade 0 (no GvHD) to grade IV (severe GvHD). The grade of GvHD has a significant impact on the survival of the patient (Gratwohl et al., 1998). With the knowledge gained the development of new treatment strategies targeting different stages and effector pathways in patients is ongoing.

5.2.3. Treatment of GvHD

The usage of immunosuppressive drugs, immunohistocompatibility matching, and T cell depletion have proven to be major advances for GvHD-free HSCT. Currently, in the clinic the first line treatment of GvHD is the systemic administration of immunosuppressive drugs, for example Methotrexate (MTX) (Storb, Epstein, Graham, & Thomas, 1970; Thomas & Ferrebee, 1962) together with anti-thymocyte globulin (Sun et al., 2010), corticosteroids and calcineurin inhibitors (Boieri et al., 2016). Several large-scale studies found that treatment of GvHD with topical steroid therapy reduces the overall symptoms and increases the survival of patients after

treatment (Blazar et al., 2012; Shlomchik, 2007). The primary mechanism of corticosteroid administration action remains unclear. Steroids have substantial side effects, including immunosuppression, hyperglycemia, and osteopenia making long-term treatment of patients a difficult task. These side effects and the risk of getting a steroid-refractory acute GvHD makes the development of second-line treatments against acute GvHD a primary research focus (Blazar et al., 2012). As discussed before, much work in the last decades showed that the clinical outcome of HSCT, especially the rate of GvHD, is influenced by many factors making different angles of treatment available for testing. Donor CD4⁺ and donor CD8⁺ T cells have been shown to have crucial roles in the pathogenesis of GvHD. Thus, the most effective approaches for GvHD prevention and therapy might focus on the depletion, tolerization, or functional incapacitation of donor T cells.

Modulating the graft composition by altering the cell properties

One option to influence cell properties is using small molecule inhibitors (SMIs). PKC isoform θ (PKC θ) has been shown to be important in GvHD induction in T cells, while only playing a minor role in pathogen-driven immune response or in GvT effects (Valenzuela et al., 2009). The PKC θ inhibitor AEB071 decreases the production of IL-2 and IFN γ by T cells and has been shown to extend the survival of rat heart and kidney allografts in primates. PKC θ inhibition decreases not only effector T cell responses but also Treg cell potency increases by mediating a negative feedback loop on Treg function (Zanin-Zhorov et al., 2010), making it an exciting target for clinical approaches. Another SMIs called Maraviroc interferes with T cell migration as it blocks CCR5, thus reducing the risk of aGvHD (Blazar et al., 2012). Besides of blocking the migration of T cells other mechanisms like inducing T cell anergy and inhibition of APCs by using Azacitidine or HDAC inhibitors (LBH589; Vorinostat), or reducing inflammation via TNF Inhibitors like Infliximab and Etanercept are also used in clinical trials (Blazar et al., 2012).

Modulating the graft composition by the administration of drugs

As GvHD is a multifactorial disease, it is not only dependent on T cell activation. It has been shown that high numbers of donor B cells correlate with the development of both acute and chronic GVHD (Shimabukuro-Vornhagen, Hallek, Storb, & Bergwelt-Baildon, 2009). New treatment protocols, leading to the depletion of B cells, like the administration of the B cell, depleting and APC inhibiting monoclonal antibody Rituximab (targeting CD20) are currently being tested in the clinic (Blazar et al., 2012). The depletion of activated T cells is also discussed as a viable option in GvHD treatment. One molecule frequently targeted is CD25, as activated

T cells upregulate CD25. The antibodies currently used in the clinic (Denileukin diftitox, Basiliximab, Daclizumab) also deplete CD25 positive Tregs (Blazar et al., 2012) and might thereby be somewhat counterproductive, as Tregs have been shown to be very important to control immune responses also in HSCT (Shlomchik, 2007; Weisdorf, 2007). In contrast to the specific depletion, one approach is to expand specific cell types selectively. The treatment with the mTOR inhibitor Rapamycin and IL2 leads to suppression of proliferation in conventional T cells and a selective expansion of functional Tregs, resulting in suppression of acute GvHD (Shin et al., 2011). *In vitro* expansion protocols using that effect resulted in a massive proliferation of human Tregs (Hippen et al., 2011) and productive Tregs in clinical treatment of GvHD (C. G. Brunstein et al., 2016; Claudio G Brunstein et al., 2011).

The considerable amount of SMIs and mAbs currently in phase I/II clinical trials make a variety of new treatment options available to clinicians, but to choose the right drug combination out of the repertoire of individual components will be one major challenge (Alousi et al., 2009).

Modulating the graft composition by choosing specific cell compartments

In addition to using drugs, it became apparent that the cell product infused in the first place has an essential role in the outcome of transfer efficacy and success of treatment. An extensive study found that KIR ligands significantly influence the outcome of HSCTs for myeloid leukemias, showing less relapse of disease but increased GvHD if there was a mismatch in KIR ligands (Miller et al., 2007), thus underscoring the importance of NK cells in both GvT and GvHD. This observation is in line with previous findings describing an increase in GvHD if there is a mismatch in the minor histocompatibility antigens. The T cell subsets contained in the T cell graft after HSCT can also have a significant impact on the outcome of HSCT and DLI. CD4 memory cells failed to induce GvHD in a mouse model of GvHD, whereas naïve CD4+ cells were able to induce experimental GvHD. The CD4 positive memory cells were still able to transfer a GvT effect (Zheng et al., 2008), potentially making the subset distribution in the graft a valuable tool to control both GvHD and GvT. In contrast to their CD4 counterpart, CD8 positive memory cells induced a GvHD reaction in addition to the GvT effect after transfer (Zheng, Matte-Martone, Jain, McNiff, & Shlomchik, 2009). Clinical trials transferring memory T cells alone might provide a practical approach to GvHD prevention or reduction. First-in-man trials showed that while there was an evident reduction in chronic GvHD, the incidence of acute GvHD was not reduced after transfer of a naïve T cell depleted T cell graft, when compared to historical controls (Bleakley et al., 2015). Additionally, no increased infection rates were observed, showing that optimizing the cell composition of Treg

grafts can dramatically decrease the incidence of GvHD after HSCT (Bleakley et al., 2015). Despite the risk of also dampening the wanted immune responses after cell transfer, one approach to better control acute GvHD could be the additional transfer of immunomodulatory cells to control the immune response early after transfer efficiently.

5.2.4. Immunomodulatory cell therapies to treat GvHD

Cell therapy aims at the reconstitution of lost, impaired, or missing biological and/or physiological functions by transferring the relevant cells and is already used in a variety of different settings. Several cell types are currently in discussion and tested to treat or preemptively inhibit GvHD in mice and man. One fascinating cell population consists of bone marrow-derived mesenchymal stem cells (MSCs). MSCs have been shown to suppress lymphocyte proliferation *in vitro* but were not able to prevent GvHD in mice (Sudres et al., 2006). In humans, on the other hand, MSCs have been shown to successfully modulate immune responses (Aggarwal & Pittenger, 2009) and after INF- γ activation have a positive effect on GvHD outcome (Polchert et al., 2011). Similar to MSCs, it was shown that cytokine-induced myeloid-derived suppressor cells (MDSCs) can inhibit GvHD and therefore might also be a valuable cell population after transfer (Highfill et al., 2010; Lechner, Liebertz, & Epstein, 2010). Donor NK cells have also been shown to have a role in the inhibition of acute GVHD. Preclinical studies indicated that donor NK cells could suppress acute GVHD and promote GVT responses (Asai et al., 1998; Olson et al., 2010). These findings are in line with the importance of KIR ligands in the outcome of HSCT (Miller et al., 2007). As described earlier, APCs are pivotal for disease induction, as especially dendritic cells play a significant role in GvHD. So it was shown that the DCs not only present antigens but also influence lymphocyte homing and can have tolerogenic functions (Blazar et al., 2012; Waller et al., 2011). However, the most promising results in treating GvHD using immunomodulatory cell therapies have been achieved by the transfer of regulatory T cells.

5.2.5. Tregs as therapeutic agent to treat GvHD

Regulatory T cells (Tregs) are essential for maintaining peripheral immune homeostasis and building up a tolerance to non-pathogenic foreign agents. These foreign agents include antigens from commensal bacteria and nutrients in mucosal areas of the intestinal tract or the airways (Josefowicz, Lu, & Rudensky, 2012; Wing & Sakaguchi, 2010). Tregs are also crucial for controlling ongoing immune responses and dampening their extent if necessary. The protective capacity of Tregs was first described when Powrie et al. adoptively transferred CD4⁺CD45RB^{high} T cells from naïve Balb/c mice into C.B-17 SCID mice and observed the

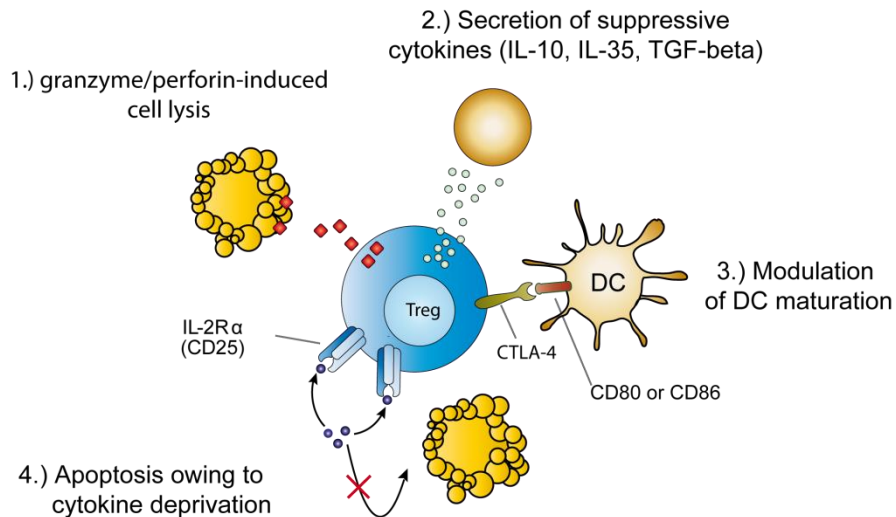


Figure 2 Mechanisms of Treg suppression: 1.) Tregs can secrete granzyme and perforin to lyse autoreactive or over-reactive cells. 2.) Tregs can also secrete a variety of different suppressive cytokines such as IL-10, IL35 and TGF-beta. Immune responses can also be influenced by the modulation of DC maturation 3.) and the preferential uptake of IL-2 depriving effector cells from the important surviving stimulus IL-2 and thereby indirectly inducing apoptosis

development of a lethal wasting disease in the recipient mice. Transfer of $CD4^+CD45RB^{low}$ cells in contrast surprisingly showed no signs of these detrimental effects (Powrie, Leach, Mauze, Caddle, & Coffman, 1993). The two subsets of CD4 positive cells seemed to have different capabilities in either inducing or regulating the immune reaction. Two years later, the $CD4^+$ T cell subset responsible for controlling the immune responses in mice was further characterized by the high constitutive expression of the IL-2R α -chain (CD25) (S Sakaguchi, Sakaguchi, Asano, Itoh, & Toda, 1995). Further analysis of the subset showed that expression of the forkhead/winged-helix family of transcription factor 3 (Foxp3) under steady state conditions to be the transcription factor driving Treg development (Fontenot, Gavin, & Rudensky, 2003; Shohei Hori, Takashi Nomura, 2002). Mutations in the Foxp3 gene were identified in an inbred mouse line named scurfy and in an analogous human genetic disorder named IPEX (immune dysregulation, polyendocrinopathy, enteropathy, X-linked syndrome). Both syndromes are characterized by a wasting illness associated with immune dysfunction, lymphoproliferation, diarrhea, rash, and other autoimmune/endocrine alterations. A similar phenotype was observed when $CD4^+CD25^+$ Tregs were deleted in mice.

CD25 and Foxp3 are also upregulated in recently activated T cells. A highly specific marker distinguishing Tregs from other CD4 T cell subsets has not yet been found (Gavin et al., 2006; Morgan et al., 2005). Tregs can either develop in the thymus (natural Treg/(nTreg)) or are generated in the periphery from naïve $CD4^+$ T cells (induced Treg/(iTreg)) (Rubtsov et al., 2010; Shimon Sakaguchi, 2004; Shimon Sakaguchi, Vignali, Rudensky, Niec, & Waldmann,

2013). Tregs suppress immune responses in several manners, including secretion of the immunosuppressive cytokines IL-10, IL-35, and TGF- β (Takahashi et al., 1998; Qizhi Tang & Bluestone, 2008; Thornton & Shevach, 1998), granzyme/perforin-induced cell lysis, inducing apoptosis via cytokine (IL-2) deprivation (Pandiyani, Zheng, Ishihara, Reed, & Lenardo, 2007), and modulation of dendritic cell function (Chung et al., 2009; Curti, Trabanelli, Salvestrini, Baccarani, & Lemoli, 2009; Sharma et al., 2009). As regulatory T cells have many immune regulatory mechanisms and the lack of Tregs leads to a severe autoimmune disease (Qin et al., 2006), regulatory T cells are a prime target for immunomodulatory cell therapy.

5.2.6. Murine Tregs in preclinical mouse models for aGvHD

In preclinical animal models of acute GvHD, the infusion of only T effectors into mice is rapidly fatal. Several groups could show that the severity and lethality of aGVHD can be diminished by the co-administration of either freshly isolated or *ex vivo* expanded Tregs with T cell effectors, when compared to mice only receiving Teff cells (Cohen, Trenado, Vasey, Klatzmann, & Salomon, 2002; Petra Hoffmann, Ermann, Edinger, Fathman, & Strober, 2002; Taylor, Lees, & Blazar, 2002). In line with that finding, the depletion of CD4⁺CD25⁺ cells from bone marrow and Treg grafts lead to a more severe aGvHD resulting in recipient mice succumbing faster to the disease (Cohen et al., 2002; Taylor et al., 2002). Further investigation revealed that only the CD62L^{high} subset of Tregs could decrease the severity and incidence of GvHD (Ermann et al., 2005). Matthias Edinger and colleagues showed that regulatory T cells could protect from lethal GVHD in an entirely MHC mismatched bone marrow transplantation model (Donor mouse: C57BL/6 (H-2^b); recipient mouse: Balb/c (H-2^d)). Treatment of recipient mice with Tregs achieved a survival rate of 89% if the Tregs were co-transfused in a 1:1 ratio with effector T cells. Most importantly, treatment with Tregs not only prevented GVHD but, in contrast to treatment with standard immune suppressive regimes, transfused tumor-specific Teffs were still able to attack and clear the tumor (Edinger et al., 2003). Surprisingly, the addition of physiologic numbers of Tregs (Treg to Teff ratio 1:10) had no beneficial effect on host survival in murine models of aGvHD. Only if the graft contained substantially elevated numbers of Tregs (i.e., Treg to Teff ratios of 1:1 or 1:2) recipient mice are protected (Cohen et al., 2002; Edinger et al., 2003; Ermann et al., 2005; Petra Hoffmann et al., 2002; Taylor et al., 2002). Although both freshly isolated and *in vitro* expanded Tregs could prevent the induction of aGVHD when co-transferred with effector T cells, data on the treatment of already established aGVHD is less clear. Depending on the model used the delayed administration of Tregs either failed or succeeded in protecting mice from lethal aGvHD. Jones et al. showed that the infusion of Tregs up to 10 days after the infusion of a graft containing CD8⁺ T cells could

prevent aGvHD lethality in an MHC-matched model, whereas it was not possible to alter the outcome in a haploidentical model (Jones, Murphy, & Korngold, 2003). However, administration of effector T cells before the injection has proven to be very beneficial for the outcome of HSCT (Bolton et al., 2015). The data suggested that Tregs play a crucial role in the early phase of aGvHD development, influencing the homing and priming of immune cells, but physiological numbers of Tregs are not able to control the disease.

5.2.7. First-in-man trials using Treg therapy to treat GvHD

Several groups already gathered some experience in the usage of regulatory T cells to either supplement immune surveillance by drugs or as the sole mediator of immunosuppression after HSCT. Different approaches are being tested at the moment, either the usage of freshly isolated regulatory cells or the extended cultivation of isolated Tregs to gather huge numbers. In a study published 2009, Trzonkowski et al. treated two patients, one suffering from aGvHD and one from cGvHD, with CD4⁺CD25⁺CD127⁻ Treg grafts containing 1×10^5 or 3×10^6 cells per kg body weight. The cells were expanded using beads coated with CD3- and CD28 specific antibodies and high dose IL-2 (1000U/ml). Tregs had a stable phenotype during expansion (~90% Foxp3 positive). In both cases, a transient clinical improvement was measured, and in one case the dose of prednisone could be reduced (Trzonkowski et al., 2009). This first-in-man use of Treg therapy led to other studies treating increased patient numbers.

Bruce Blazar's group in Minnesota published in 2011 a cohort of 23 patients which were treated using third-party cord blood-derived Treg cells. After isolation based on CD25 expression, the cells were also expanded using CD3/CD28 coated beads and IL-2 for 18 days, increasing the cell numbers 200 fold on average compared to the starting numbers. Purity for CD4 and CD25 positivity was high (~86%), but Foxp3⁺/CD127⁻ cell content was on average only around 64%. Nevertheless, a reduction of grade II-IV incidences was observed within the Treg treated group (Claudio G Brunstein et al., 2011). These promising results led to a refinement of expansion and treatment protocols, now using CD86 and CD64 expressing K562 cells (KT64/86) (Hippen et al., 2011) and thereby achieving a 13.000-fold expansion of Tregs on average. Comparison of Treg treated patients with a control group which did not receive Tregs showed an apparent reduction in aGvHD and cGvHD incidence within the first year. Furthermore, a lower infection rate was observed, but the intensity of infection was similar when infection occurred. Other parameters like hematopoietic recovery, non-relapse mortality, relapse, and disease-free survival were similar in both groups indicating that, like in the mouse model (Edinger et al., 2003), Tregs inhibit GvHD, but allow the immune system to develop normally, thereby having a GvT effect.

Unfortunately, *in vitro* expansion of Tregs is very time consuming and bears the risk of altering the cell function. Therefore, first studies tried to use freshly isolated Treg cells to circumvent the costly and possibly phenotype altering culturing of Treg cells. In a phase I trial at the University Hospital Regensburg, freshly isolated donor Tregs were transfused into nine patients with a high risk of leukemia relapse after HSCT. After abandoning of pharmacologic GVHD prophylaxis, up to 5×10^6 cells per kg body weight with a content of at least 50% FOXP3⁺ cells were administered. After an observation period of eight weeks, an additional DLI was administered to promote GvT activity. Neither GvHD nor opportunistic infections nor early disease relapses were detectable after Treg transfusion, confirming the very encouraging pre-clinical mouse data (Edinger & Hoffmann, 2011). In another recent study, a group from the University of Perugia described for the first time the prevention of GVHD in humans without any post-transplantational immunosuppression by co-infusing primary, freshly isolated Tregs along with Tregs in a haploidentical HSCT. Although the ratio between Tregs and Tregs, was never higher than 2:1 in strong contrast to studies with expanded Tregs, overall survival rates as well as GvHD associated disease symptoms were drastically reduced. This might be related to the prophylactic administration of Tregs but also to a functionally better cell product (~69% Foxp3⁺ cells).

In summary, primary Tregs – at least in a prophylactic or pre-emptive setting – seem effective for treatment, even in relatively low numbers. This also seems to be true when combined with conventional DLI treatment (Mauro Di Ianni et al., 2011), but the isolation of high enough numbers of freshly isolated regulatory T cells under GMP conditions and high purities has proven to be quite challenging (Mauro Di Ianni et al., 2011). First-in-man clinical trials and many mice experiments showed that the co-transfer of freshly isolated Tregs and T effector cells need supraphysiologic ratios of Tregs to T effectors (4:1 - 1:1) to induce protection of the graft recipient using. Physiologic cell ratios of 1:10 did not show a protective effect in mice (Engelhardt & Crowe, 2010). To this point, it is not clear if the high numbers of regulatory T cells are needed to transfer protection, or if Tregs suffer from reduced fitness. Several mechanisms could reduce the fitness and engraftment capability of regulatory T cells, thereby increasing the number of Tregs needed to control GvHD. The isolation reagents needed to specifically enrich for regulatory T cells which still stick to the cell surface after positive enrichment of Tregs could diminish the *in vivo* performance of Treg grafts both in mouse and men. These isolation reagents are built on the antigen specificity of antibodies, which are known to influence cells potentially.

5.3. Antibody-mediated effects on cells

Monoclonal antibodies (mAbs) can influence cells in a variety of ways. For example, they can block the binding pocket of surface exposed receptors, depriving the target cell of this particular signal. Moreau et al. showed in 1987 that most of the antibodies targeting the IL2 receptor α -chain (CD25) in the mouse do indeed influence cell signaling. The clone PC61, 3C7 and 7D4, which are used in many studies to isolate Treg cells, block IL2 dependent proliferation (Moreau et al., 1987). Also, the binding of the mAb can lead to conformational changes of the receptor and thereby inhibit the signal transduction. In contrast, to signal blockage, mAbs can also activate receptors in the absence of their cognate ligand thereby leading to intracellular signaling or internalization of the receptor. These traits are often actively used in research and therapy (Ghobrial RR, Boublik M, Winn HJ, 1989).

Two primary mechanisms how mAbs directly influence cells by activating the immune system have been described. One of the ways is the classical activation of the complement cascade leading to the formation of the membrane attack complex in the target cell membrane. The classical pathway plays a role in both innate and adaptive immunity. C1q connects the adaptive immune response to the complement system by binding to antibodies complexed with antigens. Binding of more than one C1q molecule to the surface causes a conformational change and an autocatalytic enzymatic activity of C1r. C1s is cleaved by C1r to generate an active serine protease. C1s enzyme acts on the next two components of the classical pathway, cleaving C4 and C2 into C4b and C2b. These two fragments together build the C3 convertase of the classical pathway. C3 convertase cleaves C3 to produce C3b molecules that coat the target surface and C3a, which initiates a local inflammatory response (Tomlinson, 1993). All three complement activation pathways merge at the formation of the C3 convertases. Several effector mechanisms are activated from this point onward. C3a initiates local inflammation, whereas the surface-bound C3b can lead to an increased uptake of the opsonized target mediated by complement receptor bearing effector cells (macrophages and DCs) or the formation of a membrane-attack complex. The result is a pore in the lipid bilayer membrane that destroys membrane integrity, killing the target by destroying the proton gradient across the target cell membrane (Charles A Janeway, Travers, Walport, & Shlomchik, 2001; Tomlinson, 1993). Antibodies eliciting complement driven killing of target cells have been recommended for use in the clinic (Nielsen et al., 2002). The ability of monoclonal antibodies

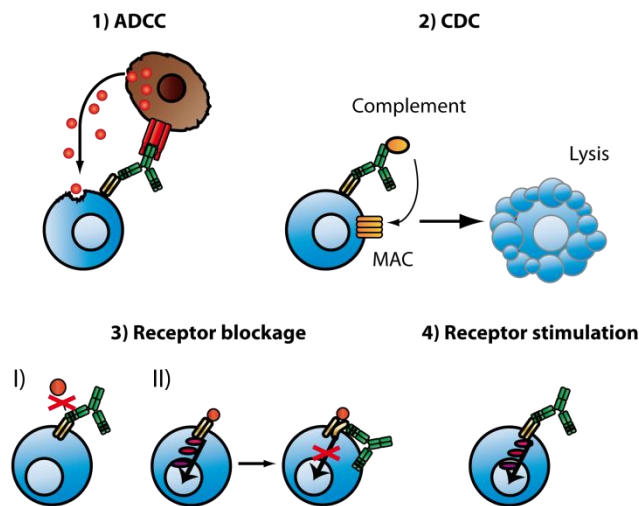


Figure 3 Antibody mediated effects on cells 1) antibody dependent cellular cytotoxicity (ADCC) surface bound antibodies can be recognized by Fc γ receptor positive immune cells (NK cells, macrophages and DCs). Activated immune cells then can kill the antibody marked target cell. 2) Complement dependent cytotoxicity (CDC) Surface bound antibodies can activate the complement system. mAbs are recognized by C1q leading to the activation of the complement cascade and the formation of the membrane attack complex (MAC). This will lead to target cell lysis. 3) Receptor blockage Antibodies bound to surface molecules can block the signaling of surface receptors by either I) blocking receptor ligand binding II) induction of structural changes in the receptor leading to a stop of signal transmission. 4) Receptor stimulation antibodies can activate intracellular signaling of surface exposed receptors without them seeing their actual ligand, leading to false signal transduction

is dependent on the surface molecule (Bindon, Hale, & Waldmann, 1988; Nielsen et al., 2002) and the Ig type of the antibody (Brüggemann et al., 1987). Activation of the immune system via the complement system is a crucial effector function of monoclonal antibodies and also readily used in the clinic, but another primary effector function has been described.

The antibody-dependent cell-mediated cytotoxicity (ADCC) is a rapid effector mechanism. It describes the killing of antibody-coated targets by cytotoxic immune cells through the release of cytotoxic agents and/or by the expression of cell death-inducing molecules. ADCC is triggered through the interaction of surface-bound antibodies (IgG/IgA/IgE) with specific Fc receptors (FcRs) (Fanger, Shen, Graziano, & Guyre, 1989; Teillaud, 2012). Several immune cells that mediate ADCC have been described, including natural killer (NK) cells, monocytes, macrophages, neutrophils, eosinophils, and dendritic cells, which due to their different localization and function have different properties in the induction of ADCC (Teillaud, 2012). Careful analysis revealed that the efficacy of ADCC is dependent on some parameters. It could be shown that the density of FcR and surface-bound mAb, which is dependent on the density and surface-stability of the antigen and the antibody affinity, can largely influence the efficacy (Teillaud, 2012). Also, not all FcR Fc-part interactions lead to the induction of ADCC. The main contributors to ADCC are the FcR Fc γ RI (CD64), Fc γ RIIa and

Fc γ RIIc (CD32), Fc γ RIIIa (CD16) in human and Fc γ RI, Fc γ RIII and Fc γ RIV in mice (Teillaud, 2012). The other Fc γ receptors seem not to play a role in ADCC induction or even counterbalance activating signals, actively suppressing ADCC (Clynes, Towers, Presta, & Ravetch, 2000). Other surface molecules (like KIRs) have also been shown to negatively regulate ADCC, which has been especially problematic in the treatment of cancer patients, where cancer surface antigens are targeted to induce ADCC in tumor cells (Seidel, Schlegel, & Lang, 2013). Several antibodies are used in the clinic to attack target cells directly by inducing ADCC. For example, Rituximab, a mAb targeting CD20 is used to target cancer cells in non-Hodgkin's lymphoma. Other mAbs targeting CLC (Obinutuzumab), neuroblastoma (Dinituximab, Hu3F8, Hul4.18K322A), breast and gastric cancer (Trastuzumab), colorectal, and head & neck cancer (Cetuximab), have also been shown to transfer their anti-tumor activity via ADCC (Wang, Erbe, Hank, Morris, & Sondel, 2015). ADCC is also used to deplete specific subsets from the patient to alter existing immune cells. Regulatory T cells are attacked by infusing antibodies targeting CD25 or CTLA-4 to boost immune responses in profoundly immuno-surveilled tumor micro-environments.

Similar to this application in the clinic, antibodies are used to rapidly deplete cell populations to answer specific questions in basic research. The administration of CD25 targeting antibodies can have an adverse effect on the success of liver transplantation, as the injection of the clone PC-61 leads to depletion of Tregs from the recipient, leading to a loss of graft acceptance (Li et al., 2006). The central mechanism of PC-61 mediated depletion has been shown to be Fc γ RIII dependent (Setiady, Coccia, & Park, 2010). Another recent study investigated the different influences an antibody can have on the target cell by generating mutant variations of the PC-61 clone and found that one antibody can mediate several effects on Tregs, like depletion and signal blockage (Huss et al., 2016). Similar to decreased transplantation success after the administration of PC-61 into recipient mice, the depletion of Tregs from a DLI graft after HSCT using the antibody 7D4, which also targets CD25, leads to an increase in morbidity and mortality in recipient mice (Taylor et al., 2002). These data not only strongly underline the importance of Tregs in transplantation settings but also show how monoclonal antibody-based isolation reagents could alter the composition of grafts. Taken together, surface-bound antibodies can lead to rapid depletion of cells from graft, blood, and primary organs by activating either effector cells or the complement cascade and can further alter their target cells by blocking or activating essential surface molecules. To avoid the potentially altering effect of isolation reagents on target cells our laboratory developed the Streptamer technology,

introducing the possibility to remove the isolation reagent from the cell surface after the positive enrichment of the target cell.

5.4. Streptamer technology

Similar to our hypothesis that monoclonal antibody-based isolation of target cells could influence the effectiveness of transferred Treg grafts, it was shown that non-reversible multimers attached to the cell surface are causing activation of the T cell in a T cell receptor (TCR) dependent manner, leading to cell activation and cell death (Whelan et al., 1999; Xu et al., 2001). MHC multimers are used to track polyclonal antigen-specific CD8⁺ T cells during the course of an immune response, as well as to assess their phenotypical and functional differentiation upon activation (Altman et al., 1996; D H Busch & Pamer, 1999; Dirk H. Busch, Pilip, Vijn, & Pamer, 1998; Stemberger et al., 2007). Monomeric MHC does not stably bind the TCRs of the cell surface, whereas multimerization of D-biotin coupled monomeric MHCs via a streptavidin backbone increases the structural avidity of the bound complex through cooperative binding, allowing stable binding of the fluorescent multimeric label to the T cell surface (Altman et al., 1996). The need to interrupt the induced signaling and the unwanted side effects led to the development of the reversible MHC Streptamer technology, permitting the disassembly of the multimeric complex into MHC monomers and the backbone, which then dissociates from the cell surface (Knabel et al., 2002). Instead of biotinylation of the MHC Monomers, a short peptide affinity tag, containing two Streptag II sequences separated by a short GS-linker (also called OneStrep-tag), was fused to the MHC monomers. The Streptag II tailed MHC-monomers were then able to be multimerized by interacting with Streptactin molecules, a streptavidin variant with an improved affinity for the Streptag II sequence. The Strep-tag II peptide binds to the Streptactin backbone with an affinity of $KD \sim 10^{-6}M$, while D-biotin still binds with an extraordinarily high affinity ($KD \sim 10^{-13}M$) to Streptactin (Voss & Skerra, 1997). Since the Streptag binds reversibly to the same pocket where the cognate ligand D-biotin is complexed, the Streptamer complex can be easily disrupted under physiologic conditions by the addition of D-biotin. Due to the spontaneous dissociation of now monomeric, weakly binding MHC molecules from the cell surface, no remaining Streptamer components are detectable after the addition of D-biotin (Knabel et al., 2002). In a functional comparison to conventional non-reversible MHC Streptamer, MHC Streptamers showed the same staining intensity, but cells isolated using them displayed better effector function than cells isolated using conventional multimers (Neudorfer et al., 2007).

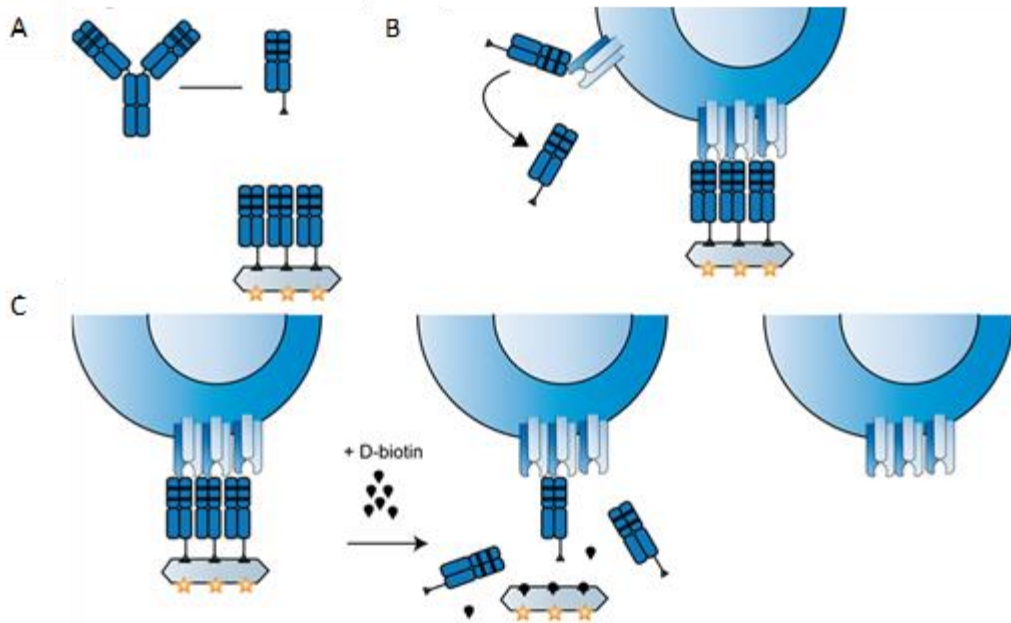


Figure 4 Illustration of the basic principle of reversible Fab-multimers. A) Fab fragments are obtained from antigen specific monoclonal antibody (upper row). Low affinity-modified Fab fragments are multimerized by Streptag-Strep-Tactin complexation (lower row). B) monomeric Fab can not bind stable to the surface receptor, but multimerized Fab does bind specific and stable to the target receptor C) Cells are labeled and isolated with Fab multimers. Subsequent treatment of stained cells with D-biotin mediates destruction of the Fab-multimer complex and results in spontaneous dissociation and complete removal of all (monomeric) components from the target cell surface

To tackle the potential problem of monoclonal antibody-based isolation reagents remaining on the cell surface and thereby influencing isolated grafts, our lab broadened the Streptamer technology. Monomeric Fab-fragments were generated from monoclonal antibodies (Abs) and, similar to the MHC-Streptamers, a One-Strep-tag was fused to the heavy chain of the Fab, allowing multimerization via Streptactin molecules (Stemberger et al., 2012). In line with the MHC Streptamers, we called these Multimers ‘Fab Streptamers’. We showed that enrichment of $CD8^+CD62L^+CD45RA^{neg}$ central memory T cells, as well as $CD4^+CD25^+CD45^+$ naturally occurring Tregs (nTregs), is possible using the Fab Streptamer technology (Stemberger et al., 2012). The Fab-technology permits the enrichment of cells and the detachment of the isolation reagent after the isolation process is finished. We already showed that the Fab Streptamer technology could be used to isolate murine regulatory T cells (Mohr, 2012; Nikolaus, 2016).

6. Aim

The aim of this Ph.D. thesis was to investigate the potency of regulatory T cells sorted by reversible staining reagents to prevent and cure autoimmune diseases. CD4⁺CD25⁺ regulatory T cells (Treg) are pivotal for the maintenance of self-tolerance. In mouse models, it could be shown that regulatory T cells prevent GvHD dependent death induced by donor CD4⁺CD25⁺ T cells from C57BL/6 animals transferred into MHC class I- and class II-mismatched BALB/c recipients.

In a first step, we used the Fab-Multimer technology developed in our laboratory to isolate minimally manipulated regulatory T cells of high purity. Therefore the isolation reagents (Fab Multimers targeting CD4 and CD25) had to be characterized and refined. Further, we wanted to compare the differentially isolated Treg grafts. To look for the potential benefits of the removal of staining reagents and to investigate the underlying mechanisms of potentially occurring differences, we wanted to investigate the engraftment capabilities of both Fab Multimer and conventionally sorted cells in different models. Our final goal was to establish a mouse model simulating a complete HLA mismatched transplantation (C57BL/6 (H-2b) -> Balb/c (H-2d)). To enable the engraftment and to mimic the situation of human cancer patients the recipient mice have been irradiated. The lympho-depleted mice also should receive a bone marrow transplantation from an HLA mismatched donor. Thereby we wanted to establish a robust protocol for the induction of an acute GvHD first and then test the either Fab Multimer- or mAb-isolated populations. In this model, we hoped to evaluate whether Fab-multimer isolated cells have a similar or maybe superior functionality compared to conventionally-sorted regulatory T cells.

7. Results

The Fab Multimer technology enables reversible staining of cell surface markers by combining the antigen specificity of monoclonal antibodies with the reversibility of the MHC-Streptamer technology (Stemberger et al., 2012). In previous work in our Lab, we already generated, optimized and tested three murine Fab-fragments, an α CD4- (parental mAb clone: GK1.5), an α CD25- (parental mAb clone: PC61) and an α CD62L Fab-fragment (parental mAb clone: MEL-14) (Mohr, 2012; Nikolaus, 2016). For functional characterization, Fab monomers were multimerized using PE-labeled Streptactin and analyzed for their capability to stain marker-positive cells specifically. All three Fab multimers identified subsets of cell populations comparable to the parental antibodies. The α CD4 Fab multimer showed a staining intensity as bright as the parental mAb, whereas the α CD25 Fab-fragment and the α CD62L Fab-fragment showed reduced staining intensities when compared to their parental mAb. Despite the reduced staining brightness, the α CD25 Fab-multimer and CD62L Fab-multimer did stain a population of similar size compared to the mAb. The α CD4 Fab fragment also stained a population very similar to the population stained with the mAb. Given that reversibility is the critical feature of the Fab multimer technology, demonstrating complete reversibility was the most crucial task. Monomerization of surface-bound Fab-multimers using D-biotin combined with subsequent washing away dissociated components, followed by re-staining of the cells with ST-PE demonstrated that the wildtype α CD4 Fab monomers could be liberated entirely from the cell surface. In contrast, the wildtype α CD62L and the α CD25 Fab Monomers could not be washed from the cell surface and resulted in re-staining with ST-PE. Therefore, we generated several mutants of the wildtype α CD4 and α CD25 Fab Monomers and identified for both Fab monomers reversible and still fully antigen-specific mutants (Mohr, 2012; Nikolaus, 2016).

7.1. Enrichment of Tregs freed from staining reagents

7.1.1. Characterization of existing and newly generated Fab multimer reagents

The previously generated Fab monomers (as summarized above) were completely reversible when tested (see Figure 6 (Mohr, 2012)), but whereas the CD4 Fab was as bright as the parental antibody, the reversible CD25 Fab lacked the staining brightness of its parental mAb. We wanted to check if other mutations could provide a brighter and still reversible Fab multimer staining. Therefore, we generated 14 new mutants and tested all of them for expression, staining brightness and reversibility. Additionally, we re-expressed the already existing mutants to

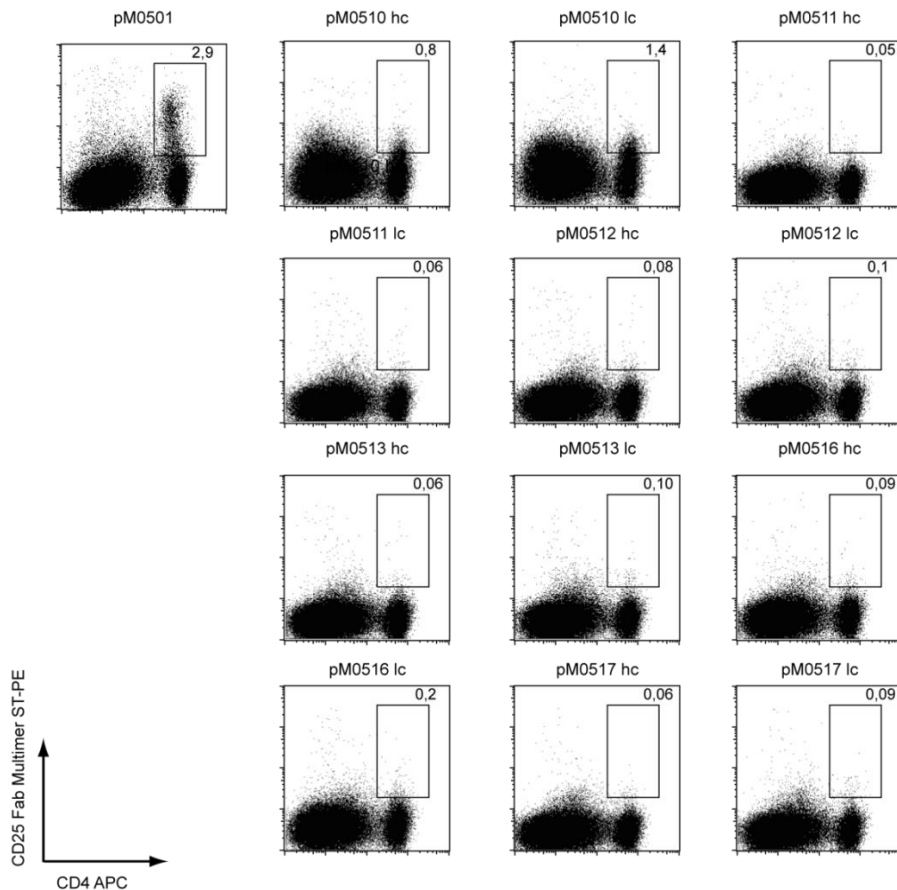


Figure 5 Test staining for newly generated Fab monomers. Newly expressed Fab monomers were multimerized using the standard protocol and ST-PE and their staining capacity was compared to the clone pM0501.

recheck them for these three parameters, in order to exclude that technical aspect during protein expression and purification did not cause the non-reversibility of Fabs in our first screening attempt. 12 out of the 14 newly generated Fab mutants could be expressed in *E. coli* and subsequently be purified and multimerized, but only two of them maintained antigen-specific staining (Figure 5 & Table 1). The mutations pM0510 hc and lc did show some staining, but way weaker than the staining of the newly expressed pM0501 (Figure 6). The mutant Fab

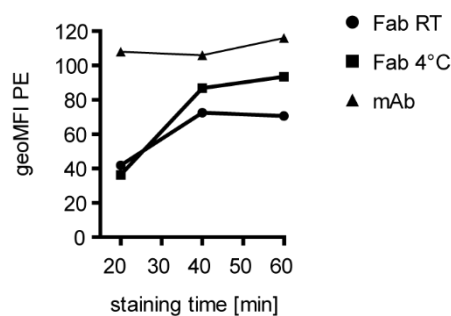


Figure 6 Prolonging staining time does increase staining brightness of α CD25 Fab multimer. Splenocytes were stained at either room temperature or 4°C and using either α CD25 Fab multimer with a Streptactin PE backbone or mAb targeting CD25. Staining brightness was measured at the indicated time points.

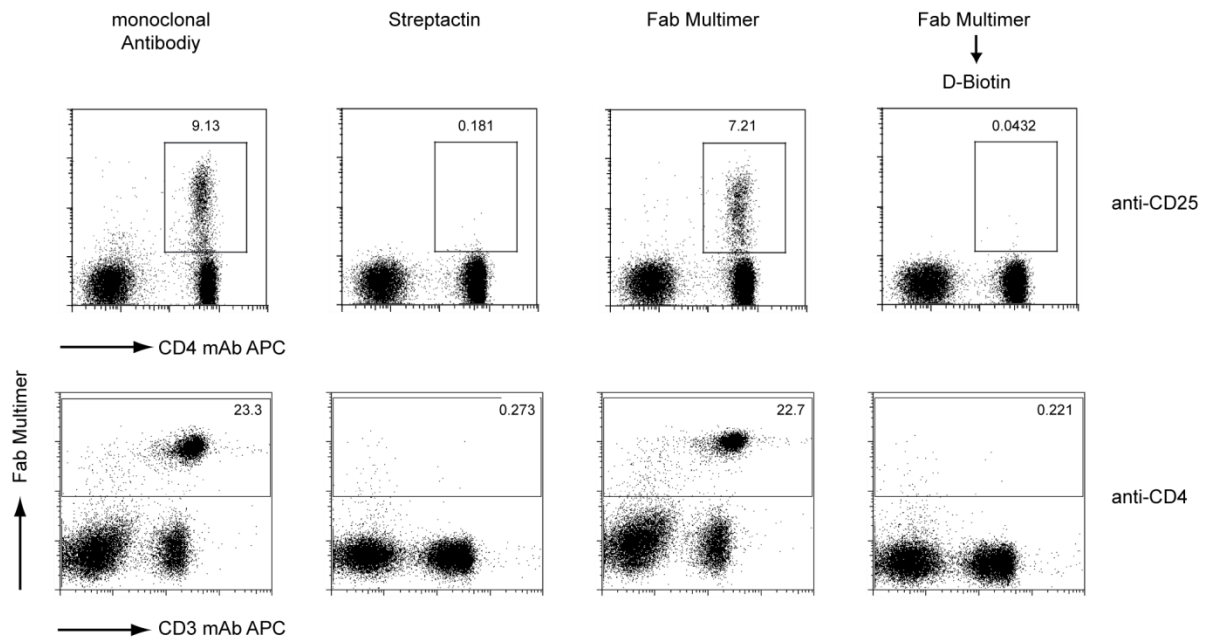


Figure 7 Reversibility test of α CD4 and α CD25 Fab staining: Upper row, reversibility of the CD25 staining; lower row CD4 staining. Depicted are the staining of the parental mAb (first column) the Streptactin background control (second column), Fab multimer staining (third column) and staining after addition and washing with D-Biotin (fourth column) in combination staining with a CD4 mAb (upper row) or a CD3 mAb (lower row)

pM0501 was the most promising candidate during our initial testing (Mohr, 2012; Nikolaus, 2016). In pM0501 the Tyrosine at position 32 of the light chain had been replaced by an alanine. To potentially enhance the staining brightness further, we tested if increased staining time and/or increased staining temperature would enhance the brightness of the Fab multimer staining. As shown in Figure 6 an extension of staining time from 20 to 40 minutes significantly increased the staining signal intensity of the α CD25 Y32A Fab. The geoMFI of pM0501 staining was almost similar to the mAb staining quality at 4°C. We then tested whether Fab multimer labeling for CD4 and CD25 can be combined in a single staining step using the above-identified best labeling conditions. As shown in Figure 7, the combined Fab multimer stainings for CD25 and CD4 were as bright as the parental Fabs, but thereby fully reversible upon exposure to D-biotin (Mohr, 2012). To further characterize the staining of Fab multimers, we next decided to determine the kinetics of spontaneous dissociation of Fab monomers from the cell surface after D-biotin addition.

Plasmid number	Plasmid backbone	Mutation	Bacterial expression	Staining	reversibility
pM0500	cDNA	wt	Yes	Yes	No
pM0501	pM0500	Y32A/light	Yes	Yes	Yes
pM0502	pM0500	W35A/light	Yes	No	-
pM0503	pM0500	Y36A/light	Yes	Yes	No
pM0504	pM0500	Y94A/light	Yes	Very weak	Yes
pM0505	pM0500	W107A/heavy	Yes	No	-
pM0506	pM0500	W108A/heavy	Yes	No	-
pM0507	pM0501	StrepTag C-Cys	Yes	Yes	Yes
pM0508	pM0501	Y32AL/LC-HIS	Yes	Yes	Yes
pM0509	pM0500	LC-HIS	No	-	-
pM0510	wt	D2HC	Yes	Very weak	Yes
pM0510	wt	D2LC	Yes	Very weak	Yes
pM0511	wt	D1HC	Yes	No	-
pM0511	wt	D1LC	Yes	No	-
pM0512	wt	D2HC	Yes	No	-
pM0512	wt	D2LC	Yes	No	-
pM0513	wt	D1HC	Yes	No	-
pM0513	wt	D1LC	Yes	No	-
pM0514	wt	D1HC/D1LC	No	-	-
pM0515	wt	D1HC/D2LC	No	-	-
pM0516	pM0511	D2HC/D1LC	Yes	No	-
pM0516	pM0513	D1HC/D1LC	Yes	No	-
pM0517	pM0511	D1HC/D2LC	Yes	No	-
pM0517	pM0513	D2HC/D2LC	Yes	No	-

Table 1 α CD25 Fab mutants

7.1.2. Measuring K_{off} rates of Fab Monomers from the cell surface

To do so, we decided to develop an assay to quantify the time how long Fab monomers stay on the cell surface after addition of D-biotin on a population level. Our lab had previously published the development of a novel assay detecting the K_{off} rates of MHC-I Streptamers on single cell level using fluorescence microscopy (Nauerth et al., 2013). Since this microscopy-based assay is quite laborious and time-consuming and since for Fab monomers analysis on the population level should be sufficient, we decided to transfer the K_{off} rate assay to a flow cytometry-based readout. Therefore, we first had to test whether it is possible to visualize fluorescence-labeled monomeric Fabs on the cell surface by flow cytometry. For this purpose, we tested two methods in parallel to approaching that problem. We either labeled the monomeric Fab molecules via a HIS-tag on light chain of the Fab using NI-NTA- dye based conjugation to Oregongreen488 (OG488) or by adding a free cysteine in the linker region and using maleimide chemistry based conjugation to Alexa488, similar to protocol used for the MHC based on rate (Nauerth et al., 2013). To do this, we mutated the pM0501 at two different sites. We added a HIS tag sequence at the end of a short linker region at the light chain of the Fab multimer to use NI-NTA dye based conjugation (Guignet, Hovius, & Vogel, 2004) or we added a free cysteine in the Streptag linker region to make maleimide-based dye coupling possible (Nauerth et al., 2013).

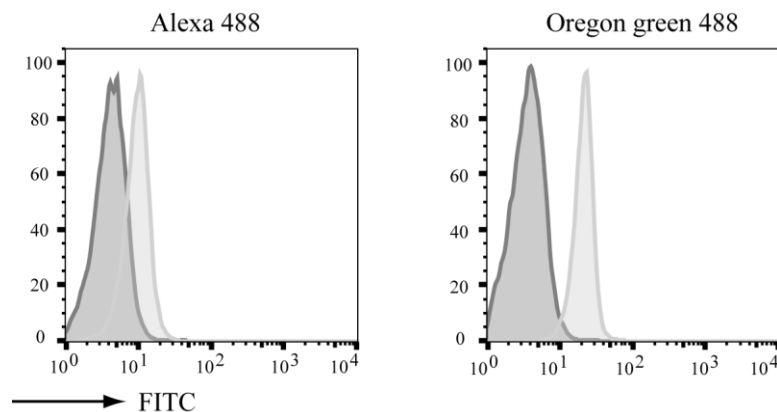


Figure 8 Dye coupling to the α CD4 Fab Monomer. Overlay of uncoupled (dark grey histogram) and coupled (light grey histogram) Fab Monomers pregated on the STPE backbone staining. Alexa 488 was coupled to the monomeric α CD4 Fab using maleimide chemistry (left side) and OG488 was coupled to Fab Monomers using NI-NTA chemistry (right side)

The mutations were generated using a mutagenesis PCR protocol, which we had established previously in our lab (Mohr, 2012). Both methods proved to make visualization of monomeric Fab on the cell surface possible, as surface accumulation with both molecules yielded a definite shift in the FITC channel after dye conjugation (Figure 8). Especially the maleimide-based dye coupling proved to be quite challenging to accomplish, as only relatively low amounts of

protein could be obtained after dye coupling. Nevertheless, we generate sufficient amounts of reagent to use them for proof-of-concept k_{off} rate measurements. For example, PBMCs stained with Streptactin APC-coupled αCD4 Fab was analyzed for 30 seconds to establish a stable starting brightness before D-biotin. For on-line measurement, we recorded the staining intensity for 15 minutes. This online measurement technique during FACS analysis had already been established previously by Mathias Schiemann to measure Ca^{2+} flux (Yu et al., 2005) and we adapted this protocol for k_{off} rate measurements. After injection of D-biotin, the Streptactin APC backbone quickly dissociates from the cell surface with a mean half-life of 10 seconds (Figure 9 right column and Table 2). The staining intensity of the monomeric Fab increases drastically after the dissociation of the backbone, most likely due to quenching of OG488

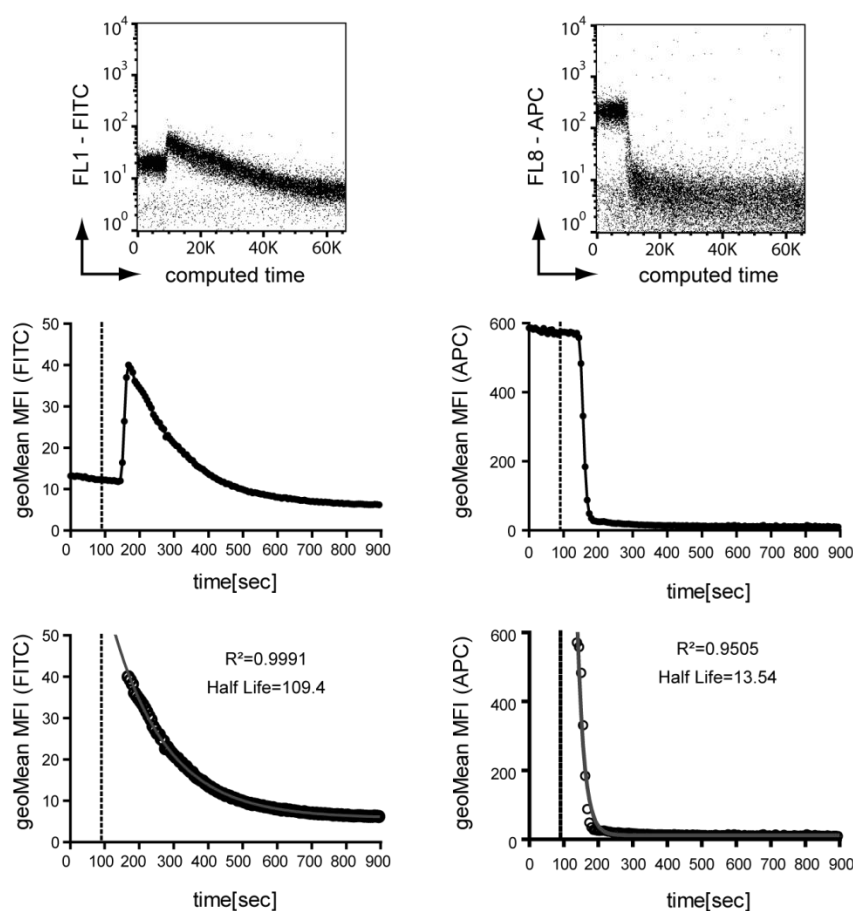


Figure 9 Analysis of flow off rate data. Upper row depicts fluorescence intensity over time for the Fab monomer conjugated with Oregon Green 488 (left side) and the streptactin APC backbone (right side). Data is converted as described in the methods part into 300 data points and plotted depicting the geometric mean of the fluorescence over time (second row). For calculation of the mean half-life times the peak of fluorescence intensity of the Fab monomer is used.

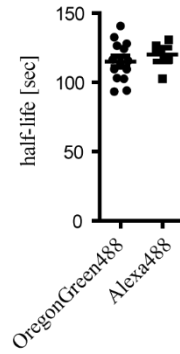


Figure 10 Comparison of half-lives of OregonGreen488 or Alexa488 dye coupled murine α CD4 Fab. Murine splenocytes were stained using either OG488 labeled or Alexa 488 α CD4 Fab multimers and the half-life of the Fab Monomers was measured using the flow based off-rate assay. (OG488 (n=12; Alexa488 n=4)

emission by the ST-APC backbone. After peaking of the staining intensity (indicating complete backbone dissociation), remaining monomeric Fabs still bound to the cell surface gradually dissociate and this kinetic can be followed by flow cytometry over time. We calculated the geometric mean fluorescent intensity and plotted it over time (Figure 9 second row). For calculation of the half-life of monomeric Fab only data points after the detachment of the ST-APC backbone (the peak of fluorescence) were used (Figure 8 third row). Using one-phase decay calculation of the GraphPad Prism 5 software, the half-life of monomeric Fab on the cell surface and the goodness of fit (R^2) was determined. The analysis revealed a mean half-life time of 109.4 seconds on the cell surface for the murine α CD4 Fab and 13.54 seconds for the Streptactin backbone (Figure 9).

Both OregonGreen488 and the Alexa488 coupled murine α CD4 Fabs detach from the cell surface with very similar kinetics (Figure 10 & Table 2), showing that the k_{off} rate is independent of the dye-coupling chemistry. These results prompted us to move forward with the NI-NTA coupled Fab monomers, as the protein expression led to higher yields. We then wanted to test whether this newly developed flow-based measurement would be comparable to the already established methods. First, we compared the flow-based results to the microscopic k_{off} rate assay, which measures the off-rate of target molecules on single cells. This assay was developed by our lab (Nauerth et al., 2013) and is a valuable tool to analyze the k_{off} -rates of MHC molecules from their cognate TCR, thereby allowing a quite precise and highly reproducible measurement of the affinity of the analyzed TCR. We stained samples with the OG488 labeled α CD4 Fab multimers and performed with one half of the sample the microscopic assay and with the other half the flow-based off-rate assay. We observed that both assays gave very similar results as the average k_{off} rate of α CD4 Fab from single cells was 123 seconds and on the flow-based population level 115 seconds, (Figure 11). These data nicely

validated the accuracy of the flow-based off-rate assay. For further validation, we went on to test if the results of our assay are also comparable to published data.

	OG488 coupled	Alexa488 coupled	ST-APC backbone OG488	ST-APC backbone Alexa488
Half-life [sec.]	115	120	11,85	10,63

Table 2 half-life of surface-bound α CD4 Fab and backbones

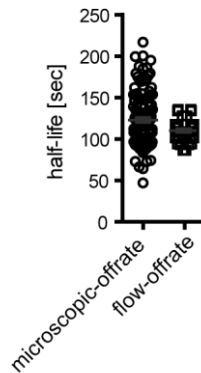


Figure 11 Comparison of microscopic and flow-based off rate measurement Murine splenocytes were stained using OG488 labeled α CD4 Fab Multimers and the half-life of the Fab Monomers was measured using either microscopic or the flow based off-rate assay.

A standard method to measure the strength of protein interaction is the Biacore measurement (Murphy et al., 2006). With this technology, one binding partner is immobilized on a sensor chip surface, and several concentrations of the binding-partner are injected and passed in solution across the chip surface. The changes in the index of refraction at the surface where binding interactions occurs can be detected and are subsequently evaluated by fitting algorithms and by comparing them to binding models. From the fitted data, several conclusions can be

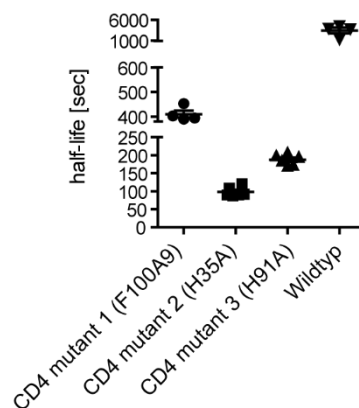


Figure 12 k_{off} -rate of human α CD4 Fabs human PBMCs were stained using OG488 labeled α CD4 Fab Multimers and the half-life of the Fab Monomers was measured using the flow based off-rate assay.

drawn. Cedric Bes and colleagues used this assay to determine the affinity of mutants of the human α CD4 Fab of the human α CD4 antibody 13B8.2 and found them to have very different binding affinities and half-life times to the CD4 antigen (Bès et al., 2003). We generated Fabs monomers containing the same mutations as well as a HIS Tag sequence coupled to the light chain to for measuring the half-life times of these clones in the flow-based k_{off} rate assay. The mutants were numbered from 1-4, with mutant 1 having a mutation at position 100 substituting a Phenylalanine with alanine, number 2 a Histidine by an Alanine at position 35 and mutant three a histidine by an alanine at position (Stemberger et al., 2012). We found that indeed the three mutated α CD4 Fabs differed profoundly in their half-life time when compared to the wildtype Fab and amongst each other (Figure 12). The results of Biacore and flow k_{off} rate data cannot be compared directly, as one technology assessed the pure protein interaction (Biacore), while the k_{off} -rate assay investigates the protein interaction in a more natural state. In Table three we ranked the wild-type and three Fab mutants we could generate according to their affinity. We observed that mutants 2 and 3, which resulted in the lowest affinities were interchanged in between Biacore and flow k_{off} rate ranking. This variation could be caused by the different environments of the binding kinetics.

We established and validated a novel setup for the recently developed microscopic Koff-rate assay, making high-throughput analyses of populations expressing the same target receptor possible. We used this novel approach to determine the half-life of the α CD4 Fab monomers (115 sec.) and α CD25 Fab (below detection limit), which we have developed for the isolation of regulatory T cells. The very fast off-rate of the α CD25 Fab indicates a very low affinity of this Fab, providing a reasonable explanation for the prolonged staining time needed to get optimal staining brightness (Figure 6) and the failure to use this Fab for magnetic selection in prior work (Mohr, 2012). As both Fabs had proven to stain very nicely for FACS analysis, we next wanted to combine these two Fab-Streptamers for a one-step selection process of regulatory T cells by flow-based cell sorting.


Affinity	Biacore	Flow off rate Assay
highest	CD4 wt	CD4 wt
	CD4 mutant 1	CD4 mutant 1
	CD4 mutant 2	CD4 mutant 3
	CD4 mutant 3	CD4 mutant 2
lowest		

Table 3 Relative affinity of human α CD4 mutant Fab Monomers

7.1.3. Development of a double Fab multimer staining

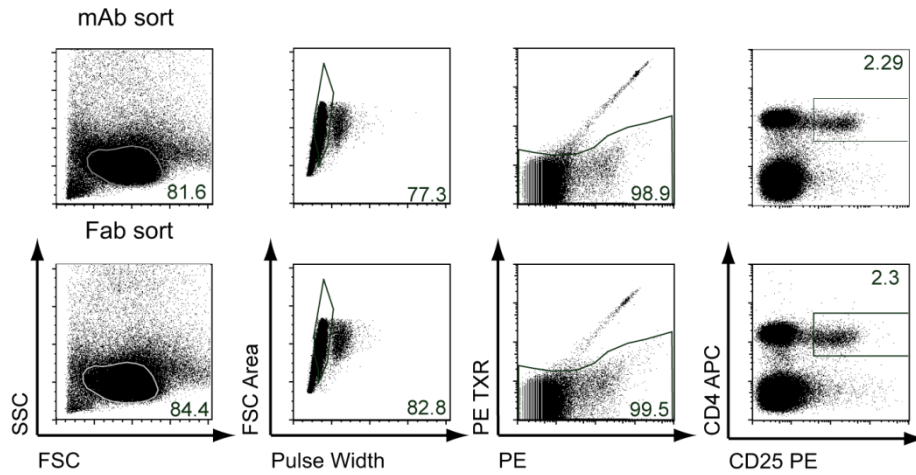


Figure 13 Isolation of regulatory T cells freed from staining reagents Gating strategy on the Moflo legacy to sort Tregs from murine splenocytes either stained with mAbs against CD4 and CD25 (upper panel) or reversible Fab multimers targeting CD4 and CD25 (lower panel). Gating on lymphocytes (first row), single (second row) and living cells (third row); representative FACS plots

To further improve the efficacy of Fab-Streptamer-based isolation of regulatory T cells and subsequent removal of the isolation reagents we wanted to combine the fully reversible stainings for CD4 and CD25. The Fab multimer double staining turned out to be more complicated as expected because we observed frequent exchange of Fab Monomers between the different (ST-PE and ST-APC) backbones (Figure 39). We first performed the stainings by directly mixing the two pre-conjugated reagents, which led to a staining smear; also extensive washing between the staining steps did not improve the staining satisfyingly (Figure. 39). Optimization of the staining procedure and inter-staining washing process guided us to a

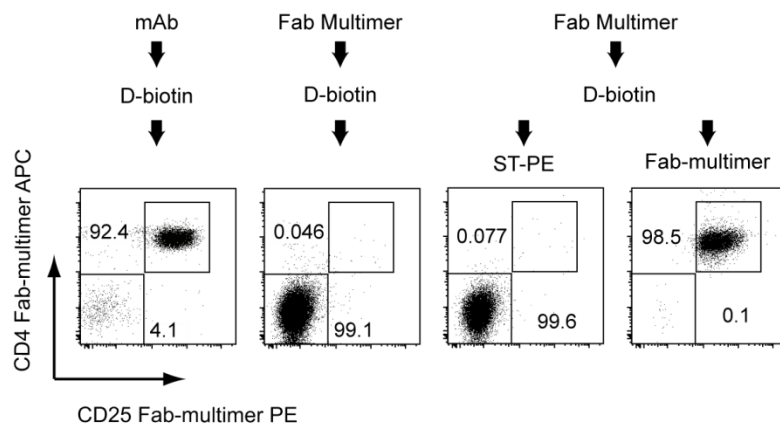


Figure 14 Reversibility of the Fab multimer double staining: mAb and Fab multimer FACS sorted cells after washing in FACS buffer containing 1mM D-biotin (left and second from left blot). Monomer reversibility test to stain for remaining Fab-Monomers we re-stained one half of the sample of Fab multimer sorted cells after D-Biotin washing and with ST-PE (second from right plot) and to make sure no more D-biotin was in the system we re-stained the second half with Fab multimers(right plot).

successful double-staining protocol with α CD25 Fabs coupled to a Streptactin PE backbone and CD4 Fab coupled to a Streptactin APC backbone in a two-step staining process (Figure 13). Comparing the staining intensity of conventional mAb and Fab multimer double stained samples on a Moflo legacy cell sorter demonstrated that cells are comparable in number and frequency of single living leucocytes. Furthermore, the staining brightness of surface markers CD4 and CD25 was nearly identical, allowing a precise identification and subsequent flow-based cell sorting of Tregs with both reagent types (Figure 13). For cell isolation, we gated on the 2-3 percent highest CD25 expressing and CD4 double-positive cells, thereby establishing a single-step isolation protocol for regulatory T cells. We then went on to confirm that an essential feature of the Fab multimer technology, the reversibility, was still preserved after co-staining and sorting.

Washing of cells with D-biotin after sorting did not lead to the removal of either the mAb staining for CD25 or the mAb staining for CD4 as seen in Figure 14 in the left panel. In contrast to that, Fab multimer-sorted and D-biotin washed cells were free of staining reagents (Figure 14 second from left panel). To confirm that not only the multimer but also monomeric Fab molecules are removed from the cell surface, we treated one half of the sorted cells with ST-PE, which would allow to re-stain non-removed monomeric Fab molecules still sticking to the cell surface, and the other half with Fab multimers to demonstrate with stable staining that all the D-Biotin had been successfully removed from the system. As seen in Figure 14, ST-PE staining was negative, whereas we were able to re-stain the isolated cells with Fab multimers, showing that the double staining of CD4 and CD25 using Fab multimers and subsequent isolation of the cells does not negatively interfere with full reversibility (backbone and Fab monomers) of the staining and yields in a highly pure population of cells.

7.1.4. Comparison of FACS isolated mAb or Fab multimer stained Tregs

To compare the cell products obtained by FACS using conventional mAb and Fab multimer-based enrichment, we analyzed the purities of the sorted cell products. FACS-based cell enrichment of Tregs from the same sample using antibodies or Fab multimers both resulted in highly pure CD4, CD25 double-positive cell products. Further analysis to check if the sorted cells had a regulatory T cell phenotype was performed looking for the Foxp3 expression in the sorted cells. Like with the surface expression of CD4 and CD25 both isolation methods yielded in a highly pure Foxp3 positive population (Figure 15A, B). To rule out that the different staining methods would prefer one of the Treg subsets, we looked for subset distribution segregating the Treg subsets by the surface markers CD27 and CD62L. We found that also there

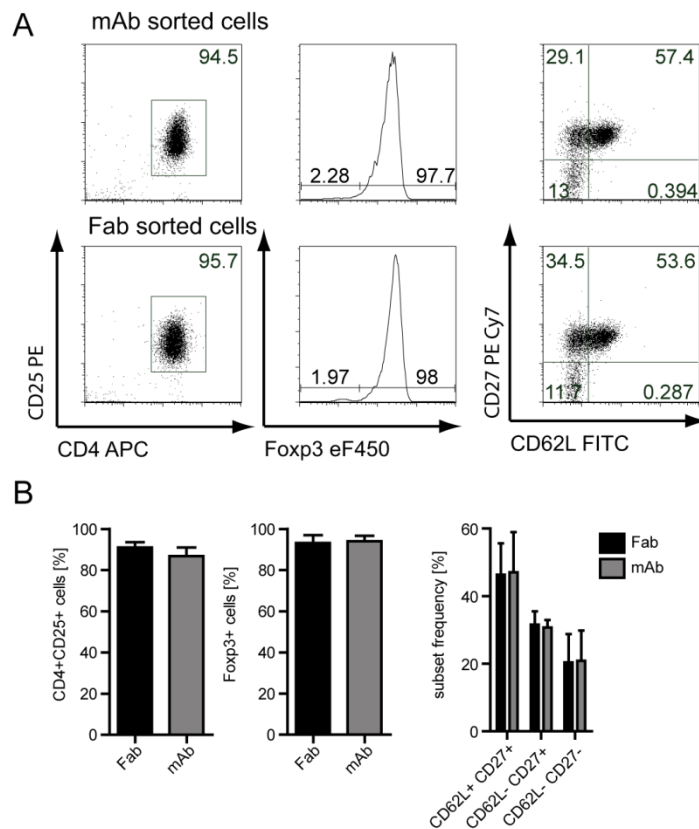


Figure 15 Treg cells after sorting Comparison of Fab Multimer and mAb Tregs after sorting **A)** exemplary FACS plots for mAb sorted cells (upper panel) and Fab Multimer (lower panel). **B)** Bar graph showing pooled analysis of 3 individual experiments

was no difference between mAb- and Fab-sorted samples, making the reversibility of the Fab multimers from the cell surface their unique distinction (Figure 15B).

From these data, we conclude that with α CD4/ α CD25 Fab multimers or mAbs identical Tregs populations can be stained and enriched by flow cytometry. Fab multimers further allow the complete removal of the staining reagents upon cell purification. Next, we wanted to know whether murine Tregs purified with conventional ‘non-reversible’ antibodies or using Fab multimers differ in their capacity to engraft and survive upon adoptive T cell transfer.

7.2. *In vivo* Engraftment

7.2.1. Transfer into wt C57BL/6 mice

After establishing that the isolation of Tregs either using conventional mAbs or reversible Fab multimers for FACS sorting lead to comparable cell products with respect to purity and cell composition, but are distinct in the capability of Fab multimer-isolated cells to be liberated from their isolation reagent. We wanted to examine whether removal of the isolation markers could be beneficial for *in vivo* engraftment and/or survival of the isolated cells. Therefore, we isolated Tregs from CD45.1 congenic donor mouse lines and transferred 20,000 Tregs per CD45.2 recipient mouse (Figure 16A). As shown in Figure 16B, we could readily recover transferred cells by a highly sensitive double staining assay for congenic markers (Figure 16B). Interestingly, we found significantly increased numbers (relative frequencies as well as absolute cell numbers) of Fab multimer-isolated cells after three weeks upon adoptive transfer in spleen and lymph nodes (Figure 16 C, D) indicating an improved engraftment and/or survival of Fab

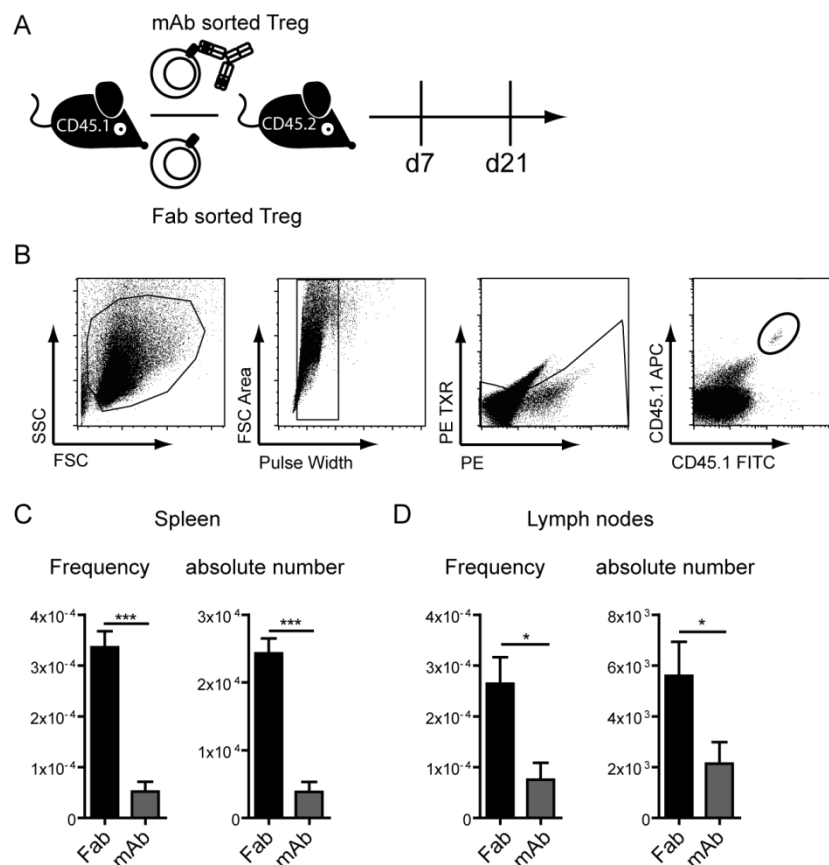


Figure 16 Transfer of differentially sorted Tregs *in vivo* A-B) 20,000 Fab multimer or mAb sorted congenically marked Tregs were transferred into wt C57BL/6 mice A) exemplary FACS plot depicting recovery of transduced cells. Tregs were detected as living lymphocytes and a double staining for CD45.1 (congenic marker). B) Frequency and absolute cell number of recovered CD45.1⁺ cells (n=4) 3 weeks after transfer statistical analysis was done using GraphPad Prism software t-test or one sample t-test; *p=0.5; ** p=0.1; ***p=0.01)

Multimer-isolated Tregs. To further consolidate these findings, we refined the experimental settings to the co-transfer of differentially isolated Tregs marked congenically with either CD90.1 or CD45.1 into wild-type (wt), CD90.2⁺ and CD45.2⁺ recipient mice.

7.2.2. Co-transfer of mAb and Fab Multimer sorted cells into wt C57BL/6 mice

To further improve our transfer system, we attempted to use the transfer of two distinct congenically marked Treg populations into one wildtype recipient mouse. Such multiplex transfers with T cells from different congenic recipients was already well established in our lab (Buchholz et al., 2013; Graef et al., 2014; Stemberger et al., 2007). We used this experience to modify the protocol established for the transfer of minimal numbers of CD8⁺ T cells to make the transfer of minimal numbers of Tregs possible. We transferred a 1:1 solution of either Fab multimer- or mAb-sorted from splenocytes (Figure 13) into C57BL/6 recipient mice. The recipient mice were sacrificed one week or three weeks after cell transfer, and both Fab- and mAb-transferred cells could be detected. For such transfer experiments, it is important to control that the congenic markers or potential genetic drifts within the donor mice have no any influence on the engraftment capability of Treg populations. Therefore, we compared the frequency of recovered cells from Fab sorted cells from a CD45.1 and a CD90.1 positive donor and found no difference in the size of the recovered populations (Figure 17 B left panel). The comparison of mAb sorted cells from both donor mouse strains showed the same result (Figure 17), demonstrating that in this setting of Treg transfer into wt C57BL/6 mice Tregs from both donor mice (CD45.1 and CD90.1) behave very similar. As an additional control, we included

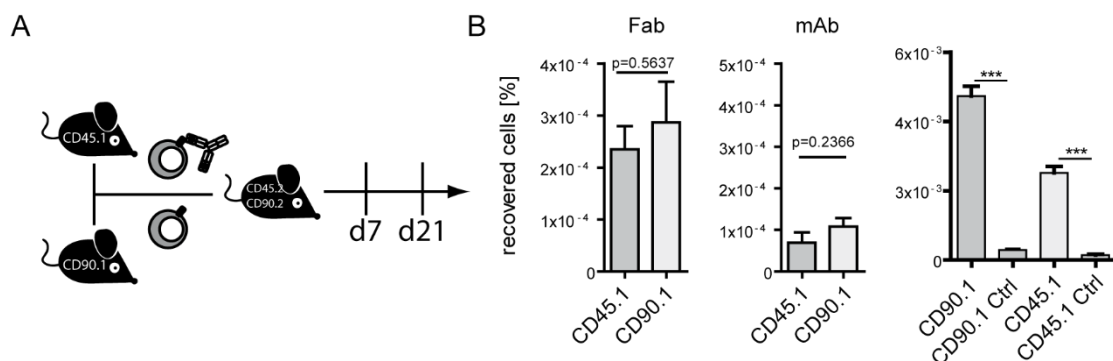


Figure 17 Co-transfer into wt C57BL/6 mice model and setup. A) Tregs were isolated either using mAbs or Fab multimers from congenically marked mice using FACS and washed in 1mM D-biotin containing FACS-Buffer afterwards and transferred into C57BL/6 wt recipient mice. Recipient mice were sacrificed on day 7 or day 21 after cell transfer. **B)** Comparison of engraftment of Fab and mAb from CD90.1 and CD45.1 donor mice at week 3 after cell transfer. Right graph show staining background in mice not receiving any cells. Statistical analysis was done using GraphPad Prism software t-test or one sample t-test (Figure 2E right panel); *p=0.05; ** p=0.01; ***p=0.001)

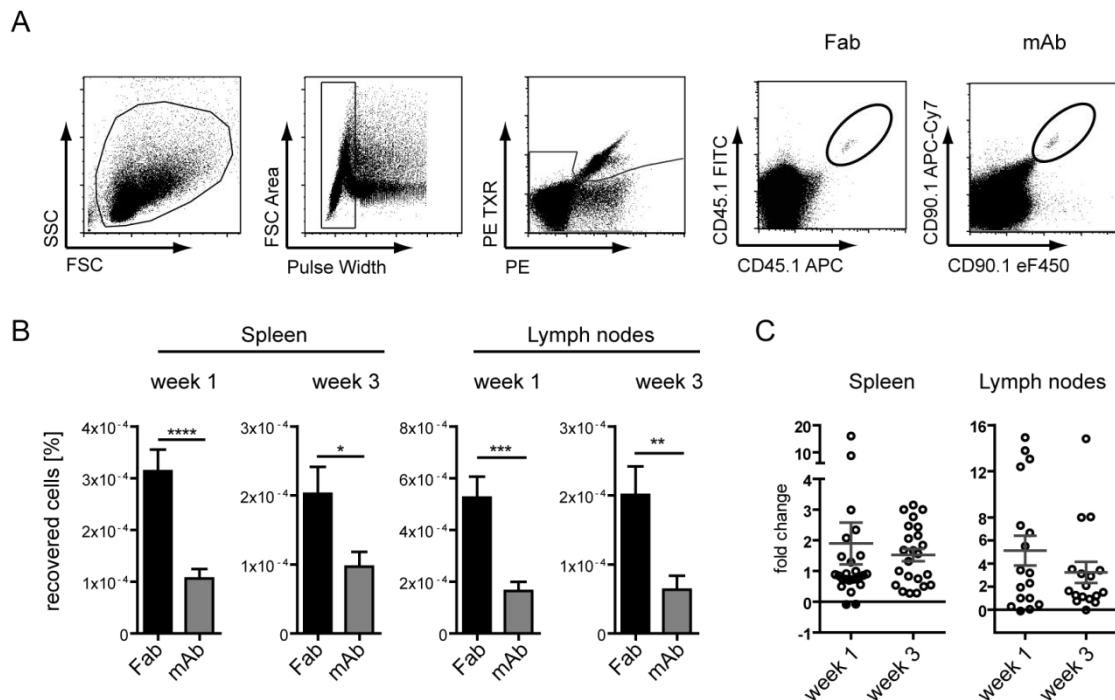


Figure 18. Co-Transfer of differentially sorted Tregs *in vivo* A-C) 2×10^4 congenically marked (either CD45.1 or CD90.1) Fab multimer and mAb sorted Tregs (1:1 solution) were co-transferred into wt C57BL/6 recipient mice. C) Exemplary FACS plots depicting recovery of transferred cells. D) frequency of recovered cells after 1 week ($n=23$) and 3 weeks ($n=23$) E) fold change for individual mice red filled circles more mAb than Fab sorted cells; empty circles more Fab than mAb sorted cells. After one week ($n=23$) and three weeks ($n=23$)

mice not receiving any Treg cells to determine the staining background and to exclude that we only detect false positive cells. These experiments demonstrated that the background was only minor in comparison to antigen-specific staining, despite the very small populations recovered.

After we established the model of co-transfer of differentially sorted Treg populations, we set out to compare the size of recovered cell populations. We analyzed primary lymphoid organs, spleen and lymph nodes one week or three weeks after cell transfer. Fab multimer-sorted Tregs were significantly more recovered after one as well as after three weeks in spleens and lymph nodes (Figure 18B). Analysis of individual mice made it possible to calculate the fold change between mAb- and Fab multimer-sorted populations. We found that in only 2 out of 48 mice we found a little more mAb-sorted cells, but the fold change was minimal (-0,079 - 0,089) (Figure 18C). Overall, a considerable improvement in engraftment capability of Fab multimer-sorted Tregs was observed, accumulating in an almost two-fold better engraftment. We further investigated if the cells we recovered had still a Treg phenotype. In line with published literature where Tregs have been described to have a very stable phenotype (Rubtsov et al., 2010), we found that transferred Tregs maintained a stable phenotype independent from the isolation method: in all cases the recovered cells were predominantly CD25, CD4 and Foxp3 positive (Figure 19 A, B). These data demonstrate that while it is possible to isolate

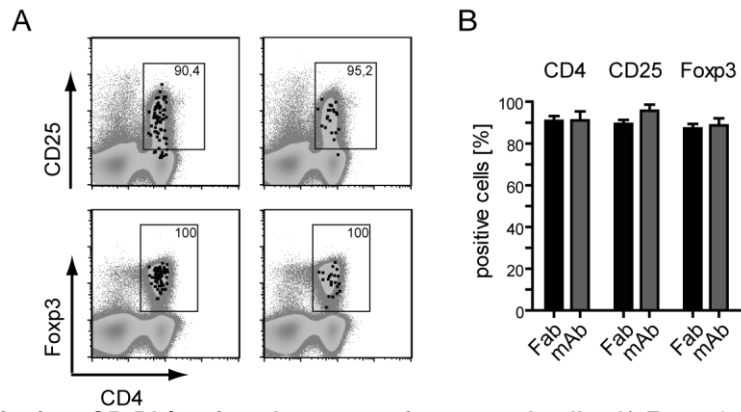


Figure 19. Co-transfer into C57BL/6 mice phenotype of recovered cells. A) Exemplary FACS plot showing phenotype of recovered cells (black dots) and endogenous cells (grey density plot) B) phenotypic analysis of recovered cells (n=17)

phenotypically stable regulatory T cells with mAbs and Fab Multimers, a number of cells recovered is substantially higher if the cells were isolated using Fab multimers and subsequently liberated from isolation reagents.

7.2.3. Co-transfer of “untouched” Tregs and “isolated reagent freed” Tregs

To test if Fab multimer-isolated Tregs perform upon adoptive transfer comparable to cells, which never came into contact with isolation reagents, we used the DEREK mouse model (Lahl et al., 2007). DEREK mice express a diphtheria toxin (DT) receptor -enhanced green fluorescent protein (eGFP) fusion protein under the control of the FOXP3 promoter (Lahl et al., 2007). This setup allows selective *in vivo* ablation of regulatory T cells by DT treatment, but also the detection of Tregs by the expression of eGFP and without additional surface staining. We sorted Tregs using either eGFP positive cells or Fab multimers (CD4/CD25) and injected a 1:1 solution into recipient mice. After one week we sacrificed the mice and analyzed spleens for recovery of both populations (Figure 20A). We found that GFP-sorted and CD4positive and CD25high Fab multimer-sorted Tregs engraft with the same frequency (Figure

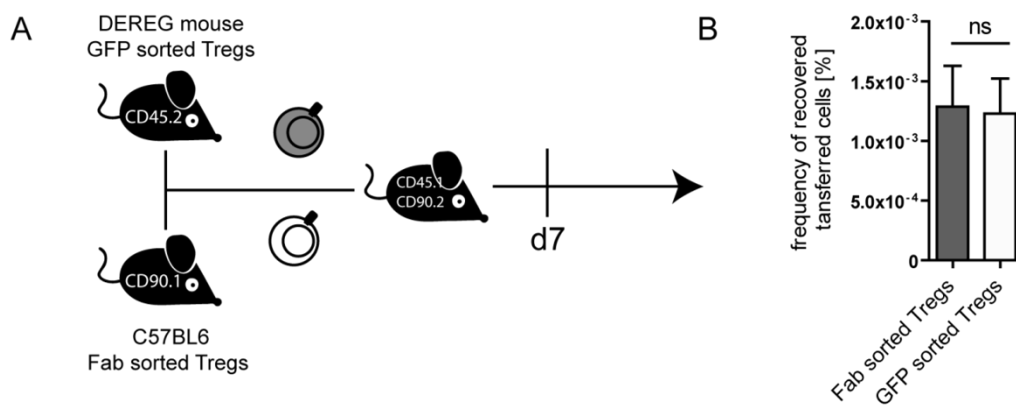


Figure 20. Co-Transfer of GFP sorted and Fab multimer sorted Tregs **A)** A 1:1 mixture from 20.000 congenically marked Tregs either sorted on GFP (DEREG mouse) or Fab multimers was injected into a CD45./CD90.2 expressing recipient mouse. The recipient mice were analyzed on day 7 after cell transfer. **B)** Bar graph of the frequency of recovered cells n=4, t test; Experiment is representative for two experiments. Statistical analysis was done using GraphPad Prism software

20B), providing strong evidence that Fab multimer-sorted cells have indeed the same engraftment capability as “never-stained” cells. As in this setup, the cells had been sorted based on different markers (DEREG: Foxp3 – C57BL/6 CD90.1: CD4/CD25), we thought of an additional experimental system in which truly the engraftment of the same population could be observed. Therefore, we injected 1:1 solutions of bulk cells with never stained (CD45.1 donor) or cell that had been exposed to Fab multimers (CD4 STAPC/CD25 STPE) or mAbs (CD4 APC/CD25 PE) and subsequent D-Biotin washing (Figure 21A). To analyze the recovery of transferred cells, we first gated on CD4 and CD25 double positive cells and then searched for the congenically marked cells. Never stained/“untouched” and reversibly Fab multimer stained cells engrafted with the same frequency into recipient mice. In sharp contrast and in line with what we observed before, Treg cells still bearing monoclonal antibodies as isolation reagents

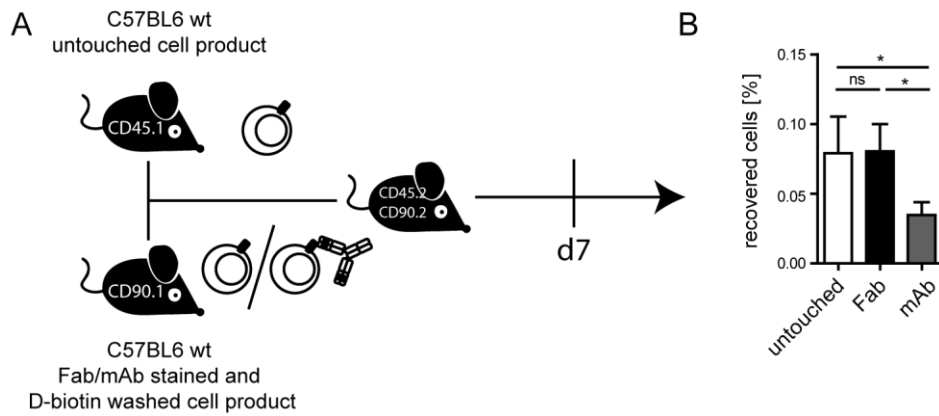


Figure 21. Co-Transfer of GFP sorted and Fab multimer sorted Tregs **A)** A 1:1 mixture from 20.000 congenically marked Tregs either sorted on GFP (DEREG mouse) or Fab multimers was injected into a CD45./CD90.2 expressing recipient mouse. The recipient mice were analyzed on day 7 after cell transfer. **B)** Bar graph of the frequency of recovered cells n=4, t test; Experiment is representative for two experiments. Statistical analysis was done using GraphPad Prism software

on the cell surface showed significantly reduced engraftment (Figure 21B). Taken together these data demonstrate that the engraftment of Fab multimer stained cells is not impaired after removal of the staining reagent when compared to either never-stained or eGFP sorted cells, whereas the engraftment of mAb-labeled cells is significantly reduced.

7.2.4. Why do Fab multimer-sorted Treg cells engraft better than mAb -sorted cells?

To test how the differences in engraftment capabilities between Fab multimer- and mAb-isolated cells are generated, we first modified our model and changed the recipient to Rag2 (recombinase activating gene 2), common γ -chain double knockout ($Rag2^{-/-}c\gamma c^{-/-}$) mice. This recipient lacks natural killer (NK) cells, T and B cells. There are some residual CD45 low cells detectable, which are of the macrophage/monocyte lineage, but even these cells are known to be severely altered in their development and functional characteristics due to the lack of functional IL-2, IL-4, IL-7, IL-9, and IL-15 receptors. This heavily immunocompromised mouse model is often used for transplantation and xenograft studies, as there are only very minor residual immune functions remaining. Using $Rag2^{-/-}$ common γ -chain $^{-/-}$ mice we wanted to examine whether Fab multimer- and mAb-sorted cells would be able to engraft and homeostatically proliferate similarly if the host is strongly immunocompromised. Analysis of engraftment showed that in comparison to the wildtype control mice, the engraftment of Treg cells in spleen, lung and bone marrow was not significantly different in $Rag2^{-/-}c\gamma c^{-/-}$ mice, but still showed a clear trend of better engraftment of Fab multimer-sorted cells (Figure 22). Due to their high immunodeficiency, $Rag2^{-/-}c\gamma c^{-/-}$ mice do not have detectable lymph nodes, so only data for the recovery from wt mice is shown this organ. In summary, these data indicate that in the absence of adaptive immunity and under conditions that have very limited immune-surveillance and strong signals for homeostatically proliferation, the difference in engraftment between Fab multimer- and mAb- sorted cells is still maintained, hinting towards an involvement of innate immune factors. As described in the introduction (5.2.7.), several ways

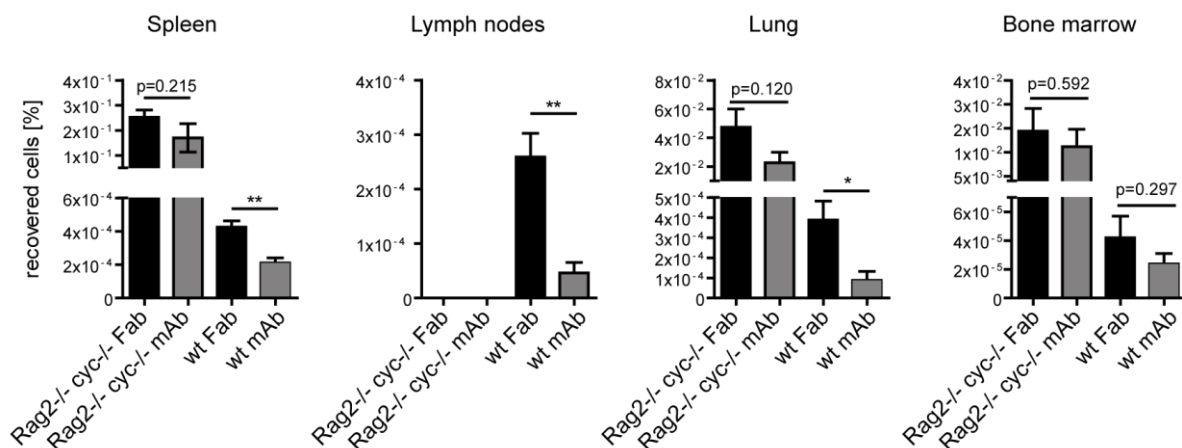


Figure 22. Engraftment of Tregs into $Rag2^{-/-}c\gamma c^{-/-}$ mice. Treg cells were isolated from congenically marked hosts either using Fab multimers or mAbs and a 1:1 solution of cells was transferred into $Rag2^{-/-}c\gamma c^{-/-}$ or wt mice. We measured recovery of transferred cells 3 weeks after cell transfer in different organs. n=7; t-test statistical analysis was done using GraphPad Prism

how antibodies can influence cells have been described in the literature. For example, antibodies can induce the complement system, activating C1q and leading to the activation of several effector mechanisms, or antibodies can activate effector cells directly via Fc Receptors. Therefore, we wanted to investigate the role of the complement system in diminishing the engraftment capability of mAb-sorted cells.

7.2.5. The role of the complement system in the depletion of mAb labeled Tregs

In vitro deposition of C3 on the cell surface

To investigate the role of complement activation we used an established complement deposition assay (AG Verschoor – Steven Broadly). In this assay, the deposition of C3 on the

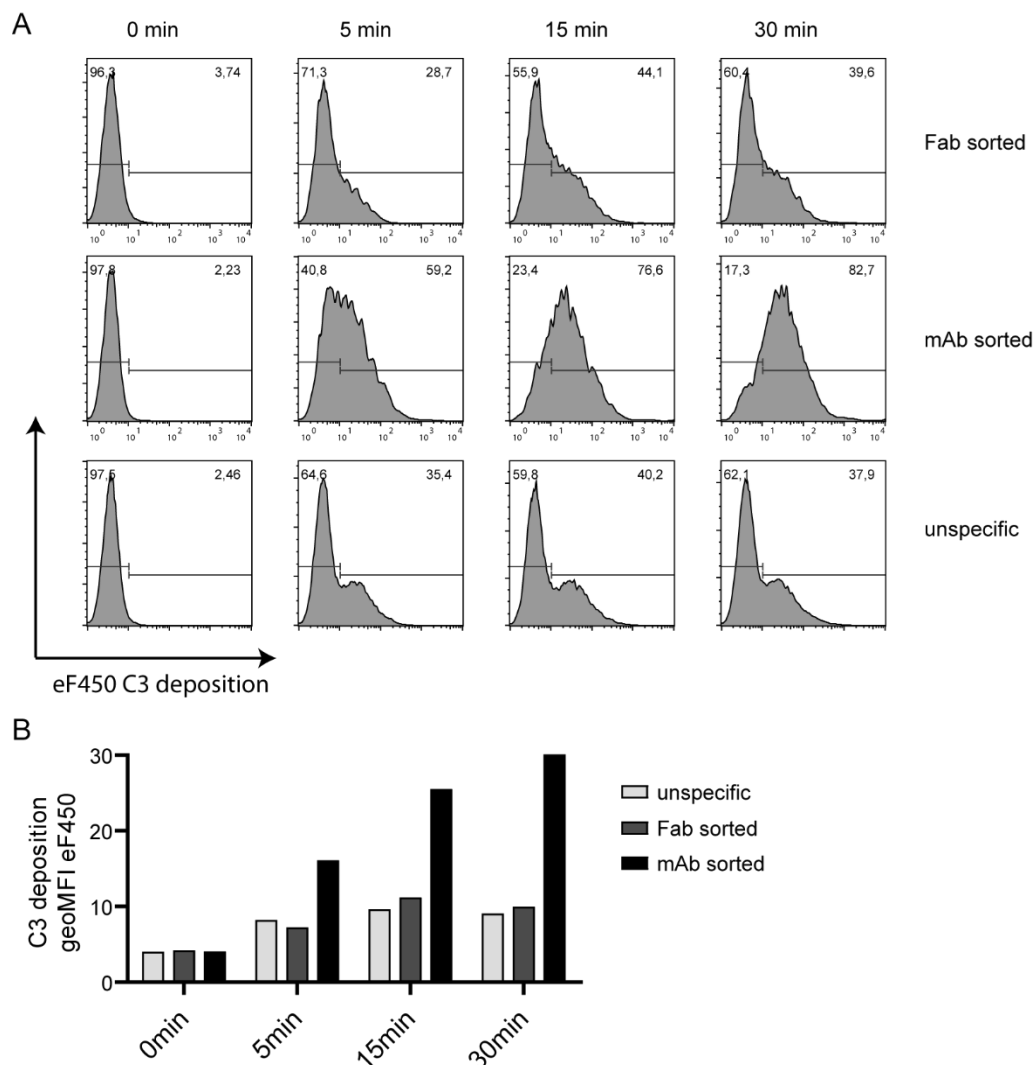


Figure 23. *in vitro* deposition of C3 on the cell surface of Tregs: A,B cells were isolated on a flow cytometer using either Fab multimer or mAb staining and after removal of Fab multimers from the cell surface cultivated for the indicated time periods in freshly prepared blood serum of C57BL/6 mice. C3 deposition was measured using a C3 specific antibody labeled with eF450 dye. A) Exemplary FACS blots showing C3 deposition at indicated time points. B) Staining intensity of C3 deposition was measured and the geoMean of fluorescence was plotted;

cell surface after getting in contact with mouse serum is measured. We performed a kinetic experiment measuring the C3 deposition 5, 15 and 30 minutes after sorted cells are re-suspended in freshly acquired C57Bl/6 wt serum. We found that approximately on one third of the cells there was mAb-unrelated deposition of C3 on the cell surface of never-stained cells (Figure 23 A), although these were only quite little amounts of C3 (Figure 23 B). Similar to this, little deposition was measured on cells, which had been isolated with Fab multimers and freed from staining reagents afterwards (Figure 23 A, B). In contrast to the other samples, mAb-sorted cells showed strong accumulation of C3 on the cell surface over the first 30 minutes after being cultivated *in vitro* with mouse serum, both in a number of cells covered with C3 and the amount of C3 on the cell surface (Figure 23 A, B). Based on these findings we suspected that complement-mediated cell death early after cell transfer might be a key player in the lowered engraftment capability of mAb-sorted Tregs and set out to analyze this in *in vivo* knockout models.

Engraftment of mAb and Fab Multimer sorted Tregs in C3 deficient mice

To test, if complement activation indeed is a critical player in the lowered engraftment capability of mAb-sorted Tregs, we transferred 20.000 congenically distinguishable Fab multimer-sorted or mAb-sorted Tregs into wildtype or C3^{-/-} mice. The formation of C3 convertase activity is crucial for the activation of the complement pathway, leading to the production of the primary effector molecules and uniting the three distinct complement activation pathways (Tomlinson, 1993). Our *in vitro* data already demonstrated increased C3 deposition on the cell surface of mAb-sorted Tregs, so we expected the difference between Fab Multimer- and mAb-sorted Treg populations to be reduced or gone when we transferred cells into C3^{-/-} mice. However, when we determined the recovery after three weeks, we found that in contrast to our expectations there was still a significant difference in the size of Fab Multimer- and mAb-sorted populations. This difference was detectable on the frequency level as well as on the total population size in the spleen (Figure 24 A, D). The same observation was made when analyzing the frequency and total cell number of recovered cells in the lymph nodes (Figure 24 G; J). We further found that Tregs isolated with Fab Multimers were somewhat increased in recipient mice when these mice lack C3 (Figure 24 B, E, H, K). This finding could not be explained so far and might hint towards an enhanced proliferation of transferred cells. When calculating the fold-change from mAb-sorted to Fab Multimer-sorted cells, we found that in both recipients the same fold change was observed (Figure 24 C, F, I, L). This finding was also in line with our previous findings describing a two-fold increase in cell number. The data demonstrate that while antibodies increase the amount of C3 deposition on the cell surface, the complement driven pathway of immune-mediated antibody-dependent cytotoxicity does not play a significant role in the reduced engraftment capability of mAb-isolated Tregs. The second major pathway activated by surface-bound antibodies is the cellular cytotoxicity (ADCC). Therefore, we next set out to investigate if ADCC plays a role in the diminished engraftment numbers of mAb sorted Tregs.

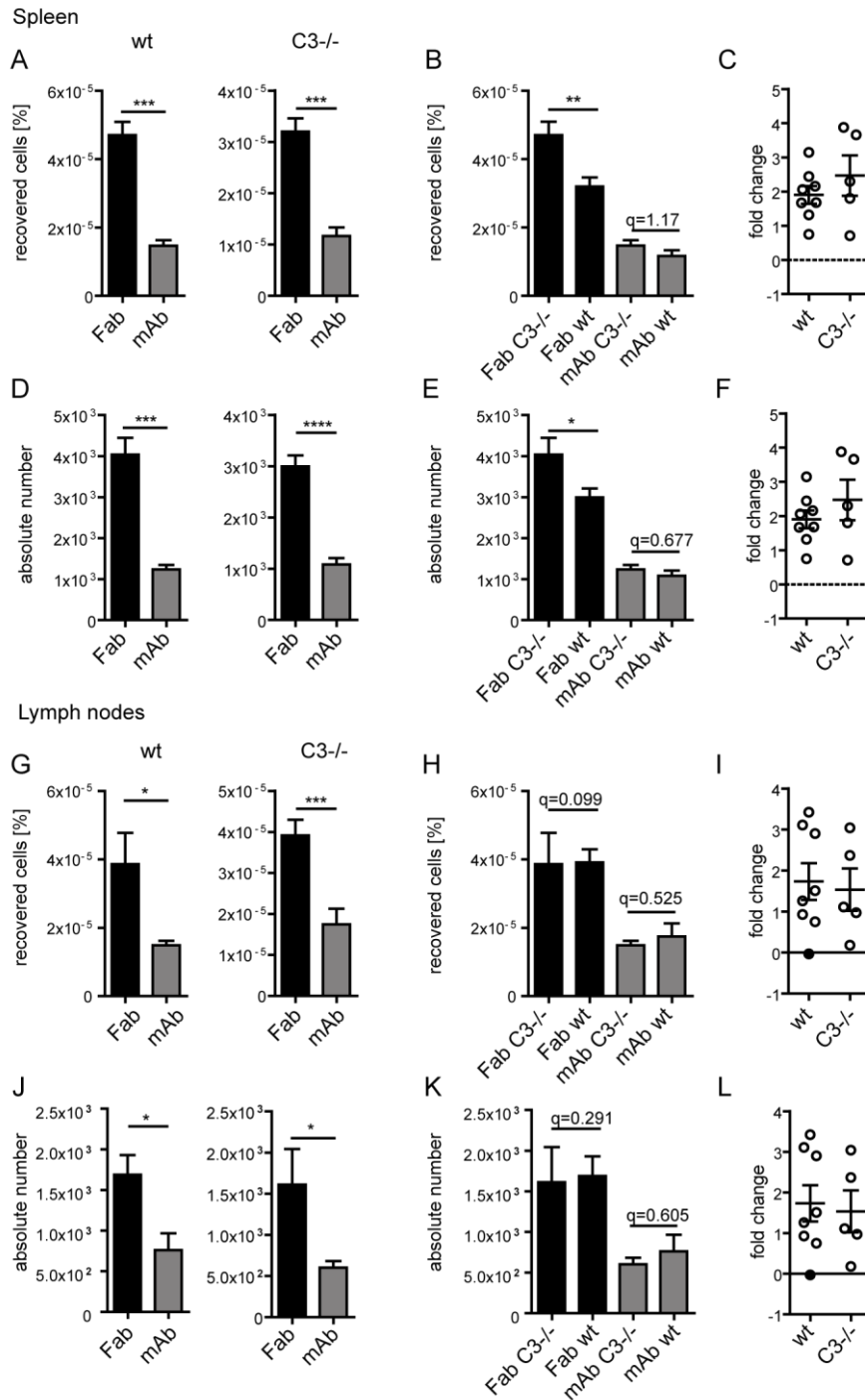


Figure 24. Transfer of Fab multimer- and mAb-sorted Tregs into C3^{-/-} mice: A-L 1:1 solution of congenically marked Fab multimer and mAb sorted cells were transferred into C3^{-/-} or wt recipient mice and looked for recovery after 3 weeks: A-F) in spleen A) frequency B) frequency comparing wt and C3^{-/-} C) fold change on frequency level D) absolute number of recovered cells E) absolute number comparing wt and ^{-/-} F) fold change on absolute number levels G-L) in lymph nodes G) frequency H) frequency comparing wt and C3^{-/-} I) fold change on frequency level J) absolute number of recovered cells K) absolute number comparing wt and ^{-/-} L) fold change on absolute number levels; n=8 t-test all statistics with GraphPad Prism; representative for two experiments

7.2.6. Antibody-dependent cell-mediated cytotoxicity as reason for diminished engraftment of mAb labeled cells

Antibody-dependent cell-mediated cytotoxicity (ADCC) is the second central effector mechanism described to be elicited by surface-bound antibodies. In ADCC, effector immune cells attack targets whose surface antigens have been marked by antibodies. Main effector cells of ADCC are natural killer (NK) cells; but macrophages, neutrophils, and eosinophils have also been described to be important mediators of ADCC. After showing that complement-induced cytotoxicity has no or only a minor role in the reduced engraftment of mAb-sorted Tregs, we investigated the influence of Fc γ Receptor-positive effector immune cells on the engraftment of mAb-marked Tregs. In mice, the Fc γ receptors (Fc γ R) are the primary mediator of ADCC. Therefore, we used mice with a knock-out for the Fc γ R subdomain, knocking out the Fc γ receptors Fc γ R I (pairing with CD64), Fc γ R III (pairing with CD16), Fc γ R IV (pairing with CD16-2) and Fc ϵ RI and a knock-out for Fc γ RII (CD32), which does not require the Fc γ R subpart to be surface exposed. Fc ϵ RI is a high-affinity receptor found on epidermal Langerhans cells, eosinophils, mast cells and basophils (Teillaud, 2012). The Fc γ Rs are the most critical Fc receptors for inducing phagocytosis of opsonized targets and also induce efficient killing of targets.

To analyze whether knock-out of Fc γ R would alter the engraftment of mAb- or Fab-sorted cells and maybe diminish the difference in engraftment capability, we utilized our already established transfer model. As shown in Figure 25, the recovery of transferred Tregs cells after 3 weeks was independent of the isolation reagent used (Figure 25A), strongly

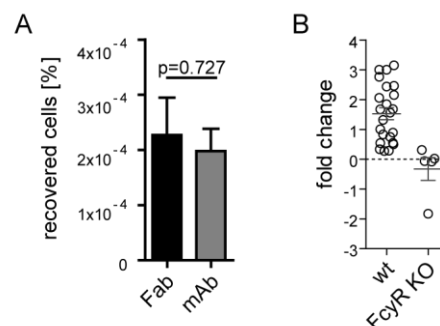


Figure 25. Transfer of Fab multimer- and mAb-sorted Tregs into Fc γ R^{-/-} mice. A 1:1 solution of 20.000 Tregs was i.v. injected into recipient mice and recovery was checked after 3 weeks. A) Frequency of recovered Treg cells n=5 B) Fold change between mAb and Fab Multimer sorted Tregs

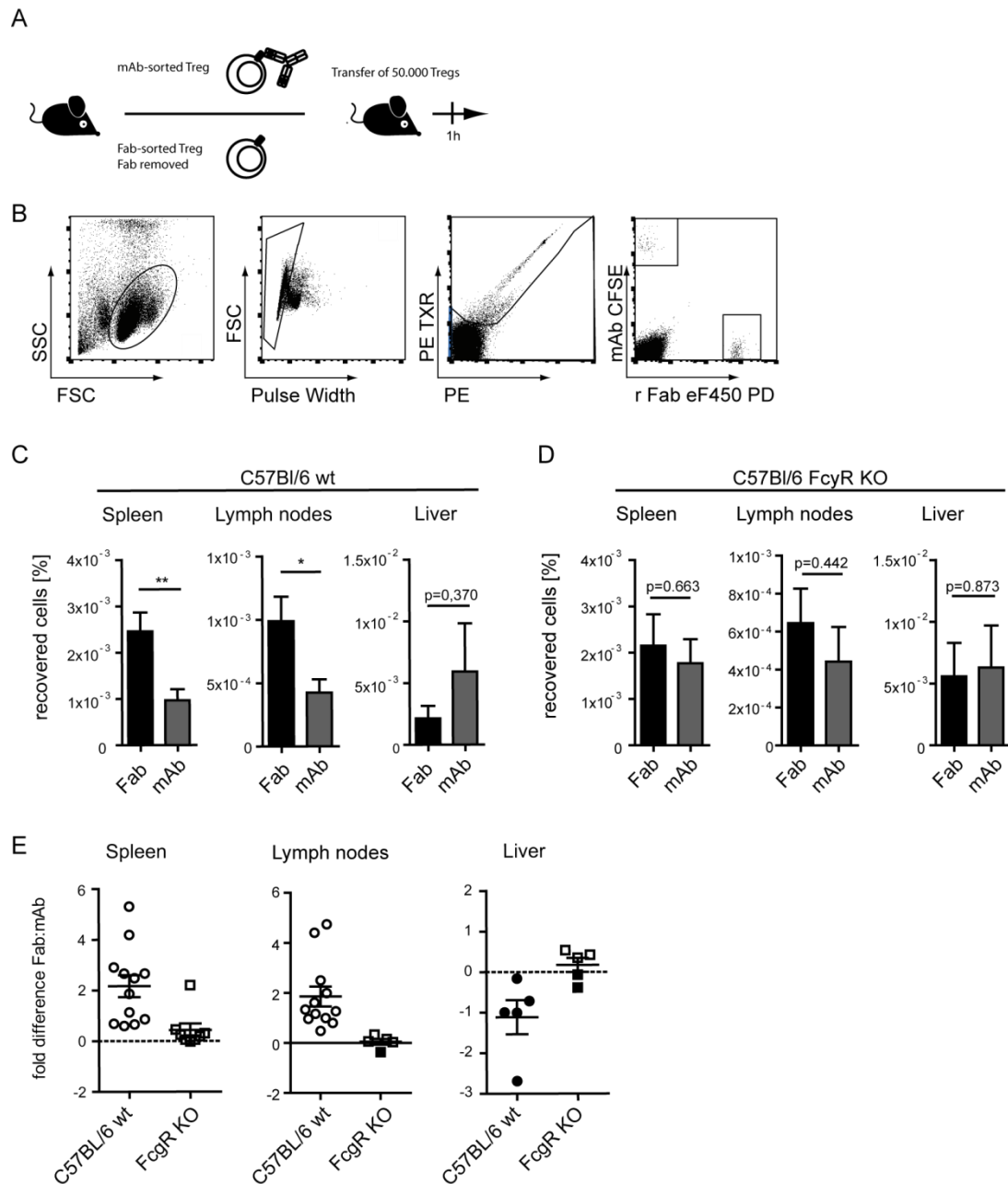


Figure 26. Early recovery of transferred Tregs 1 hour after transfer A-D) 100,000 cells of a 1:1 mixture of proliferation dye marked (CFSE; eF450PD; eF670 PD) Fab and mAb sorted Tregs population were injected into recipient mice. After 1 hour the recipient mice were sacrificed and different organs were analyzed. **A)** exemplary gating strategy to recover transferred Treg cells **B)** frequency of the recovered transferred cells after transfer into C57Bl/6 wt mice in spleen (n=12) and liver (n=6) (pooled from 4 Experiments; One-Way Anova with Dunnetts Posttest) **C)** Frequency of recovered cells after adoptive co-transfer into FcγR KO mice in spleen (n=9) and liver (n=6) **D)** fold change for individual mice red filled circles more mAb than Fab sorted cells; empty circles more Fab than mAb sorted cells; red filled circle more mAb than Fab sorted cells recovered; all statistics was done using GraphPad Prism; t test *p=0.5; ** p=0.1)

suggesting that the interaction of the Fc part of the antibody and endogenous Fc receptor-bearing cells is the driving force of the diminished engraftment capability of mAb-isolated Treg cells. Furthermore, we did not detect any ‘fold change’ in individual mice (Figure 25B). To further confirm this finding, we changed our transfer protocol as Fc-dependent mechanisms are

described to be very rapid occurring cellular responses. We marked Fab multimer- and mAb-sorted cells with proliferation dyes (PD) after sorting and transferred them into wt recipient mice (Figure 26A). Subsequent determination of recovered cell frequencies at a very early time point after adoptive transfer (1h) revealed a clear distinction between the transferred populations and to the endogenous cells (Figure 26B). One hour after transfer the frequencies of mAb-sorted cells in wild-type mice were already significantly reduced in spleen and lymph nodes, but interestingly slightly elevated in the liver (Figure 26C), showing that the difference in engraftment capability of Fab Multimer- and mAb-isolated Treg grafts is indeed established very early. The antibody clone PC 61 has been described to mediate trapping and killing of Tregs by Fc- γ -receptor (Fc γ R) after injection *in vivo* (Setiady et al., 2010). To test experimentally if the rapidly occurring differences shown in Figure 25C are caused by the Fc part of the parental antibody, we transferred both populations into Fc γ R KO mice. Moreover, as shown in Figure 24, at a later time point we could not find differences in recovered population sizes in Fc γ R KO mice in spleen and lymph nodes (Figure 26D). Calculation of the fold change between Fab multimer- and mAb-sorted cells revealed that transfer in wildtype C57BL/6 resulted in 2 fold higher frequencies of Fab multimer-sorted cells in spleen and lymph nodes and one-fold higher frequency of mAb sorted cells in the liver whereas there was no change observed in the Fc γ R KO mice (Figure 26E). These data demonstrate that rapid clearing of Tregs isolated with mAb-based isolation reagents on the surface is mediated to a large extent by Fc γ R-mediated mechanisms.

7.2.7. Fab removed to Fab non-removed

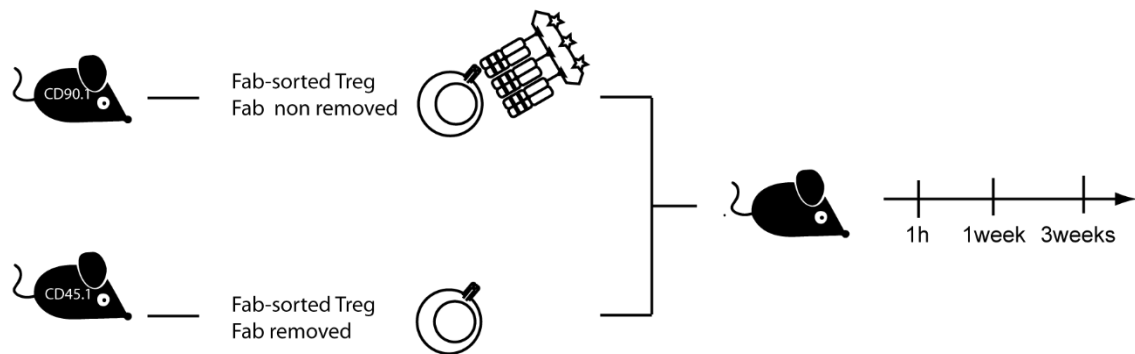


Figure 27. Schematic experimental setup: Can the recovery of cell subsets be affected by other isolation reagents despite mAbs as well. Co-transfer of either 100.000 (1 hour measurement) or 20.000 (1 week & 5 week measurement) congenically marked Fab multimer isolated Tregs. One group washed in D-biotin after isolation, whereas the other group was washed in FACS buffer. A 1:1 solution of both cell populations was transferred into recipient mice. Recipient mice were analyzed 1 hour, 1week or three weeks after cell transfer.

Besides the early Fc γ R-mediated influence of Treg recovery, we wanted to test whether long-term recovery could also be affected by additional mechanisms of cell label interference. To test this experimentally, we transferred Fab multimer-sorted Tregs either with non-removed or removed Fab multimers into wt recipients and analyzed Treg recovery after 1 hour, one week and five weeks (Figure 27). We sorted single living Treg cells, as depicted in Figure 27. After the sorting, one sample was washed in FACS buffer containing 1mM D-biotin whereas the other sample was washed in FACS buffer without D-Biotin. The sort purity was high in both samples (Figure 28). With this enrichment strategy, we had two congenically distinct cell populations, one still carrying the sorting reagent without Fc part on the cell surface, and the other one as a label-free population. With this setup, we investigated the influence of labeling reagents besides the Fc part-mediated effects described earlier. A 1:1 solution of both cell

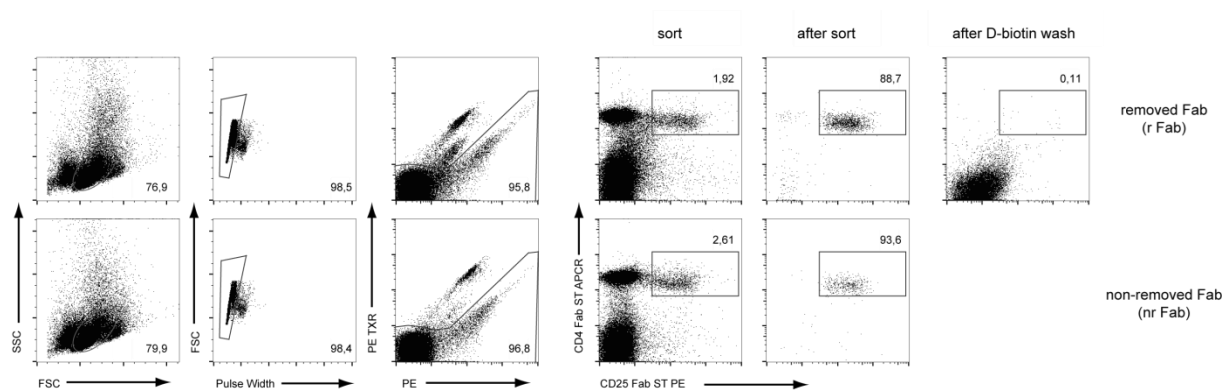


Figure 28. Sorting strategy for label free and Fc-free labeled cells. Cells were pregated on single living lymphocytes. The sort gate was set on CD4 APC CD25-PE double positive cells. Purity control and sorting were performed on the Moflo Legacy.

populations was injected into C57BL/6 mice. As shown in Figure 29A, removal of Fab multimers had no additional effect on Treg recovery 1 hour after adoptive transfer when compared to non-removed Fab multimers. In contrast to the early reduction observed when Tregs still bear mAbs on the cell surface, remaining Fab multimers do not lead to rapid decrease in cell number. However, at later time points removal of Fab Multimers led to significantly enhanced Treg recoveries both after one and five weeks in the spleen (Figure 29A). Additional analysis of the lymph nodes revealed the same phenotype. While after 1 hour no difference in numbers of recovered Tregs was observed, a clear difference was visible after one week (Figure 29B). The fold change from non-removed Fab to removed Fab increased from none after one hour to ~1x after one week and stayed stable until week five in spleen (Figure 29C) and lymph nodes (Figure 29D), indicating an influence of remaining staining reagents on cell engraftment within the first week independent of Fc recognition. This difference does not increase over time, indicating that both cell populations have the same capacity to maintain themselves after surviving the initial phase of the adoptive transfer (Figure 29C). We speculated that this effect could be mediated via blocking of IL2 signaling by the isolation reagents on the cell surface.

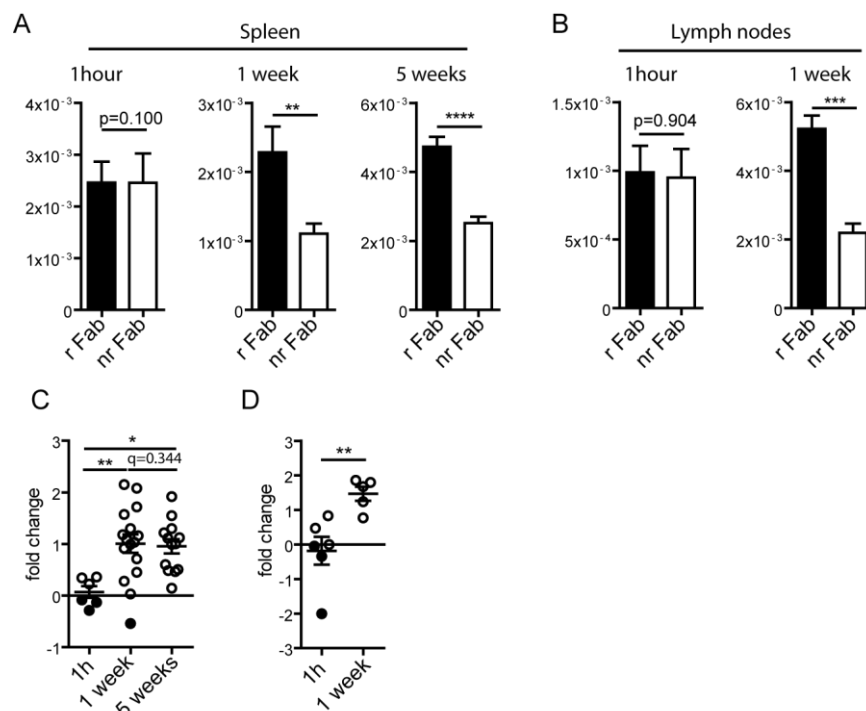


Figure 29. Removal of Fab multimers from the cell surface is important A) 1 hour 100.000 cells of a 1:1 mixture of proliferation dye marked (alternating; CFSE – ef450PD – eF670 PE) D-biotin treated Fab sorted (r Fab) and non-D-biotin treated Fab sorted (nr Fab) Tregs population were injected into recipient mice. After 1 hour the recipient mice were sacrificed and the spleen was analyzed. (t test) 1/5 weeks 40.000 cells of a 1:1 solution of congenically marked r Fab or nr Fab Tregs were injected into recipient wt C57BL/6 mice and recovery of both groups was checked after one (n=16) and five (n=12) weeks (t test) C) Fold change of recovered Tregs within one mouse 1 hour, one week and 5 weeks (One way Anova with Dunetts Post test)

We had already established an assay to measure STAT5 phosphorylation of Tregs in our lab (Mohr, 2012). To test if the IL2 induced signaling of labeled cells or freed cells was different, we stimulated Tregs for 15 minutes at 37°C with 50µg IL2. Subsequently, we performed western blot analysis and stained for the phosphorylation of STAT5, the primary signaling molecule in the IL2 pathway (Malek, 2008). We found while IL2 signaling was blocked by the addition of αCD25 antibody (clone: PC61) neither the addition of monomeric or multimeric Fab did abrogate the IL2 signaling completely (Figure 30 left panel). Washing with D-biotin led only to minor changes in the IL2 signaling (Figure 30). To test if these small changes could be responsible for the changes seen *in vivo* (Figure 29), we investigated the *in vitro* proliferation of Tregs induced by IL2. We isolated Tregs with Fab multimers, split them into removed and non-removed groups and analyzed for *in vitro* CFSE dilution at day 4. As summarized in Figure 31, both groups proliferated slowly, but the removal of staining reagents

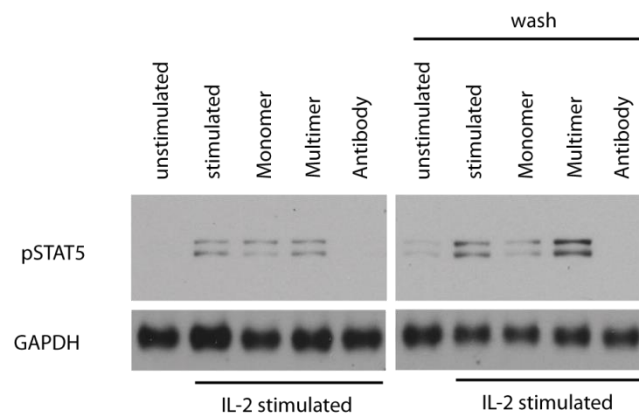


Figure 30. Intracellular IL2 signaling 5×10^6 cells were stained with the standard staining protocol and transferred in a 96-well flat bottom plate. For Fab-multimer and Antibody wash fractions 1.5×10^7 cells were stained and washed according to standard staining and D-biotin removal protocol. 5×10^6 cells were transferred to the 96-well flat bottom plate. All cells were incubated for 30 minutes at 37°C and afterwards stimulated with 50U IL-2 for 15 minutes. After stimulation cells were lysed and Blotted as described in material part.

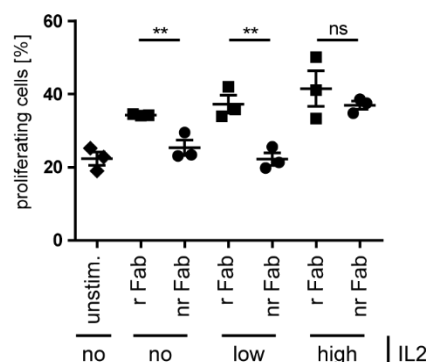


Figure 31. *In vitro* proliferation of r Fab and nr Fab sorted Tregs. Different doses of IL-2 were added to the cell culture and CFSE dilution was measured. (t test; exemplary for 3 independent experiments) statistical analysis as indicated was done using GraphPad Prism software; *p=0.5; ** p=0.1; ***p=0.01

led to a significantly increased proliferation rate of Tregs after treatment with low dosages of IL-2. High dose IL-2 treatment could overcome this proliferative disadvantage *in vitro*. These results indicate that remaining surface bound Fab multimers might also block the IL-2 receptor and thereby affect cell survival and/or proliferation of labeled Tregs.

In summary, we established that Fc γ -receptor-mediated killing of Tregs initially diminished the engraftment capability of labeled Tregs when compared to label-free Tregs, but that also other effects, like the blockage of IL2 signaling, can further alter the engraftment of cells. However, whether these strong effects are also relevant for the functionality of Treg grafts has so far not been shown. Therefore, we next wanted to examine whether label-removed Tregs would also have a superior function when compared to selection-reagent bearing cells.

7.3. Functionality of Fab Multimer isolated Tregs

After having shown that remaining isolation reagents on the cell surface can have tremendous effects on the engraftment capability, we wanted to investigate if remaining staining reagents have a detectable influence on the functional capability of Treg grafts. For this purpose, we first decided to determine the *in vitro* functionality of Tregs either isolated by Fab multimers or mAbs.

7.3.1. *In vitro* functionality

To determine the *in vitro* functionality of Tregs, we sorted CD8 effector T cells based on CD8 expression into a CD3/CD28 pre-coated 96 well plate and titrated either Fab multimer- or mAb-sorted Tregs into the assay. We observed that stimulated Teffs proliferated vigorously until day three in the absence of Tregs. The addition of either Fab multimer- or mAb-sorted Tregs at a ratio of 1:1 led to drastically reduced proliferation (Figure 32 left panel). However, we did not observe a difference in reduction of proliferation when comparing Fab multimer- and mAb-sorted cells. When lowering the amount of Tregs used in the assay to a Teff to Treg ratio of 4:1, we observed still a significant reduction of proliferation after addition of either Fab multimer- or mAb-sorted Tregs, but there was a significantly higher reduction of proliferation in the presence of Fab multimer-sorted cells. This hints towards an improved suppressive capability of Fab multimer isolated cells (Figure 32 right panel). To test both isolation methods in a clinically relevant system, we next tested differently isolated Tregs in an already established mouse model of acute graft-versus-host disease.

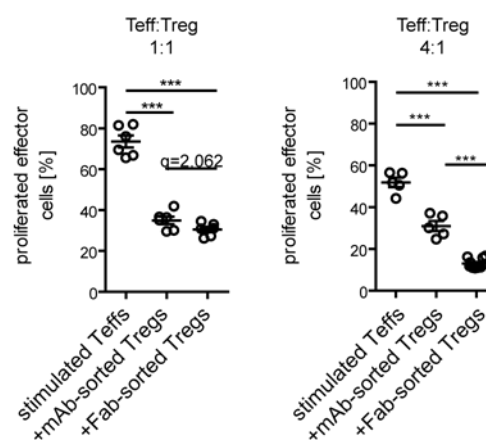


Figure 32. *In vitro* Treg suppression Assay: Proliferation of CD3/28 stimulated effector cells (CD8+) was measured on day 4 after stimulation by measuring the CFSE dilution. Tregs were added at the indicated ratios. Statistical analysis as indicated was done using GraphPad Prism software; One-way Anova with Bonferroni posttest * $p=0.05$; ** $p=0.01$; *** $p=0.001$

7.3.2. *In vivo* functionality of Fab Multimer isolated Tregs

We utilized an established acute GvHD model (aGvHD) to test in a preclinical setting whether removal of staining reagents upon purification of Tregs affects the outcome of adoptive Treg therapy of aGvHD. Bone marrow (BM) and effector T cells (Teff) from C57BL/6 donor mice were injected into lethally irradiated BALB/C recipients. Subsequently, Fab multimer- or mAb-sorted Tregs grafts were transferred in different ratios (in relation to the number of transferred Teff) and survival and weight loss over time were monitored. We observed that the mice had a substantial irradiation-induced weight loss until day 7/8, but almost all mice recovered from the irradiation-induced weight loss till day 12/13. Mice receiving only bone marrow recovered well from irradiation caused weight loss. Starting from the recovery point, mice receiving Teff cells, but not receiving Tregs showed rapid weight loss. In line with the published literature, the transfer of Tregs at a Teff to Treg ratio of 1:1 led to reduced weight loss, both after transfer with Fab multimer- or mAb-sorted cells. However, whereas Fab multimer-sorted Tregs conferred a rapid recovery of weight and constant weight gain, the transfer of mAb-sorted Tregs only had a small effect, and most animals continued to lose weight over time (Figure 33A).

A further reduction of the total number of transferred regulatory T cells to a Teff to Treg ratio of 4:1 showed that it was not beneficial to transfer mAb-sorted Tregs at this ratio. In contrast, the transfer of Fab multimer-sorted Tregs had still a significant positive effect on the weight loss of recipient mice (Figure 33A). At a Treg to Teff ratio of 1:1, only 42.9% of all mice survived when treated with mAb-sorted Tregs, whereas 100% of all mice treated with Fab multimer-isolated Tregs survived (Figure 33B). Even under reduced conditions, when recipient animals were treated with a Treg to Teff ratio of only 1:4, 69.2% of all mice treated with Fab multimer-isolated Tregs survived whereas only 10% of all mice treated with mAb-sorted Tregs have survived until day 50 (Figure 33C). The in this thesis newly established isolation protocol using a double staining with two reversible Fab Multimer, FACS enrichment, and subsequent label removal appears to have clear *in vivo* advantages over currently used technologies for Treg isolation. We demonstrate that in a model of acute Graft versus Host disease these minimally manipulated regulatory T cell grafts have a superior *in vivo* potency when compared to conventional non-reversible mAb staining, allowing to detect therapeutic activity even at largely reduced input cell numbers.

As described earlier, human naturally occurring Tregs, like murine Tregs, are most commonly characterized by surface expression of CD4, CD25 and constitutive expression of Foxp3. In contrast to the mouse, the characterization of Tregs only by the surface markers CD4 and CD25 is often not sufficient to isolate pure Treg populations, leading to the necessity of

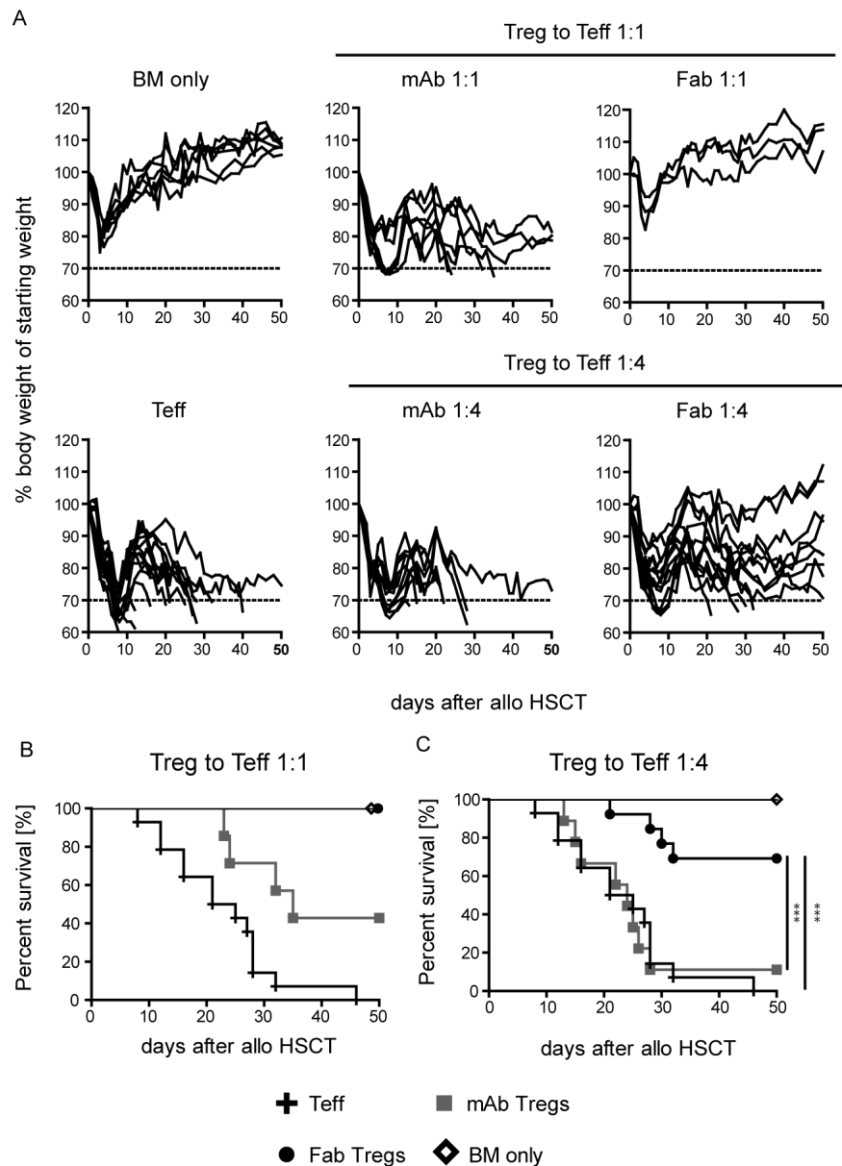


Figure 33. GvHD therapy using isolation reagent freed Tregs A-C) Recipient Balb/c mice were treated as indicated in the methods. Teffs, Fab multimer- and mAb-sorted Treg grafts were co-transferred at the indicated ratios. **A)** Changes in weight after cell transfer were monitored over 50 days. Each line represents a single mouse. **B)** Survival of mice receiving Tregs at Treg to Teff ratio of 1:1 **C)** Survival of mice receiving Tregs at Treg to Teff ratio of 1:4 Data was pooled from 3 independent experiments; Mantel Cox test; Statistic was performed using GraphPad Prism

having at least an additional third marker, further distinguishing Tregs from activated effector T cells. Our current protocol utilized the fact that double staining with two reversible Fab multimers is possible, but due to the lack of other backbone-dye combinations, a triple Fab multimer staining was so far not possible to perform. Therefore, we wanted to establish a setup where also triple Fab multimer labeling can be demonstrated.

7.4. Enrichment of Treg subpopulations using Fab multimers

To test the enrichment for three markers in our murine mouse model, we first had to define which additional marker to use. We decided to target the CD62L subpopulations, as Tregs being CD62L positive have been claimed to have enhanced protective capacity when compared to CD62L negative cells (Ermann et al., 2005). We isolated and expressed a Fab multimer targeting CD62L based on the mAb clone Mel-14 and mutated it successfully to stain cells reversible (Table 4) (Mohr, 2012). The mutated clone pM0306 was expressed well, stained very good and showed satisfying removal from the cell surface after washing with D-biotin. We, therefore, decided to use this clone for our triple enrichment approach. After re-expression of the clone pM306, we wanted to develop a suitable isolation protocol.

Plasmid name	Plasmid backbone	Mutation	Expression	Staining	removal
pM0300	cDNA	wt	Yes	Yes	No
pM0301	wt	91A1ight	Very weak	Yes	Yes
pM0302	wt	36Aheavy	Yes	Yes	No
pM0303	wt	108Aheavy	Yes	Yes	No
pM0304	pM0304	StrepTag C-Cys	Yes	Yes	No
pM0305	pM0304	P53Aheavy	Yes	Yes	No
pM0306	pM0304	Y36A1ight	Yes	Yes	Yes
pM0307	pM0304	P53Aheavy/Y36A1ight	Yes	weak	Yes

Table 4 α CD62L Fab mutants

Cell separation with magnetic particles is an important method used in laboratory and clinical practice to isolate cells. Our Lab already showed that serial magnetic enrichment using Streptactin coated paramagnetic beads can be used to separate distinct T cell subsets from human blood (Stemberger et al., 2012). We already developed a protocol making the enrichment of murine CD4 positive cells using Fab multimer in high purities (>90%) possible, but the obtained yields were very poor, as the paramagnetic beads coupled with Streptactin led to the formation of indispensable clusters of murine splenocytes. During this time the basis of the T-CATCH technology was developed by Herbert Stadler and Sabine Przybilla. This technique uses Streptactin-coated agarose beads as binding matrix and allowed the purification of human cell subsets. Due to their different size, we decided to try to use the agarose-bead based enrichment also for the murine cells.

7.4.1. Enrichment for three markers of murine Tregs using Fab multimers

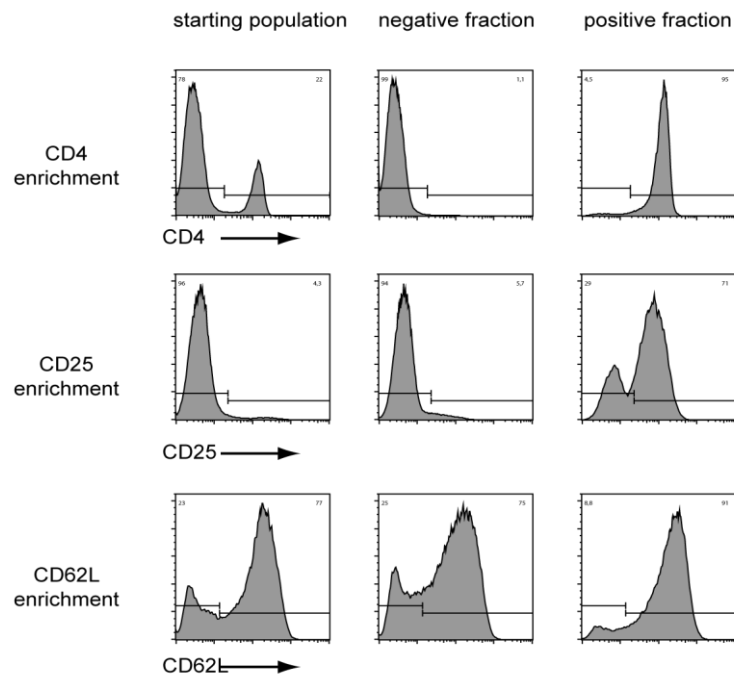


Figure 34. Representative FACS blots depicting single living lymphocytes before and after enrichment. Starting population shows the percentage of positive cells prior to enrichment. The negative fraction describes the flow through, showing how many cells are not binding to the agarose beads. Positive fraction shows the cell product after washing with D-biotin

We decided to utilize the T-CATCH technology as a pre-enrichment step. First, we adapted the isolation protocol used for human PBMCs for mouse lymphocytes, finding that additional washing steps and slower flow rate lead to increased purity and better yields. Further, we found that enrichment success was independent of erythrocyte lysis making direct isolation of Fab multimer-stained populations out single cell solutions possible. Next, we tested if the surface markers CD4, CD62L and CD25 are equally suited to be used in the pre-enrichment step. Enrichment with either CD25 or CD62L Fab multimers was successful (Figure 34), but in both cases the purity and the yield were low (Figure 34 & Figure 35). We speculated that the low affinity of the CD25 Fab might interfere with the enrichment success, similarly to what we already observed when using paramagnetic beads. The low yield of CD62L positive cells was most likely caused by the large amounts of cells being CD62L positive and the limited binding capacity of the 1000 μ l resin. The low purity might be caused by shedding of the molecule after enrichment. Shedding of CD62L by matrix metalloproteinases was already observed when enriching human cells. While CD62L and CD25 only were suboptimal for good pre-enrichment (CD25 purity: 48.38%; yield: 36.62%; CD62L purity 80.79%; yield: 69.69%) the usage of α CD4 Fab multimer in the agarose loaded tips proofed to be highly efficient. In 29 runs we obtained on average a purity of 92.94% and a yield of 80.55% (Figure 35). The pre-enrichment

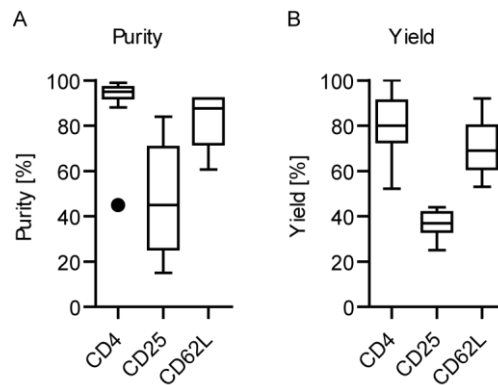


Figure 35. Cumulative enrichment data using enrichment columns: data showing enrichment purity and the yield of positive cells obtained by the enrichment. Box-Whisker Blot: Tukey; CD4 n=29; CD25 n=8; CD62L n=7

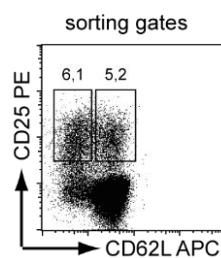


Figure 36. Sorting Gates for CD62Lhigh and low, CD25 positive cells. After CD4 enrichment using affinity columns Tregs cells were sorted based on CD25 staining using the α CD25 multimer coupled with ST-PE backbone and the α CD62L multimer coupled to ST-APC backbone on the Moflo Legacy. Cells were pre-gated on single, living lymphocytes (representative FACS plot)

using α CD4 Fab multimer-loaded tips allowed us to use the α CD25 and α CD62L Fab multimers for a double staining to isolate either CD62L low or CD62L high Treg subpopulations. As shown in Figure 35 simultaneous staining with both Fab multimers is possible and allows flow-cytometric sorting of CD25 positive and either CD62L low and high populations (Figure 36). To test if the label-free Treg subsets are still capable of engrafting into C57BL/6 hosts and to then track their behavior over time, we utilized the beforehand described engraftment model for Tregs established in our lab.

7.4.2. In vivo growth of CD62L high and low Fab, multimer sorted cells

To test if it is possible to isolate stable CD62L positive and negative subsets using Fab multimers and the two-step enrichment process described before, we isolated CD62L positive and negative subsets from congenically marked donor mice and injected a 1:1 ratio of both subsets into recipient C57BL/6 mice. We observed that both subsets were detectable after one week in similar frequencies. At week three the size of the CD62L negatively-sorted subset had grown substantially whereas the size of the CD62L⁺ subset stayed the same (Figure 37A). As we used the congenic marker to distinguish both populations this growth in population size

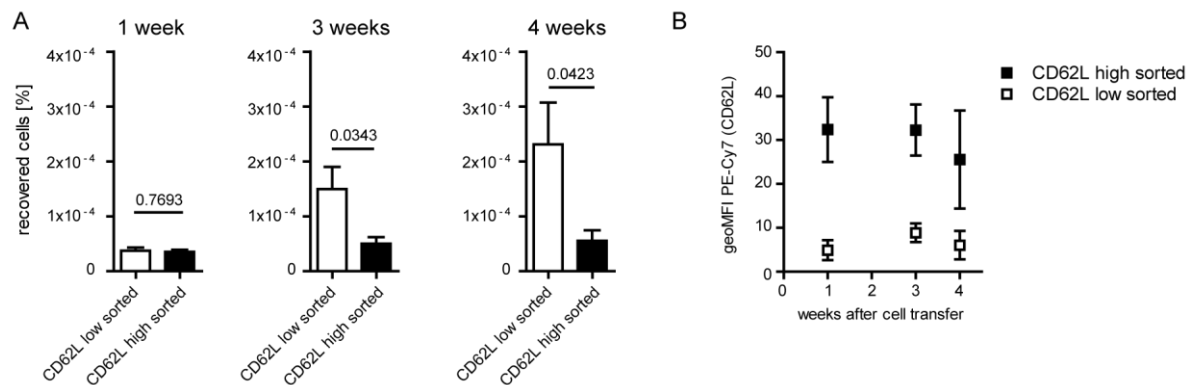


Figure 37. *In vivo* engraftment and growth of CD62L subpopulations. A 1:1 ratio of congenically marked CD62L^{high} and CD62L^{low}, Fab multimer sorted cells was injected into C57BL/6 wt recipient mice. A) Recovery of cell populations after one, three and four weeks are shown. B) Geometric mean fluorescence of recovered CD62L high and low populations is shown at week one, three and four. n=8 t-test, statistic was done using GraphPad Prism software data was combined from 3 individual experiments

cannot be explained by the replenishment of CD62L low cells from the CD62L high cell compartment, but instead is due to the homeostatic proliferation of the cell compartment. The growth of population size was also observed in week four after cell transfer (Figure 37A). Remarkably the population kept their CD62L high and respective low phenotype, at least until week four after cell transfer (Figure 37B), indicating that CD62L high and low Tregs might be stable subsets. These findings are in line with results of other groups showing that only the CD62L high regulatory T cells are protective in a setting of experimental acute GvHD (Ermann et al., 2005). These findings clearly show that also an enrichment of murine regulatory T cell subsets using Fab multimers is possible and feasible and further shows that CD62L high and low Tregs are stable under steady-state conditions for extended periods of time after adoptive cell transfer.

8. Discussion

The infusion of either freshly isolated or *ex vivo* expanded Tregs can improve survival of recipients in acute GVHD, but it is believed that large numbers of Tregs are required to achieve therapeutic effects (C. G. Brunstein et al., 2016; Claudio G Brunstein et al., 2011; Cohen et al., 2002; Mauro Di Ianni et al., 2011; Edinger et al., 2003; Edinger & Hoffmann, 2011; P. Hoffmann, Ermann, Edinger, Fathman, & Strober, 2002; Taylor et al., 2002). Due to the relatively low frequency of natural Tregs in circulation of only 1-2% of total CD4⁺ T cell population in adult humans (Baecher-Allan, Brown, Freeman, & Hafler, 2001) the purification of sufficiently large numbers of Tregs has been challenging or might not even been feasible in clinical practice without *in vitro* expansion (C. G. Brunstein et al., 2016; Claudio G Brunstein et al., 2011; M Di Ianni et al., 2009; Haase et al., 2015; Petra Hoffmann, Boeld, et al., 2006; Kleinewietfeld et al., 2009).

We hypothesized that isolation reagents remaining on the cell surface upon conventional cell enrichment technologies are diminishing the potency of the Treg graft, which would explain the non-physiologically high numbers of Tregs needed to control aGVHD. To test this hypothesis, we established a protocol, based on reversible Fab multimer staining, enabling the purification of Tregs and subsequent removal of isolation reagents in a one-step enrichment process. The obtained Treg population was in purity and subset composition not different from Tregs isolated with conventional non-reversible monoclonal antibodies. However, Fab multimer-isolated Tregs engrafted substantially better upon adoptive transfer into recipient mice. The substantial difference was reflected on the level of frequency as well as absolute cell numbers recovered upon various time points upon transfer and was mediated by Fc γ receptor-dependent as well as Fc γ receptor-independent effects triggered by isolation reagents remaining on the cell surface. The engraftment benefit translated into a more potent suppression of aGVHD by adoptively transferred Tregs in a preclinical mouse model. These data demonstrate a substantial benefit of entirely removing isolation reagents from the cell surface of Tregs. In order to get to this findings, we had to overcome several hurdles:

8.1. Choosing the right Fab Monomers

In previous work, we already generated and tested three murine Fab-fragments, an α CD4 Fab-fragment (parental mAb clone: GK1.5), an α CD25 Fab-fragment (parental mAb clone: PC61) and an α CD62L (parental mAb clone: MEL-14) (Mohr, 2012; Nikolaus, 2016). We were able to express Fab monomers for all three target molecules and could show specificity of the obtained Fab molecules. The removal of monomeric Fab-fragments using the D-biotin washing protocol followed by staining the cells with ST-PE showed that, while the wildtype

α CD4 Fab Monomers could be liberated entirely from the cell surface, the wildtype α CD62L and α CD25 Fab Monomers could not be washed away from the cell surface. Obviously, the binding affinity was despite the introduced mutation still too strong to support reversible cell staining. Therefore, we had to generate more mutants of wildtype α CD62L and α CD25 Fab monomers to search for Fabs that maintain the binding specificity of the parental antibody as multimer but dissociate from the surface upon monomerization. Fortunately, we found for both specificities a reversible and still specific mutant Fab molecule, making reversible multimer staining possible.

For fast isolation of highly pure Treg populations, we wanted to enrich murine CD4 positive and CD25 positive cells in an easy and quick manner using Fab multimers. In order to establish the one-step purification system, we first needed to establish a specific and as bright as possible Fab multimer staining that was still fully reversible. As the α CD4 Fab staining had already been optimized, we concentrated next on the α CD25 Fab. Several α CD25 mutants had previously been generated and successfully tested, but none was able to stain as bright as the parental mAb clone in our initial tests and also enrichment with paramagnetic beads was not possible, suggesting that the Fab mutant might have too low affinity for these applications (Mohr, 2012). For the generation of new mutants, we used cDNA from a different hybridoma PC61 (IgG1 λ antibodies against murine CD25) as starting material. We generated and screened multiple new mutants of the α CD25 Fab to check if we would find a better-suited candidate for our cell enrichment protocols. Unfortunately, most of the introduced mutations led to a loss of functionality, meaning that the Fab multimers were not able to bind the cell surface (Figure 5 & Table 1). We never observed any unspecific binding/staining but instead found that the generated Fab mutations were not binding at all (Figure 4; Table 1). This can be explained by the nature of the mutations introduced by us: we did not alter the antigen-recognizing region of the Fab but tried instead to allow more freedom in the backbone structure of the generated Fab molecules by replacing “bulky” amino acids through smaller ones (Bès et al., 2003; Stemberger et al., 2012).

We also tried to introduce a higher amount of refolding/binding flexibility in the protein by mutating the linker regions in-between the variable and the constant region of the Fab multimers. Three of the mutations led to proteins which were not able to be expressed in significant amounts in *E. coli* (Table 1 pM0509, pM0514, pM0515). These proteins are most likely toxic for *E. coli*, as we observed a drastic reduction in the OD600 values after induction of protein production, most likely caused by cell death of the protein expressing bacteria. When (re-)testing all newly generated and the already existing Fab multimers, we found that the Fab

monomers having a mutation at position 32 substituting a Tyrosine by an Alanine showed the best staining while still being fully reversible. When staining with Fab multimer for 20 minutes at 4°C, the staining brightness was weaker than the staining with the parental antibody. After we decided to use this clone, we wanted to check if prolonged staining time would lead to a brighter and still reversible staining. We found that extending the staining time to 40 minutes did indeed improve the brightness significantly (Figure 6). This improvement cannot be seen when using the parental monoclonal antibody and is most likely due to the low affinity of the α CD25 Fab pM0502. The more prolonged incubation time allows the less affine Fab multimer to accumulate further on the cell surface thereby increasing the staining brightness. We choose to proceed with the wt α CD4 Fab and the pM0502 α CD25 Fab mutant and producing large batches of both. After re-checking the staining and reversibility to exclude batch to batch variations (Figure 7), we went on to better define this Fab Monomers.

8.2. Defining the of the Fab Monomers using a flow-based k_{off} rate assay

As the removal of monomeric Fab molecules is the key component of our enrichment protocol, we needed to demonstrate efficient removal of the single Fab molecules from the cell surface. Our lab had previously developed an assay to quantify the half-life of single MHC Streptamers on the cell surface using a microscopic assay (Nauerth et al., 2013). Utilizing that assay, the affinity (better Koff rate) of the T cell receptor (TCR) bound by the MHC Streptamer can be analyzed. To do so, the monomeric MHC molecule had to be visualized on the cell surface. Therefore, a dye had to be coupled directly to the monomeric MHC molecule. During her Ph.D. thesis, Magdalena Nauerth identified three sites in the Streptag III region of the MHC molecule as potential dye coupling sites. One conjugation site in the GS-linker between MHC C-terminal end and the first Streptag II sequence (I), the second (II) between the two Streptag II sequences and the third (III) at the end of the Streptag II region. The dye conjugation sites were generated by insertion of a cysteine for conjugation sites I and II or a cysteine combined with a short GS linker for conjugation site III by mutagenesis PCR of the MHC vector. The dye-conjugation on-site III so far turned out to be the best in previous studies. For visualization of monomeric Fab molecules as well as to test the interaction time of Fab monomers and their target molecules we first tried to use the dye coupling site III. We mutated a cysteine into the Streptag III sequence of the murine α CD4 Fab and conjugated the fluorescent dye Alexa488 to it. We tested the staining with the STPE backbone and found that both the backbone and Alexa488 fluorescence were detectable by flow cytometry (Figure 8 Dye coupling to the α CD4 Fab Monomer. Overlay of uncoupled (dark grey histogram) and coupled (light grey histogram) Fab Monomers pregated on the STPE backbone staining. Alexa 488 was coupled to the

monomeric α CD4 Fab using maleimide chemistry (left side) and OG488 was coupled to Fab Monomers using NI-NTA chemistry (right side). While the obtained murine α CD4 Fab Multimers did show a staining for CD4 (Figure 8) the yield of protein production was meager. As correct folding of the monomeric Fab protein needs the cysteine bonds stabilizing the protein (Goto & Hamaguchi, 1982b, 1982a), the additional free cysteine introduced via mutagenesis PCR for dye coupling most likely interfered with the correct folding of the monomeric Fab, leading to nonsense protein clusters within the protein-producing *E. coli* bacteria. In order to circumvent this problem, we set out to introduce a new staining method for the monomeric Fab molecules. We found that adding a HIS tag sequence on the light chain of the Fab and using $N\alpha$, $N\alpha$ -bis(carboxymethyl)-L-lysine, Nickel(II) complex (NI-NTA) conjugated to OregonGreen488 led to bright staining of monomeric Fabs on the cell surface (Figure 8). NI-NTA is specific for polyhistidine tags with minimal cross-reactivity (Guignet et al., 2004). The yield of protein production was also way higher compared to the protein obtained using cysteine-based dye conjugation.

After labeling, the k_{off} rate of MHC molecules bound to surface-expressed TCRs can be monitored by real-time microscopy in a highly reliable manner on the single cell level (Nauerth et al., 2013). As for the Fab monomers, we were mainly interested in the k_{off} rate on a population level (and not for the k_{off} rate on a single cell basis), we established an assay to measure the k_{off} rate of Fab Monomers using flow cytometry (Figure 9). For this, we injected 2mM D-biotin for online measurement after 40 seconds to a Fab multimer-stained cell solution and recorded the staining intensity for 15 minutes. The online measurement during FACS analysis was already established by Matthias Schiemann to measure Ca^{2+} flux (Yu et al., 2005). This assay proved to produce similar results than the microscopic k_{off} rate measurement (Figure 11) and showed that mutants of monomeric Fab, shown before to have different affinities to the CD4 molecule (Figure 12) (Bès et al., 2003; Stemberger et al., 2012), also have different k_{off} rates from living cells. This data validated the flow-based k_{off} rate measurement on a population level to be a valuable tool for rapid k_{off} analysis. We found that the wt murine CD4 Fab had a relatively high k_{off} rate (half-life >100 sec.), whereas the pM0502 mutant of the CD25 Fab had a very fast k_{off} rate (under detection limit) (Table 2). This finding is in line with the enrichment and staining data, which already hinted towards a very low-affinity mutant Fab (Mohr, 2012). After establishment, the assay was also adapted to MHC-I Streptamers by Magdalena Nauerth, who further validated the findings that microscopic and flow based k_{off} rate assays lead to the same k_{off} rates (Nauerth et al., 2016). These data showed that the flow-based k_{off} rate assay could be a valuable tool for population-based affinity assessment. After characterizing the Fab

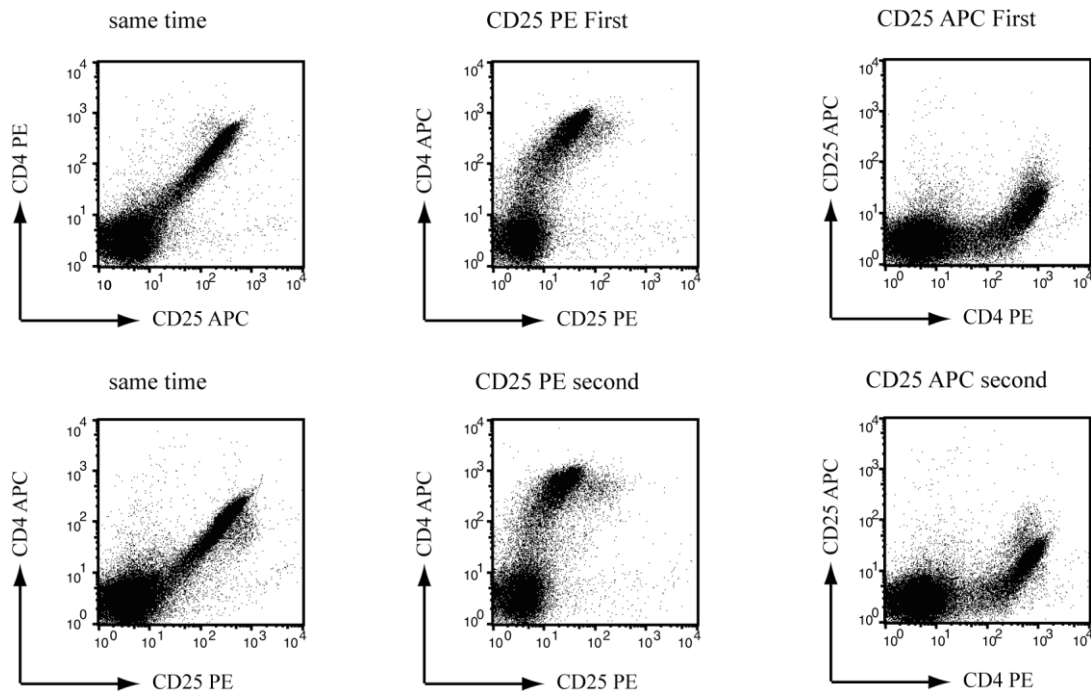


Figure 38. Isolation of regulatory T cells using Fab multimer double staining. The Fab multimers were used in the indicated order. 1st column both Fab multimers were used at the same time. In the following stainings both staining steps were separated by a washing step using FACS buffer. In the 2nd column the α CD25 Fab was coupled to the ST PE backbone and either used 1st (upper) or 2nd (lower). In the third column the α CD25 Fab was multimerized using STAPC backbone and either used 1st (upper) or 2nd (lower).

monomers, we wanted to combine the α CD25 and α CD4 Fab multimer staining to establish a protocol to stain them in parallel for rapid isolation of regulatory T cells.

8.3. Development of a double multimer staining

Combining the α CD25 and the α CD4 Fab multimer staining led to considerable problems. When using both pre-conjugated Fab multimers at the same time, we detected only double positive cells (Figure 38 left column). This could be explained by interchanging of α CD4 and α CD25 monomers generating chimeric α CD4/ α CD25 Fab multimers with either Streptactin PE or Streptactin APC backbones. The strong interchanging was not expected, but it might be that residual (unbound) monomeric Fab was binding to the wrong backbone. Additionally, it could be possible that the Streptactin backbones are not fully saturated, facilitating binding of free Fab monomers. To circumvent this problem, we combined the two surface stainings subsequently and not in parallel at the same time. This required two separate staining steps with one washing step in between. When analyzing our samples at the FACS analyzer, we still could detect interchanging and smearing of the Fab multimer staining (Figure 38 middle and right column), independent of which multimer was used first. This staining was considerably better than the co-staining at the same time, as less interchanging was observed, but still did not make sorting of Tregs possible. Therefore, we further optimized our staining protocol, finding that a

staining with α CD25 Fab coupled by ST-PE backbone followed by three washing steps in a big volume (10ml) and subsequent staining with pre-conjugated α CD4 Fab monomers coupled by ST-APC backbones led to a staining, which was very similar to that of a mAb double staining (Figure 13). Due to their different susceptibility to unspecific staining, it was essential to start with the ST-PE coupled backbone. PE is known to be bound by some B cells and thereby can induce “unspecific” staining. The extensive washing before applying the second Fab multimer led to reduced false positive cells. After establishing the double staining, we set out to compare Fab multimer and mAb sorted cells. We stained splenocytes from the same donor mice and sorted them on the Moflo XDP sorted. We found that both staining protocols led to very similar cell products in cell death, composition and staining brightness (Figure 13) and that in contrast to a staining with mAbs the double multimer staining was fully reversible (Figure 14). In spite of being free of isolation reagents, the sorted cell product was not different in any of the parameters assessed (Figure 15). After setting up the enrichment process, we investigated if, as we hypothesized, the isolation reagents do influence the Treg graft.

8.4. *In vivo* engraftment

In order to test whether the capacity to engraft and survive upon adoptive T cell transfer was changed, we set up two models to examine the engraftment. For the first, we isolated Tregs from CD45.1 congenic donor mouse line and transferred 20.000 Tregs per CD45.2 recipient mouse. The second model used the same setup, but was more sophisticated, as it allowed to compare both Fab multimer- and mAb-sorted Treg grafts in one recipient mouse. We found that in both models the frequency and the absolute number of recoverable Tregs was significantly different between Fab multimer- and mAb-sorted cells (Figure 16 & Figure 18) independent of the congenic marker used to identify the transferred cell populations (Figure 17). After cell transfer, no difference in Foxp3, CD25 and CD4 expression was detectable when comparing Fab multimer- and mAb-sorted Tregs, indicating that surface-bound PC-61 and Gk1.5 mAbs seem to have no or only little influence on the phenotype of transferred cells, but a significant impact on the overall recoverable cell number (Figure 19).

In order to have a better understanding of these findings, we checked if the isolation reagent freed cells would engraft as good as never-stained cells. When checking if Fab multimer-stained and liberated Tregs engraft similar to never touched Tregs, we found in two different systems that the engraftment capability of Tregs was not diminished or enhanced when compared to untouched cells (Figure 20 & Figure 21). This finding also ruled out that Fab multimer isolation did indeed improve the engraftment capability of regulatory T cells. We next wanted to answer the question, why Fab multimer-sorted Treg cells do engraft better than mAb

sorted cells. As discussed before, several mechanisms how monoclonal antibodies could influence cells are known. We adopted our transfer model to Rag2 (recombinase activating gene 2), common γ -chain double knockout (Rag2^{-/-}c γ c^{-/-}) recipient mice, to check if the immune system plays a role in the diminished engraftment capability of isolation-reagent bearing cells. This mouse model lacks natural killer (NK) cells, T and B cells. There are some residual CD45 low cells detectable, which are of the macrophage/monocyte lineage but are severely altered in their development and functional characteristics due to the lack of functional IL2, IL4, IL7, IL9, and IL15 receptors (Mazurier et al., 1999). We found that while there was a trend of better engraftment of Fab multimer-sorted cells in all organs analyzed, no significant difference between Fab multimer- and mAb-sorted cells in engraftment and homeostatic proliferation was detected in this strongly immune-compromised recipients (Figure 22).

The antibody clone PC-61 has been shown to block IL-2 signaling induced proliferation (Moreau et al., 1987) and could account for the trend towards better proliferation of Fab multimer-sorted cells, as IL-2 signaling is essential to stabilize the Foxp3-driven Treg phenotype and to prevent Foxp3-driven apoptosis of regulatory T cells (Pierson et al., 2013; Tai et al., 2013). The vast amount of free cytokines in the Rag2^{-/-}c γ c^{-/-} mouse model most likely abrogates the effect of IL2 receptor blockage, as it leads to an increased homeostatic proliferation of transferred cells, hiding proliferative differences occurring early. Nevertheless, the data strongly suggested that the observed difference between isolation reagent-bearing and -freed cells is based on an immune system associated effect. Based on that finding, we then focused on other immune system associated knock-out mouse-models to delineate the mechanisms behind the observed differences. As described in the introduction (5.2.7.), several ways how antibodies can influence marked cells have been described in the literature. For example, antibodies can induce the complement system, activating C1q and leading to the activation of several effector mechanisms, or antibodies can activate effector cells directly via Fc Receptors (Ghobrial RR, Boublik M, Winn HJ, 1989; Rashid, Auchincloss, & Sharon, 1992; Setiady et al., 2010). Therefore, we wanted to investigate the role of the complement system in diminishing the engraftment capability of mAb-sorted cells.

We found that while having monoclonal antibodies on the cell surface did lead to increased deposition of C3 convertase on the cell surface (Figure 23), the engraftment into C3 KO mice was not improved (Figure 24), showing that the engraftment of Tregs is not diminished by a complement driven mechanism. As the ability of monoclonal antibodies to activate the immune system is dependent on the target surface molecule (Bindon et al., 1988; Nielsen et al., 2002) and the Ig type of the antibody (Brüggemann et al., 1987), we concluded

that the mAb clones PC-61 and Gk1.5 seem not to elicit strong complement activated killing *in vivo* but might instead lead to ADCC.

We then went on to check the influence of Fc γ -Receptor – Fc-part of the monoclonal antibodies interaction might have on the diminished engraftment. We analyzed whether transfer into Fc γ R^{-/-} mice would prevent differences in engraftment between Fab multimer- and mAb-sorted cells. And indeed, no detectable difference in the cell recovery was observed in short-term and long-term transfer experiments (Figure 25 & Figure 26). This data fits well to already published data showing that the CD25-targeting clone PC-61 and the α CD4 Gk1.5 can deplete – at least partially – Tregs *in vivo* (Alters, Sakai, Steinman, & Oi, 1990; Ghobrial RR, Boublik M, Winn HJ, 1989; Rashid et al., 1992; Setiady et al., 2010). This depletion was shown to depend on Fc γ receptor-bearing cells in the liver (Setiady et al., 2010). These data would suggest that just the use of isolation reagents not containing the Fc part of an antibody, instead of complete antibodies for cell selection, could be sufficient to improve *in vivo* survival of transferred cells.

In order to test this hypothesis, we performed transfer-experiments using Fab multimers and compared the engraftment of Treg cells either still having the Fab multimer on the cell surface or being released of the Fab multimer (Figure 27). To test the influence of surface-bound Fab multimers *in vivo*, we used our already well-established transfer model. In short-term transfer experiments, we found high recovery rates of Fab multimer-sorted Tregs without reagent removal, and isolation reagent freed cells and no significant difference between the two groups (Figure 29). However, further long-term follow up of recovery rates of Fab multimer-removed and non-removed Treg grafts revealed additional negative influences of remaining isolation reagents independent from Fc γ R as we found a reduced recovery rate after one week (Figure 29). Therefore, we analyzed whether the Fab multimers are still stably bound to the transferred cells in the blood stream, as published data showed that endogenous D biotin in the serum (Plebani, Avanzini, Massa, & Ugazio, 1984) could have an effect on Streptavidin binding *in vivo* (Rusckowski, Fogarasi, Fritz, & Hnatowich, 1997). We were wondering if the serum D biotin also affects the binding of Fab multimers or if the Fab multimer would be stable. Therefore, we treated Fab multimer stained cells *in vitro* with either whole blood or just serum at 37°C for 30 minutes under constant agitation. We only saw a little shift in the MFI but no shift in Fab multimer-positive cells showing that the majority of Fab multimer-positive cells does not lose the surface-bound Fab multimers (Figure 39). We concluded from this data that the still surface bound Fab Multimer might influence the recovery efficacy and suspected that a partial blockage of IL2 signaling might be responsible for that.

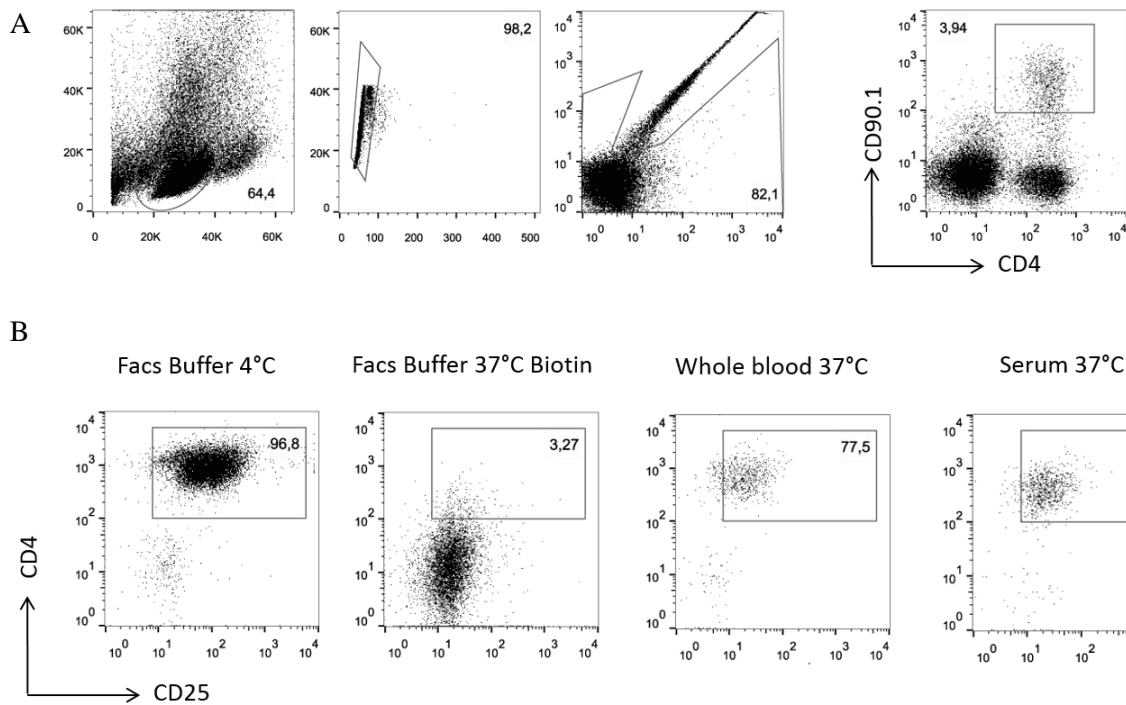


Figure 39. Influence of blood D-Biotin on Multimer stability: A) gating strategy for single living lymphocytes B) staining for CD4 and CD25 for the different groups

Therefore, we tested *in vitro* if IL2 signaling could be involved in the decreased maintenance of non-released Fab multimer-sorted Tregs. We found that, while IL2 signaling is not entirely abrogated like in the mAb-treated Tregs, the IL2 signaling was be diminished (Figure 30). Western Blot analysis might not be sensitive enough to detect the impact of reduced IL2 signaling, so we also checked the proliferation of CD3/CD28 stimulated regulatory T cells and found that Tregs still having Fab multimers bound to their surface are proliferating significantly worse *in vitro* when compared to isolation reagent-free Treg cells (Figure 31).

Overall, our analyses of adoptive transfer recoveries using purified primary (non-cultured) Tregs demonstrated that complete removal of isolation reagents prior to transfer is highly beneficial for engraftment and maintenance. After having established the improved engraftment capability of Fab Multimer sorted Tregs we checked if the *in vitro* and *in vivo* functionality of the Tregs was also improved.

8.5. Improved Functionality of isolation reagent freed cells

In order to test the *in vitro* functionality of Fab multimer-sorted and -isolated Tregs, we used a standard Treg suppression assay measuring the abrogation of Teff proliferation by addition of Tregs in a CD3/CD28 pre-coated 96 well plate. This assay showed a significant reduction of proliferation of Teff cells after addition of either Fab multimer- or mAb-sorted Tregs, but there was a significantly higher reduction of proliferation in the presence of Fab multimer-sorted cells, hinting towards improved suppressive capabilities of Fab multimer-isolated cells (Figure

32). We next went on to check for *in vivo* functionality of Fab multimer-isolated Treg grafts. Our analyses of adoptive transfer recoveries using purified primary (non-cultured) Tregs demonstrated that complete removal of isolation reagents prior to transfer is highly beneficial for engraftment and maintenance and therefore we next checked whether Fab multimer-isolated Tregs would also be beneficial in an *in vivo* disease setting and not only be dominant in numbers. Treg therapy has a lot of potential in different disease settings, like diabetes, multiple sclerosis and other auto-immune diseases (von Boehmer & Daniel, 2012; Zaiss et al., 2013), but the most convincing data for successful Treg therapy are currently in the context of treatment of problems caused by GvHD after alloHSCT.

Treatment with Tregs not only can prevent experimental aGvHD but, in contrast to treatment with standard immune suppressive regimes, transfused tumor-specific Tregs were still able to attack and clear the tumor (Edinger et al., 2003). The addition of physiologic numbers of Tregs (Treg to Teff ratio 1:10) had no beneficial effect on host survival in murine models of aGvHD. Only if the graft contained substantially elevated numbers of Tregs (i.e., Treg to Teff ratios of 1:1 or 1:2), recipient mice were found to be protected (Cohen et al., 2002; Edinger et al., 2003; Ermann et al., 2005; Petra Hoffmann et al., 2002; Taylor et al., 2002). As recently reviewed by Engelhardt and Crowe, it is still believed that in preclinical aGvHD models Teff to Treg ratios of minimally 1:1 or even 1:2 are needed to induce disease suppression (Engelhardt & Crowe, 2010). However, in an animal model of aGvHD we were able to demonstrate that Treg selection label removal translates into improved disease protection when compared to conventionally isolated Treg grafts. Our experiments confirmed these published data when Tregs were purified using antibodies that cannot be removed from the cell surface. However, after label removal, the majority of mice was protected even at a Teff to Treg ratio of 4:1. To our knowledge this is the first report of aGvHD protection with Tregs at such a low ratio and with such a low amount of Tregs. Based on these findings, primary Fab multimer-isolated Tregs could become an exciting source for clinical applications.

8.6. Enrichment for three parameters – the gate to Treg subpopulations

Similar to CD45RA in humans, the marker L-selectin (CD62L) can be used as an additional surface label to define a more potent Treg graft (Ermann et al., 2005). Due to their self-renewal and high suppressive capacities, CD45RA⁺ Tregs represent a very interesting subset for cell therapy in humans. We wanted to broaden our isolation protocol to make it possible to isolate CD4, CD25, and CD62L triple positive Tregs from murine single cell suspensions. Therefore, we adopted a system, which was in parallel developed for human applications, to isolate murine

cells from splenocytes single cell suspension using agarose beads coated with Streptactin and Fab multimers. We successfully developed a protocol to isolate CD4 positive CD25 positive and CD62L positive cells (Figure 34 & Figure 35). In between the different surface molecules, we found considerable differences for cell enrichment properties. The enrichment for CD4 has proven to be the most reliable one in terms of purity of the cell product and the yield of the enrichment. CD25 was the worst surface marker for cell enrichment. We hypothesize that this is due to the very low affinity of the CD25 targeting mutated Fab fragment. The enrichment for CD62L showed decent purities but had a lower yield than the enrichment of CD4 positive cells. Based on their findings, we decided to incorporate an enrichment step prior to sorting the cells, as we had only Streptactin coupled to two different fluorescent dyes available. After enriching the cells using the Fab coated agarose beads we went on to stain the cells with the two reversible stainings for CD25 (multimerized with STPE) and CD62L (multimerized with STAPC) (Figure 36) and sorted these cells by flow cytometry. This turned out to be a fast and reliable protocol to obtain highly purified Treg subsets.

In order to test if the sorted Treg subsets were functional *in vivo*, we transferred the cells in our already established Treg transfer system and found that both subsets stayed stable over time under steady-state conditions (Figure 37). Furthermore, the CD62L low subset proliferated vigorously over time (Figure 37).

8.7. Human application

Induction of immunologic tolerance is essential to improving outcomes of organ transplantation, both for solid organs and the hematopoietic system. Regulatory T cells are essential for the success of the transplantation, as they induce tolerance (Q. Tang & Bluestone, 2013). Their therapeutic efficacy is well documented in animal models. None of the current immunosuppressive drugs can suppress the immune response to the graft without potentially altering immune response toward tumor antigens and microbial pathogens (Singer, King, & D'Alessio, 2014). After Edinger et al., could show that Tregs can discriminate between beneficial and malignant immune responses, Tregs became very interesting for therapy in humans as well (Edinger et al., 2003; Edinger & Hoffmann, 2011).

Human naturally occurring Tregs, like murine Tregs, are most commonly characterized by surface expression of CD4, CD25 and constitutive expression of Foxp3. Only the surface markers CD4 and CD25 are available for staining and isolation, which is often not sufficient to isolate pure Treg populations, as also activated effector T cells display CD25 on the cell surface. Several other markers have been discussed. Tregs can be distinguished from activated CD4⁺CD25⁺ effector T cells by their low or absent surface expression of CD127 as well as

some other markers like CD49d (negative) and CD45RA (positive) (Miyara et al. 2009). Marker combinations using CD4⁺CD25⁺ and CD45RA⁺ cell (Hoffmann et al. 2006) and CD49d- and CD127⁻ cells (Haase et al. 2015; Brunstein et al. 2015; Brunstein et al. 2011) have been tested in pre-clinical and clinical settings. In man, the markers CD45RO and CD45RA distinguish Treg subsets with different proliferative potential and migratory characteristics (Booth et al., 2010). As described in the mouse system, Tregs numbers needed to confer protection are very high (a ratio of 1:1 at least) depending on the model used. This shortage in Treg numbers may be overcome by *in vitro* expansion of the cells especially of CD45RA⁺ naive Tregs (Hoffmann et al. 2006). The co-expression of CD25 and CD45RA is restricted mainly to Tregs, and the isolation of CD4⁺CD25⁺CD45RA⁺ further not only delineates functional differentiation of different Foxp3⁺ Treg subsets but also reduces the risk of contamination with activated CD25⁺ CD4⁺ T effs, which are mostly CD45RA negative (Petra Hoffmann, Eder, et al., 2006). In addition, CD45RA⁺ Tregs were shown to have a stable phenotype, function, and stability of Foxp3 expression even after extended *in vitro* expansion (Petra Hoffmann, Eder, et al., 2006; Miyara et al., 2009). For clinical application of Treg therapy using freshly isolated highly pure Treg products, the enrichment for three parameters seems to be crucial. We have already shown that it is possible to isolate human CD4⁺CD25⁺CD45RA⁺ regulatory T cells with high purity using Fab multimer-coated beads and serial magnetic enrichment (Stemberger et al., 2012). This enrichment leads to a cell product with predominantly Foxp3-positive cells, making freshly isolated, highly pure label-free Tregs available for human therapy as well.

9. Summary

The infusion of either freshly isolated or *ex vivo* expanded Tregs can improve survival of recipients in acute GVHD, but it is generally believed that vast numbers of Tregs are required to achieve therapeutic effects (C. G. Brunstein et al., 2016; Claudio G Brunstein et al., 2011; Cohen et al., 2002; Mauro Di Ianni et al., 2011; Edinger et al., 2003; Edinger & Hoffmann, 2011; P. Hoffmann et al., 2002; Taylor et al., 2002). Due to the relatively low frequency of nTregs in circulation of only 1-2% of total CD4⁺ T cell population in adult humans (Baecher-Allan et al., 2001), the purification of sufficiently large numbers of Tregs for therapy has been challenging or might not even been feasible in clinical practice without *in vitro* expansion (C. G. Brunstein et al., 2016; Claudio G Brunstein et al., 2011; M Di Ianni et al., 2009; Haase et al., 2015; Petra Hoffmann, Boeld, et al., 2006; Kleinewietfeld et al., 2009).

We hypothesized that isolation reagents remaining on the cell surface are diminishing the potency of the Treg graft, which would explain the non-physiologically high numbers of Tregs needed to control aGvHD. The reversible Fab multimer-based Treg purification developed during this thesis can prevent conventional antibody label-induced interferences *in vitro* and *in vivo*. A substantial increase in engraftment efficacy in C57BL/6 wildtype mice was observed when the cells were released from isolation reagents. This difference in engraftment efficacy was mediated by Fc- γ -receptor- as well as IL-2 receptor-dependent mechanisms. We tested the differentially isolated T regs grafts (Fab Multimer/conventioally) in a pre-clinical model for acute GvHD, showing that 'label-freed' Tregs are protective at substantially lower cell numbers as compared to Tregs isolated using conventional non-reversible antibody staining, translating into significantly improved survival of mice treated with minimally manipulated Tregs. These findings might have significant clinical relevance for future Treg-based cell therapies.

10. Acknowledgement

An dieser Stelle möchte ich die Gelegenheit wahrnehmen all denen zu danken, die mich während meiner Doktorarbeit praktisch, geistig oder auch seelisch unterstützt habe.

Zuerst möchte ich mich bei Professor Busch für die Möglichkeit in seinem Labor zu arbeiten und für die Unterstützung während der Arbeit und das mir entgegengebrachte Vertrauen danken.

Dank gilt auch Christian Stemberger und Stefan Dreher für ihre Freundschaft und die Einführung in das praktische Arbeiten in der Immunologie, sowie Herbert Stadler für immer inspirierende und spannende Gespräche.

Meinen vielen Freunden, die ich am Institut gewonnen habe möchte ich auch einen besonderen Dank aussprechen und um nur einige hier namentlich zu erwähnen Thomas, Marten, Manuel, Katherine, Inge, Anna, Philipp, Simon, Immanuel, Shwetha, Patrick, Ronny, Ann, Steven und all den anderen tollen Kollegen/Freunden.

Als letztes möchte ich meinen Dank meinen Eltern Heribert & Rosmarie, meinem Bruder Daniel und meiner Liebe Tina aussprechen, die mit ihrem Zuspruch, Rat und Unterstützung und Verständnis meine Arbeit ermöglicht haben.

11. Material and Methods

11.1. Plastic

item	manufacturer	
1.0ml Eppendorf	Zefa	Munich Germany
1.5ml Eppendorf	Zefa	Munich Germany
15ml Falcon Cell Star	Greiner bio-one	Heidelberg, Germany
2.0ml Eppendorf	Zefa	Munich Germany
50ml Falcon Cell Star	Greiner bio-one	Heidelberg, Germany
70µm Nylon Cell Strainer	BD Falcon	Heidelberg, Germany
Electroporation cuvette	Sigma Aldrich	Hamburg, Germany
Inject 5ml	Braun	Melsungen, Germany
PCR Eppendorf	Zefa	Munich, Germany
petri-dish	BD Falcon	Heidelberg, Germany
SuperRX	FujiFilm	Düsseldorf, Germany

11.2. Fab Streptamers & plasmids

epitope	parental clone	plasmid
αCD4 wt	GK1.5	pASGwt2
αCD25-Y32A _{light}	PC61	pASGwt2

11.3. Antibodies

FACS Staining (All experiments were conducted with mAbs targeting murine epitopes)

epitope	dye	dilution	manufacturer	
aCD8	FITC	1:200	Caltag	London, UK
aCD3	PE	1:250	eBioscience	San Diego, USA
α CD4	PE	1:250	BD	Heidelberg, Germany
aCD8	PE	1:200	eBioscience	San Diego, USA
α CD25	PE	1:100	eBioscience	San Diego, USA
aCD3	PE- Cy7	1:100	eBioscience	San Diego, USA
α CD4	eF450	1:100	eBioscience	San Diego, USA
α CD127	eF450	1:100	eBioscience	San Diego, USA
Foxp3	eF450	1:100	eBioscience	San Diego, USA
α CD62L	FITC	1:100	eBioscience	San Diego, USA

Stimulation Assays (All experiments were conducted with mAbs targeting murine epitopes)

epitope	dye	dilution	manufacturer	
aCD3	PE	variable	eBioscience	San Diego, USA
α CD25	PE	variable	eBioscience	San Diego, USA

Western blot (All experiments were conducted with mAbs targeting murine epitopes)

epitope	dilution	manufacturer		
pY-STAT5	1:1000	Cell signaling	Danvers, USA	
pY-STAT3	1:1000	Cell signaling	Danvers, USA	
beta-actin	1:4000	Cell signaling	Danvers, USA	
Goat anti-rabbit HRP	IgG- 1:5000	Santa Biotechnology	Cruz	Heidelberg, Germany

11.4. Buffer

5xloading dye	200mM Tris-HCl pH 6,8 400mM DTT 10% (w/v) SDS 16% (v/v) Glycerol 2g/l Bromphenolblue
blocking buffer	PBT 0.5% (w/v) milk powder
Blotting buffer	20% (v/v) methanol 10% (v/v) 10x Tris Glycin 70% (v/v) bi-distilled H ₂ O
Developer solution	Na ₂ CO ₃ solution 0.2% (v/v) Na-Thiosulfate stock solution 0.05% (v/v) formaldehyde (37%)
ethanol-solution	50% (v/v) ethanol (100%) 50% (v/v) bi-distilled H ₂ O
EZ-Running buffer	90% (v/v) bi-distilled H ₂ O 10% EZ-Running buffer stock solution (Fisher Scientific)
FACS buffer	PBS Dulbecco 0.5% (w/v) BSA
fixation-solution	50% (v/v) methanol 120% (v/v) acetic acid 38% (v/v) bi-distilled H ₂ O
Lysis buffer	20 - 150mM NaCl 1mM DTT 1mM Na ₂ EDTA 1mM EGTA 0,5% (v/v) Nonident P-40 10% (v/v) Glycerol 20mM beta-Glycerolphosphat 1mM Na ₃ VO ₄ 0,4mM PMSF 1 Tablet Protease Inhibitor Cocktail (EDTA free)

	1mM NaF
Na ₂ CO ₃ solution	bi-distilled H ₂ O
	6% (w/v) dehydrated N a ₂ CO ₃
Na-thiosulfate-solution	10% (v/v) Na-thiosulfate stock solution
	90% (v/v) bi-distilled H ₂ O
Na-thiosulfate-stock solution	bi-distilled H ₂ O
	2% (w/v) Na-thiosulfate
PBS Dulbecco	ready to use preparation
PBT	PBS Dulbecco
	0.5% (v/v) Tween 10
Puffer E	100mM Tris·Cl
	150mM NaCl
	1mM EDTA
	2.5mM desthiobiotin, pH 8
Puffer P	100mM Tris/HCl pH8
	500mM sucrose
	1mM EDTA
Puffer W	100mM Tris/HCl pH 8
	150mM NaCl
	1mM EDTA
Silver-nitrate solution	bi-distilled H ₂ O
	0.4% (w/v) silver-nitrate AgNO ₃
	0.76% (w/v) formaldehyde (37%)

11.5. Solutions and chemicals

	manufacturer	
Acrylamide	Sigma-Aldrich	Taufkirchen, Germany
Agarose	Invitrogen, Paisley,	United Kingdom
AgNO ₃	Sigma-Aldrich	Taufkirchen, Germany
AHT	IBA lifescience	Göttingen, Germany
APS	Sigma-Aldrich	Taufkirchen, Germany
Bromphenolblue	Sigma-Aldrich	Taufkirchen, Germany
BSA	Roth	Karlsruhe, Germany
D-biotin	Sigma-Aldrich	Taufkirchen, Germany
dehydrated N a ₂ CO ₃	Sigma-Aldrich	Taufkirchen, Germany
desthiobiotin	IBA lifescience	
DTT	Sigma-Aldrich	Taufkirchen, Germany
EGTA	Sigma-Aldrich	Taufkirchen, Germany
EGTA	Sigma-Aldrich	Taufkirchen, Germany
ethanol	Klinikum rechts der Isar,	Munich, Germany
Formaldehyde	Sigma-Aldrich	Taufkirchen, Germany
Glycerol	Sigma-Aldrich	Taufkirchen, Germany
methanol	Klinikum rechts der Isar,	Munich, Germany
NaCl	Sigma-Aldrich	Taufkirchen, Germany
SDS	Sigma-Aldrich	Taufkirchen, Germany
silver-nitrate AgNO ₃	Sigma-Aldrich	Taufkirchen, Germany
sucrose	Sigma-Aldrich	Taufkirchen, Germany
TEMED	Invitrogen, Paisley,	United Kingdom
Tris HCl	Sigma-Aldrich	Taufkirchen, Germany
Western Lightning Plus ECL	Perkin Elmer	Heidelberg, Germany
β-mercaptoethanol	Agilent Technologies, Inc.,	Santa Clara ,USA

11.6. Software

Software	manufacturer	
Flowjo 10	Treestar	Ashland, USA
Office Word 10	Microsoft	Unterschleißheim, Germany
Office Excel 10	Microsoft	Unterschleißheim, Germany
GraphPad Prism 5	GraphPad	San Diego, USA
Summit 4.3.01	DakoCytomation	Golstrup, Denmark

11.7. Organisms

Organisms	strain	manufacturer	
<i>E. coli</i>	<i>JM83</i>	IBA,	Göttingen, Germany
<i>Mouse</i>	<i>C57BL/6 45.1</i>	Klinikum Rechts der Isar	Munich, Germany
<i>Mouse</i>	<i>C57BL/6 45.2</i>	Harlan	
<i>Mouse</i>	<i>RAG2 -/- cgamma-</i> <i>/-</i>	Klinikum Rechts der Isar	Munich, Germany
<i>Mouse</i>	<i>C57BL/6 90.1</i>	Klinikum Rechts der Isar	Munich, Germany
<i>Mouse</i>	<i>C57BL/6 C3 KO</i>	Klinikum Rechts der Isar	Munich, Germany
<i>Mouse</i>	<i>C57BL/6 FcyR KO</i>	Klinikum Rechts der Isar	Munich, Germany

11.8. Enzymes

Name	manufacturer	
Herculase	Stratagene	London, UK
Benzonase	Sigma-Aldrich	Taufkirchen, Germany
Collagenase V	Sigma-Aldrich	Taufkirchen, Germany
DNase	Sigma-Aldrich	Taufkirchen, Germany

11.9. Machines

machine	name	supplier
	T3000 Thermocycler	Biometra, Göttingen, Germany
	SE250/260	HOEFER, Holliston, USA
	gene pulser	Biorad, Munich, Germany
	Multifuge 3 S-R	Heraeus , Hanau, Germany
	Ultraspec3000 pro	Amersham <i>Bioscience</i> , Freiburg, Germany
centrifuge	Sorvall 6+ Centrifuge	Thermo Scientific, Bonn, Germany
electroporator	pulse controller	Biorad, Munich, Germany
FACS Sorter	MoFloII	Beckman Coulter, Krefeld, Germany
flow cytometer	CyAn ADP	DakoCytomation, Golstrup, Denmark
gel chamber	HE33 mini horizontal submarine unit	Amersham, Freiburg, Germany
gel documentation system	Eagle Eye	Biorad, Munich, Germany
photometer	BioPhotometer	eppendorf, Hauppau, USA
power supply	Electrophoresis Power Supply EPS	Amersham, Freiburg, Germany
radiographic cassette	radiographic cassette	Dr. Goos-Suprema, Heidelberg, Germany
spectrophotometer	NanoDrop	Kisker-Biotech, Steinfurt, Germany
table centrifuge	Biofuge fresco	Heraeus, Hanau, Germany
Thermocycler	T3 Thermocycler	Biometra, Göttingen, Germany
water bath	E100	LAUDA, Königshofen, Germany

12. Methods

12.1. Production of electrical competent *E.coli* JM83

For the production of electrocompetent *E.coli* JM83, bacteria were cultured in 5ml LB medium overnight at 37°C under constant agitation (150 rpm). Afterwards 1l LB₀ was inoculated with 5ml pre-culture and incubated (37°C, 150 rpm) until an OD₆₀₀ of 0.5 to 0.6 was reached. The cells were transferred on ice for 10min and centrifuged (4000g; 15min; 4°C). The supernatant was discarded and the pellet resuspended in 5ml ice-cold 1mM HEPES buffer. After resuspension, another 350ml ice-cold 1mM HEPES was added. The washing procedure was repeated twice. Afterwards, the pellet was resuspended in 5ml ice-cold 10% glycerin and centrifuged (4000g; 15min; 4°C). Finally, the pellet was resuspended in 2ml ice-cold 10% glycerin, divided into aliquots of 40µl, shock-frozen in liquid nitrogen and stored at -80°C.

12.2. Mutagenesis PCR

A point mutation can be incorporated if the primer used carries the one non-complementary base and is long enough to have sufficient complementary sequence for stable hybridization on both sides of the "wrong" base. The mutagenesis PCR was used to target small changes in the sequence of the produced murine Fabs. The DNA templates were already cloned plasmid DNA, so that an amplification could be carried out according to the principle of an inverse PCR. With only one primer pair, the entire vector sequence was thus amplified. The specially designed mutagenesis primers spanned the position to be mutually by about 20 bp each. The melting temperature of the two areas did not deviate more than 2 ° C.

Reaction solution:

5µL	5xHerculase reaction buffer	
100ng	DNA template	
1µl	Forward primer	10µM
1µl	Reverse primer	10µM
0,5µl	dNTP mix	100µM
1µl	HerculaseII	1U/µl
Filled up to 50µl	H ₂ O bidest	

Thermocycler program:

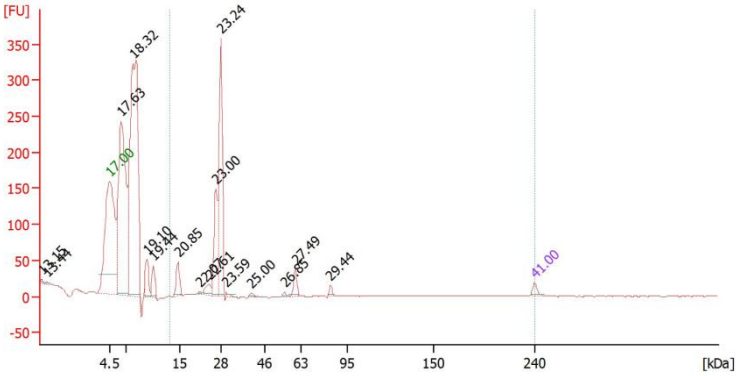
1.	Initial denature	95°C	2min
2.	Denature	95°C	1min
3.	Annealing	48-58°C	45sec
4.	Elongation	68-72°C	1min/kb
5.	Synthesis	68-72°C	3min
6.	Storage	4°C	

12.3. Periplasmic Fab- expression

For periplasmic expression, one aliquot of the *E. coli* expression lineage *JM83* stock was thawed on ice and attenuated with 100µl sterile bi-distilled H₂O. 80µl of *JM83*-solution was transferred into a precooled 1.5ml Eppendorf tube and 1µl (100ng) of target plasmid was added. After mixing the solution was transferred into an electroporation cuvette (optical path 1mm (Sigma)) (. The cells were transformed with the target plasmid using electroporation (400 Ω 25µF and 2.5 kV; Pulse Controler & Gene Pulser (Biorad). After electroporation bacteria were immediately supplemented with 1ml pre-warmed (37°C) LB-medium and transferred to an Eppendorf tube. The cells were incubated for one hour at 37°C to give the cells time to develop antibiotic resistance. Then 500µl were transferred into 4ml LB_{Ampi} (100mg/L) and incubated under constant agitation (150rpm) overnight at 37°C. Next day 2ml of the overnight culture was transferred to a 200ml Erlenmeyer flask and incubated for 24h at 22°C and 150rpm. To start the main culture 25ml were transferred into a two-liter flask which was then filled up to a total volume of one liter with LB_{Ampi}. The bacteria were incubated at 22°C and 150 rpm until an OD₆₀₀ of 0.5-0.6 was reached. For induction of protein expression, AHT was added at a ratio of 1:10000. After incubation for another three hours, the OD₆₀₀ was measured and the bacteria harvested. The cells were centrifuged at 5000g for 12min at 4°C and the pellet stored at -80°C. To extract the Fab-fragment, the pellet was thawed and resuspended in 20ml buffer P at 4°C. After 30min incubation on ice, the cells were centrifuged at 15000rpm for 15min at 4°C (Sorval 6+ Centrifuge SA300 rotor). The supernatant was transferred into a falcon tube and contaminating nucleic acids were enzymatically digested using Benzonase (125U). The cells were kept on ice for 30min, and afterward sterile filtered using a 0.22µm filter. The filtered periplasmic extract was transferred onto a *Strep*-Tactin-Superflow column (IBA Göttingen), which was previously equilibrated twice with 2.5 column volumes ice-cold buffer W. Afterwards the column was washed five times with buffer W. The Fab-fragment was eluted

using buffer E. Three elution samples were collected (0.8ml, 1.5ml, 1.0ml). The second elution sample having the highest protein content was dialyzed against sterile PBS pH 7.4 at a ratio of 1:1000000 using a cut off dialyzer flexible tube (14kDa). After dialysis, the samples were analyzed for total protein content using the 2100 Bioanalyzer by Agilent and the Protein 80 kit according to manufacturer's protocol.

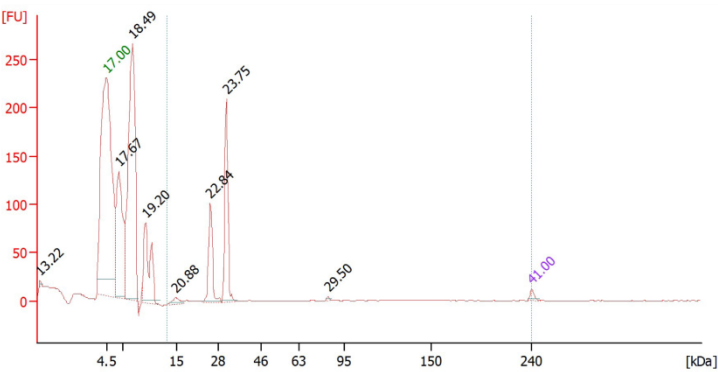
mCD4 batch generated and used for all experiments:



Peak table for sample 1 : mCD4

Peak	Size (kDa)	Rel. Conc. (ng/μl)	Calib. Conc. (ng/μl)	% of Total	Observations
1	0.2	0.0	0.0	0.0	
2	0.5	0.0	0.0	0.0	
3	4.5	0.0	0.0	0.0	Lower Marker
4	6.3	0.0	0.0	0.0	System Peak
5	8.1	0.0	0.0	0.0	System Peak
6	10.2	0.0	0.0	0.0	System Peak
7	11.1	0.0	0.0	0.0	System Peak
8	14.8	218.8	0.0	8.2	
9	21.3	13.4	0.0	0.5	
10	24.2	105.6	0.0	4.0	
11	26.4	616.6	0.0	23.1	
12	27.8	1,468.0	0.0	55.0	
13	30.2	21.5	0.0	0.8	
14	40.6	25.7	0.0	1.0	
15	55.1	21.5	0.0	0.8	
16	60.2	134.8	0.0	5.1	
17	82.9	42.9	0.0	1.5	
18	240.0	60.0	0.0	0.0	Upper Marker

mCD25 batch generated and used for all experiments:



Peak table for sample 2 : mCD25

Peak	Size [kDa]	Rel. Conc. [ng/μl]	Calib. Conc. [ng/μl]	% of Total	Observations
1	0.2	0.0	0.0	0.0	
2	4.5	0.0	0.0	0.0	Lower Marker
3	6.4	0.0	0.0	0.0	System Peak
4	8.5	0.0	0.0	0.0	System Peak
5	10.4	0.0	0.0	0.0	System Peak
6	14.8	123.0	0.0	5.0	
7	25.5	848.2	0.0	34.5	
8	31.4	1,466.6	0.0	59.7	
9	83.7	20.6	0.0	0.8	
10	240.0	60.0	0.0	0.0	Upper Marker

12.4. Preparation of mouse organs – spleen & lymph nodes

Mice were sacrificed using cervical dislocation and spleen, and lymph nodes were aseptically removed. The organs were immediately transferred to ice cold RPMI10+. The tissue was homogenized by filtering through a 70μm mesh. The cell suspension was transferred to a 15ml falcon tube, and ice cold RPMI10+ was added to a total volume of 15ml. After centrifugation (6min, 1500 rpm, 4°C) the supernatant was discarded and the pellet resuspended in 3ml ACT per spleen. The solution was incubated 3min at room temperature with the tube being inverted two to three times. Afterwards, the 15ml Falcon was filled up with ice-cold RPMI10+ and centrifuged for 6min at 1500rpm. Then the supernatant was discarded, and the cell pellet resuspended in 10ml FACS buffer and filtered one more time through a 70μm mesh. The cell number was determined using a Neubauer counting chamber.

12.5. IL-2 stimulation assay

The aim of this assay was to collect experimental data on the potential influence of surface-bound CD25 staining reagents on cell signaling. Therefore an antibody targeting CD25 and the corresponding Fab-fragment were used. As the antibody clone PC61 is described to be a blocking antibody (Lowenthal et al. 1985a) the same properties were expected to apply for the Fab-multimer. To obtain data on the blockage the cells were isolated, stained, and stimulated before being lysed and analyzed for their intracellular signaling. Also, the influence of staining and washing the cells afterward was of interest and investigated during the experiment. Murine splenocytes were prepared according to standard procedures (9.4). Afterwards, 5×10^6 splenocytes were transferred to the wells of a 96-well round-bottom plate. To assess if the washing has any influence 1.5×10^7 cells were transferred into falcon tubes. The cells were stained following the staining protocol adapted to the cell count (9.8.2) and if the cells were stained in a falcon tube washed with the D-biotin washing protocol. After the staining the cells were rested for 30min at 37°C and afterward stimulated with 50U IL-2 for 15min before being transferred on ice. 50μl ice-cold PBS was added to each well and the content of each well transferred into a pre-cooled Eppendorf tube. After centrifugation (1min; 13.000rpm; 4°C; Biofuge fresco) cells were washed once in 100μl ice-cold PBS. The pellet was resuspended in

50µl lysis-buffer and incubated for 5-10min.. Afterwards, cells were centrifuged at 13000rpm for 10min at 4°C. The supernatant was collected and transferred to a new pre-cooled Eppendorf tube and stored at -20°C. The probes were analyzed via SDS-PAGE and western blot.

12.6. SDS-PAGE and analysis

12.6.1. SDS-PAGE

After assembling the gel chamber, the separation gel was cast into the gel chamber and covered with isopropyl alcohol. By covering the gel air bubbles are prevented and a clear horizontal top edge is formed. After polymerization of the separation gel, the stacking gel was applied, and the comb was placed into the gel. The following reagents and volumes were used:

<u>12% SDS-PAGE</u>		
	Separation gel	Stacking gel
acrylamide	12ml	2.6ml
1.5 M Tris-HCl pH8.8	7.5ml	-
2.0 M Tris-HCl pH6.8	-	1.25ml
SDS 10% (w/v)	300µl	800µl
H ₂ O	9.9ml	15.7ml
TEMED	15µl	20µl
APS 10% (w/v)	150µl	100µl

Table: components for 12% SDS Gel

For analysis 12µl 5x loading buffer were mixed with 50µl of the probe and boiled at 95°C for 5min. After a short spin (5sec, to avoid concentration alterations due to condensation during boiling), 20µl of the sample was loaded into the pocket of a prepared SDS Gel. 80V of voltage was applied until the dye front reaches the end of the stacking gel; then the voltage was increased to 120V. The gel run was stopped when the 10kDa marker band reached the bottom edge of the gel.

12.6.2. Silver staining

Silver staining is a sensitive method to detect trace amounts of proteins in SDS-PAGE gels. It is possible to identify or quantitatively determine the components of protein mixtures. Silver staining was used to analyze the purity of expressed Fab-fragments after purification. The SDS-gel was incubated in the fixation solution for 30min and afterwards washed three times for 15min in the ethanol solution. After discarding the ethanol solution, the gel was incubated in the thiosulfate-solution for one minute. After washing the gel three times in bi-distilled H₂O for 20 seconds each, the silver nitrate solution was added, and the gel was incubated for 20min. After washing the gel twice in bi-distilled H₂O for 30 seconds, the developer solution was added. The staining process was stopped by adding the fixation solution when an optimal staining intensity was achieved. For conservation stained gels were incubated in sealing buffer for 10min and finally sealed between two layers of cellophane.

12.6.3. Western blot analysis

12.6.3.1. Semi-dry - blot

For the detection of a protein using a specific antibody western blot analysis was performed. In detail, the gel was applied on two layers of Whatman paper (7cm x 18cm for a large gel and 7cm x 9cm for a small gel) wetted with blotting buffer and a layer of nitrocellulose membrane (6x18cm for large gels, 6x9cm for small gels). After adding a small volume of blotting buffer, the gel was strimmed smooth to the surface, and another two layers of Whatman paper soaked with blotting buffer were applied on top. The blotting chamber was assembled and connected to the power supply. The power supply was set to a maximum of 25V and 1.2A/cm² gel and the transfer time was limited to 1h 40min. Afterwards, the gel and the Whatman paper were disposed, the nitrocellulose membrane was blocked in blocking buffer for one hour at 4°C and subsequently washed twice in PBT for 2min each. After washing the nitrocellulose membrane was transferred into a falcon tube containing 2ml of the primary antibody solution. The primary mAb was diluted as recommended by the manufacturer (usually in a ratio of 1:1000) and incubated at 4°C overnight on a rolling incubator. The next morning the membrane was washed three times in PBT for 10min each, followed by secondary mAb incubation for one hour. After incubation, the membrane was washed four times in PBT for 5min and two times in PBS for 5min. After washing the membrane was incubated for one minute with Western Lightning ECLplus (enhanced chemiluminescence lightning solution) and stored in a radiographic cassette. X-ray films were exposed for different time intervals on the membrane in the darkroom and afterwards developed.

12.7. Suppression assay

One C57BL/6 mouse of each congenic marker (CD45.2; CD45.1) was sacrificed, and cells from spleen and lymph nodes were isolated and counted according to the protocol (8.4). Subsequently, cells from the CD45.1⁺ mouse were used as effector cells and were initially stained with CFSE (8.8.1). Subsequently, the cells were stained with mAbs against CD3, CD4, and CD25 according to the standard staining protocol (8.8.3) and FACS sorted for CD3⁺CD4⁺CD25⁻. Cells isolated from CD45.2⁺ mice were used to isolate regulatory T-cells and feeder cells. The isolated cells were stained with mAbs against CD3 and CD4 and either antibodies or Fab-multimers against CD25 according to the standard staining protocol (8.8.3), and FACS sorted for CD3⁻ (feeder cells) and CD3⁺CD4⁺CD25⁺ (Treg cells). Subsequently, Fab-multimer isolated cells were washed once in 200µl FACS-buffer containing 1mM D-biotin for 10min and afterwards twice with RPMI10⁺ for 10min. After FACS sorting 1.5 million feeder cells the falcon tube was filled up with 1ml filtered pure FCS and irradiated with 25Gy. 24.000 effector cells were sorted into each well of a 96-round-well plate (Figure 1.) with each well containing 30µl FCS (1mM D-biotin). 8.000 regulatory T cells were sorted into the first two rows with one row containing Fab-multimer labeled the other mAb stained regulatory T-cells. 75.000 of irradiated feeder cells were added to each well. For the following culture, cells were resuspended in 150µl RPMI10⁺ and stored in the incubator at 37°C for four days. For FACS analysis cells were stained with mAbs against CD45.1 according to the standard staining protocol (8.8.3) and analyzed on a CyanADP flow-cytometer for reduction of the CFSE signal within the CD45.1⁺ effector cells. Experiments were analyzed with FlowJo software, and statistical analysis was performed using Prism Software.

12.8. In vitro Proliferation measurement

FACS isolated regulatory T cells either isolated using Fab multimers or mAbs were labeled using CFSE according to manufacturer's protocol. Labeled cells were transferred into a pre-coated MaxiSorp flat bottom 96-well plate (NUNC). For pre-coating, 96-well plates were incubated over night at 4°C with PBS containing 5µg/ml purified αCD3 mAb(145-2C11 eBioscience) and 2.5 µg/ml αCD28 mAb (37.51 BD). Plates were washed and incubated for 2 hours with FCS. Cells were cultivated for three days at 37°C in RPMI containing 10%FCS and analyzed for CFSE dilution at day three.

12.9. Cell staining

12.9.1. CFSE staining

Isolated lymphocytes were diluted to 2×10^7 cells/ml in PBS at room temperature, and the designated amount of cells was transferred into a 15ml falcon tube. Carboxyfluorescein diacetate succinimidyl ester (CFDA-SE) was added to a final concentration of $1.5 \mu\text{M}$, vortexed gently and kept in the dark at room temperature for 8min. After 3min cells the falcon conatining the cells was filled up with RP10+ medium and put into a 37°C water bath for 10min. The cells were centrifuged for 6min at 1500rpm, and the supernatant was discarded. The cells were then washed two more times with 1ml PBS per 10^6 cells. After the last washing step, the cells were resuspended in an appropriated amount of FACS buffer for further use.

12.9.2. Fluorescence-activated cell analysis

Flow cytometric cell sorting and the trademark name fluorescence-activated cell sorting (FACS) are often used as equivalent. FACS uses a laser directed onto a hydrodynamically-focused stream of liquid to detect the combination of scattered and fluorescent emitted light. The fluorescent light can be emitted by excitation of fluorescent dyes with narrow excitation and emission spectra coupled to mAbs that specifically bind to cell surface markers. The sorting of cells is achieved, by breaking the fluid stream into a series of small droplets, with one cell per droplet, quickly measure and analyze the light properties of each droplet. If a droplet contains a single cell emitting the desired light spectra, it is electrostatically charged and separated from the fluid stream by deflecting it into collection tubes during their flight in the air. Due to its high specificity and the high sorting purity is FACS an essential tool in basic research, clinical diagnostics and cell selection for preclinical models. Although several smaller studies investigated the use of FACS for clinical trials, it has not yet been approved by government officials due to concerns about patient safety (Jaye et al. 2012).

Conventional FACS systems have emerged as essential tools in modern biological laboratories. The FACS machine creates a hydrodynamically focused stream of cell suspension which is analyzed using a laser beam and an array of photodetectors. Fluorescent labels are attached to one or more cell types in a heterogeneous suspension, and the cells are analyzed or sorted individually based on how they scatter the incident laser light and the wavelength of light they emit.

For fluorescence-activated cell analysis (FACS) cells were stained after the isolation from mouse organs. In the standard staining protocol, 5×10^6 cells were resuspended in $50 \mu\text{l}$ FACS-

buffer and transferred to a 96-well plate. The staining procedure was performed at 4°C and as dark as possible. Each fluorochrome used in the actual experiment also had to be displayed as a single color. For single-colors, 2x10⁶ cells were stained with a single antibody carrying the needed fluorochrome needed for compensating spectra interference between some fluorochromes. The mAbs were added to the 50µl cell solution according to their titrated dilution. For staining with Fab-multimers 1µg Fab was incubated with 3µl *Strep*-Tactin coupled with a fluorochrome (either PE: ST-PE or APC: ST-APC). After addition of the dye-labeled staining, reagent cells were incubated for 20min at 4°C in the dark. Afterwards 150ml the cells were centrifuged at 1500 rpm at 4°C for 3min, the supernatant discarded and resuspended 200ml FACS-buffer. The cells were centrifuged at 1500 rpm at 4°C for 3min. The washing step was repeated once. For analysis cells were resuspended in 200ml FACS-buffer and transferred to FACS-tubes. Before measurement 100µl PI (final concentration 1µg/ml) were added for differentiation of living and dead cells. Fluorescence was measured on a CyanADP flow-cytometer. The acquired data were analyzed using the FlowJo software.

12.9.3. Fluorescence-activated cell sorting

For sort experiments, the amount of staining reagents was linearly scaled up to the respective starting cell number. Staining procedures and incubation times were as described in the standard staining protocol. FACS sort was performed on a Moflo II, or Aria.

12.10. Using Affinity Catch columns for enrichment

Fab: mαCD4 (Munich): 18µg

600µl Matrix

Cells: single cell solution of two mixed C57Bl/10 Spleens

Starting population: 2*10⁸ cells in

Protocol:

S-1000

	Volume [ml]	Speed [ml/min]
Fab	3	1.5
Cells	10	2.5
Wash	10	10
Wash	10	10
Wash	10	10
D-biotin	10	5

D-biotin	10	5
Wash	10	10
Wash	10	10

12.11. Removal of Fab-multimers from the cell surface using D-biotin

After the staining/labeling of cells with dye-conjugated *Strep*-Tactin or with magnetic beads conjugated with *Strep*-Tactin and the following experimental procedures the Fab - multimer can be removed from the cell surface. Therefore the cells were transferred to a 15ml Falcon and filled up to 10ml with D-biotin (1mM final concentration). The cells were incubated for 10min at 4°C and inverted 4-5 times during the incubation time. Afterwards, the cells were spun down at 1500rpm for 6min at 4°C. The supernatant was discarded, and the cell pellet was resuspended in 1mM D-biotin; the D-biotin step and the washing step were repeated once. To remove remaining D-biotin and monomeric Fab-fragments the cells were resuspended in 10ml FACS-buffer and washed twice.

12.12. Cell transfer

Wt C57BL/6 (H-2k^b CD90.2⁺ CD45.2⁺) mice were obtained from Harlan Winkelmann. BALB/c (H-2k^d, CD90.2⁺) were purchased from Janvier Labs (France). Congenically marked mice were bred in house C57BL/6 (CD90.1⁺ CD45.2⁺ and CD90.2⁺ CD45.1⁺). All mice were housed under specific pathogen-free conditions at the mouse facility at the Technical University Munich. For all experiments freshly isolated splenocytes and lymph nodes cells were obtained from 6-8 week old sex-matched mice. Animal experiments were approved by the local authorities. Treg transfers into different mice (C57BL / 6, RAG - / -, DREG) were performed. For the transfer of a spleen cell suspension, the spleens of a donor mice were prepared as indicated and enriched by FACS sorting. Prior to transfer the Tregs were washed 2x in 1 mM D-biotin after FACS sorting to replace the reagent. Afterwards the cells were transferred i.v. transferred in 200µl of sterile PBS.

12.12.1. Long-term Engraftment Experiments

Congenically marked cells were stained according to protocol and sorted using the Moflo Legacy (Beckmann Coulter) or the FACS Aria II (BD). Sorted and washed cells (if indicated with 1mM D-biotin) cells were injected i.v. into recipient mice. For co-transfer models differentially congenically (CD90.1/CD45.1) cells a 1:1 solution of cells was used and transferred in one single injection. Recipient mice were sacrificed at the indicated time points and different organs were analyzed.

12.12.2. Short-term Engraftment Experiments

Cells were sorted as described above. After sorting the populations were stained using different Proliferation dyes (CFSE/eF450 PD/eF670 PD, eBioscience). To exclude influences of cell labeling we interchanged PD, between different experiments.

12.12.3. GvHD model

Allogeneic bone marrow transplants were performed as previously described (Jankovic et al., 2013). Briefly, female, 6-8 weeks old BALB/c recipients received lethal total body irradiation (TBI) with 2x4.5Gy. Directly after the second irradiation step mice received 5×10^6 T cell depleted bone marrow cells for reconstitution with or without T effector and T regulatory cells as indicated in the text and figures. T cell depletion of freshly isolated BM cells was performed using CD90.2 microbeads (Miltenyi). The survival and appearance of mice were monitored daily. Body weight was measured daily for at least three weeks and afterwards every 2 to 3 days. Mice were observed for 50 days.

13. List of abbreviations

μ F	Micro Faraday
aGvHD	Acute Graft-versus-Host disease
APC	Antigen-presenting cell
APC	Allophycocyanin / Antigen-presenting cell
B-cell	B-lymphocyte
BCR	B cell receptor
BSA	Bovine serum albumin
CD	cluster of differentiation
cGvHD	Chronic Graft-versus-Host disease
Ch	heavy chain constant region
Cl	Light chain constant region
<i>CMV</i>	<i>Cytomegalovirus</i>
CTL	Cytotoxic T lymphocyte
d	day
DC	Dendritic cell
ddH ₂ O	Distilled, deionized water
DNA	Deoxyribonucleic acid
dNTP	Deoxynucleoside-triphosphate
<i>E. coli</i>	<i>Escherichia coli</i>
<i>EBV</i>	<i>Eppstein-Barr virus</i>
EDTA	Ethylenediaminetetraacetate
FACS	Fluorescence-activated cell sorting
FITC	Fluorescein-isothiocyanat
FoxP3	Forkhead box P3
GATA3	Transacting T-cell-specific transcription factor
GvHD	Graft versus Host Disease
GvL	Graft versus leukemia effect
GvT	Graft versus tumor effect
HC	Heavy chain
HLA	Human leukocyte antigen
HZDM	High-density media
IFN	Interferon
Ig	Immunoglobulin

IL	Interleukin
ITAM	Immunoreceptor tyrosine activatory motif
ITIM	Immunoreceptor tyrosine inhibitory motif
kDa	Kilodalton
LB	Luria-Bertoni Medium
LB _{Amp}	Luria-Bertoni Medium + Ampicillin
Lc	Light chain
LN	Lymph node
LPS	Lipopolysaccharide
mAb	Monoclonal antibody
MHC-I/II	Major histocompatibility complex class I/II
NK cell	Natural killer cell
OD	Optical density
PBS	Phosphate buffered saline
PCR	Polymerase chain reaction
PE	Phycoerythrin
PI	Propidium iodide
PRR	Pattern recognition receptor
ROR γ	RAR-related orphan receptor gamma
rpm	Rounds per minute
RT	Room temperature
SDS	Sodium dodecyl sulfate
SMI	Small molecule inhibitor
ST	Strep-Tactin
STAT	signal transducer and activator of transcription
T-cell	T lymphocyte
TCR	T cell receptor
TEMED	N, N, N', N'-Tetramethylethylenediamine
TLR	Toll-like receptor
Treg	Regulatory T Cell
Tris	Tris-(Hydroxymethyl-)Aminomethane
Vh	Heavy chain variable region
VI	light chain variable Region
Ω	Ohm

14. Table of literature

- Aggarwal, S., & Pittenger, M. F. (2009). Human mesenchymal stem cells modulate allogeneic immune cell responses. *Transplantation*, *105*(4), 1815–1822. <http://doi.org/10.1182/blood-2004-04-1559>. Supported
- Alousi, A. M., Weisdorf, D. J., Logan, B. R., Bolan, J., Carter, S., Difrongo, N., ... Horowitz, M. M. (2009). Etanercept, mycophenolate, denileukin, or pentostatin plus corticosteroids for acute graft-versus-host disease: a randomized phase 2 trial from the Blood and Marrow Transplant Clinical Trials Network, *114*(3), 511–517. <http://doi.org/10.1182/blood-2009-03-212290>. Previously
- Alters, S. E., Sakai, K., Steinman, L., & Oi, V. T. (1990). Mechanisms of anti-CD4-mediated depletion and immunotherapy. A study using a set of chimeric anti-CD4 antibodies. *Journal of Immunology (Baltimore, Md. : 1950)*, *144*(12), 4587–4592.
- Altman, J. D., Moss, P. A., Goulder, P. J., Barouch, D. H., McHeyzer-Williams, M. G., Bell, J. I., ... Davis, M. M. (1996). Phenotypic analysis of antigen-specific T lymphocytes. *Science (New York, N.Y.)*, *274*(5284), 94–6. Retrieved from http://www.ncbi.nlm.nih.gov/entrez/query.fcgi?cmd=Retrieve&db=PubMed&dopt=Citation&list_uids=8810254
- Alyea, E. P., Kim, H. T., Ho, V., Cutler, C., DeAngelo, D. J., Stone, R., ... Soiffer, R. J. (2006). Impact of conditioning regimen intensity on outcome of allogeneic hematopoietic cell transplantation for advanced acute myelogenous leukemia and myelodysplastic syndrome. *Biology of Blood and Marrow Transplantation: Journal of the American Society for Blood and Marrow Transplantation*, *12*(10), 1047–55. <http://doi.org/10.1016/j.bbmt.2006.06.003>
- Asai, O., Longo, D. L., Tian, Z. G., Hornung, R. L., Taub, D. D., Ruscetti, F. W., & Murphy, W. J. (1998). Suppression of graft-versus-host disease and amplification of graft-versus-tumor effects by activated natural killer cells after allogeneic bone marrow transplantation. *The Journal of Clinical Investigation*, *101*(9), 1835–1842. <http://doi.org/10.1172/JCI1268>
- Baecher-Allan, C., Brown, J. A., Freeman, G. J., & Hafler, D. A. (2001). CD4+CD25high regulatory cells in human peripheral blood. *Journal of Immunology (Baltimore, Md. : 1950)*, *167*(3), 1245–53. <http://doi.org/10.4049/jimmunol.167.3.1245>
- Barnes, D. W., & Loutit, J. F. (1957). Treatment of murine leukaemia with x-rays and homologous bone marrow. II. *British Journal of Haematology*, *3*(3), 241–52. Retrieved from <http://www.ncbi.nlm.nih.gov/pubmed/13460193>
- Barnes, D. W., Loutit, J. F., & Micklem, H. S. (1962). “Secondary disease” of radiation chimeras: a syndrome due to lymphoid aplasia. *Annals of the New York Academy of Sciences*, *99*, 374–85.

Retrieved from <http://www.ncbi.nlm.nih.gov/pubmed/13969359>

- Barnes DW, Corp MJ, Loutit JF, N. F. (1956). Treatment of murine leukaemia with X rays and homologous bone marrow; preliminary communication. *British Medical Journal*, 2(4993), 626–7. <http://doi.org/10.1136/bmj.2.4993.626>
- Baron, F. (2005). Graft-Versus-Tumor Effects After Allogeneic Hematopoietic Cell Transplantation With Nonmyeloablative Conditioning. *Journal of Clinical Oncology*, 23(9), 1993–2003. <http://doi.org/10.1200/JCO.2005.08.136>
- Baron, F., Maris, M. B., Sandmaier, B. M., Storer, B. E., Sorror, M., Diaconescu, R., ... Storb, R. (2005). Graft-versus-tumor effects after allogeneic hematopoietic cell transplantation with nonmyeloablative conditioning. *Journal of Clinical Oncology : Official Journal of the American Society of Clinical Oncology*, 23(9), 1993–2003. <http://doi.org/10.1200/JCO.2005.08.136>
- Bès, C., Briant-Longuet, L., Cerutti, M., Heitz, F., Troadec, S., Pugnière, M., ... Chardes, T. (2003). Mapping the paratope of anti-CD4 recombinant Fab 13B8.2 by combining parallel peptide synthesis and site-directed mutagenesis. *The Journal of Biological Chemistry*, 278(16), 14265–73. <http://doi.org/10.1074/jbc.M210694200>
- Billingham, R. E. (1966). The biology of graft-versus-host reactions. *Harvey Lectures*, 62, 21–78. Retrieved from <http://www.ncbi.nlm.nih.gov/pubmed/4875305>
- Bindon, C. I., Hale, G., & Waldmann, H. (1988). Importance of antigen specificity for complement-mediated lysis by monoclonal antibodies. *European Journal of Immunology*, 18(10), 1507–14. <http://doi.org/10.1002/eji.1830181006>
- Blazar, B. R., Murphy, W. J., & Abedi, M. (2012). Advances in graft-versus-host disease biology and therapy. *Nature Reviews Immunology*, 12(6), 443–458. <http://doi.org/10.1038/nri3212>
- Bleakley, M., Heimfeld, S., Loeb, K. R., Jones, L. a, Chaney, C., Seropian, S., ... Shlomchik, W. D. (2015). Outcomes of acute leukemia patients transplanted with naive T cell – depleted stem cell grafts. *Journal of Clinical Investigation*, 125(13), 1–13. <http://doi.org/10.1172/JCI81229>
- Boieri M, Shah P, Dressel R, I. M. (2016). The Role of Animal Models in the Study of Hematopoietic Stem Cell Transplantation and GvHD: A Historical Overview. *Frontiers in Immunology*, 7(August). <http://doi.org/10.3389/fimmu.2016.00333>
- Boieri, M., Shah, P., Dressel, R., & Inngjerdingen, M. (2016). The Role of Animal Models in the Study of Hematopoietic Stem Cell Transplantation and GvHD: A Historical Overview. *Frontiers in Immunology*, 7. <http://doi.org/10.3389/fimmu.2016.00333>
- Bolton, H. A., Zhu, E., Terry, A. M., Guy, T. V, Koh, W., Tan, S., ... de St. Groth, B. F. (2015). Selective

- Treg reconstitution during lymphopenia normalizes DC costimulation and prevents graft-versus-host disease. *Journal of Clinical Investigation*, 125(9), 3627–3641. <http://doi.org/10.1172/JCI76031>
- Booth, N. J., McQuaid, A. J., Sobande, T., Kissane, S., Agius, E., Jackson, S. E., ... Vukmanovic-Stejic, M. (2010). Different proliferative potential and migratory characteristics of human CD4+ regulatory T cells that express either CD45RA or CD45RO. *Journal of Immunology (Baltimore, Md. : 1950)*, 184(8), 4317–26. <http://doi.org/10.4049/jimmunol.0903781>
- Brüggemann, M., Williams, G. T., Bindon, C. I., Clark, M. R., Walker, M. R., Jefferis, R., ... Neuberger, M. S. (1987). Comparison of the effector functions of human immunoglobulins using a matched set of chimeric antibodies. *The Journal of Experimental Medicine*, 166(5), 1351–61. Retrieved from <http://www.ncbi.nlm.nih.gov/pubmed/3500259>
- Brunstein, C. G., Miller, J. S., Cao, Q., McKenna, D. H., Hippen, K. L., Curtsinger, J., ... Wagner, J. E. (2011). Infusion of ex vivo expanded T regulatory cells in adults transplanted with umbilical cord blood : safety profile and detection kinetics Infusion of ex vivo expanded T regulatory cells in adults transplanted with umbilical cord blood : safety profile and. *Blood*, 117(3), 1061–1070. <http://doi.org/10.1182/blood-2010-07-293795>
- Brunstein, C. G., Miller, J. S., McKenna, D. H., Hippen, K. L., DeFor, T. E., Sumstad, D., ... Wagner, J. E. (2016). Umbilical cord blood-derived T regulatory cells to prevent GVHD: kinetics, toxicity profile, and clinical effect. *Blood*, 127(8), 1044–1051. <http://doi.org/10.1182/blood-2015-06-653667>
- Buchholz, V. R., Flossdorf, M., Hensel, I., Kretschmer, L., Weissbrich, B., Gräf, P., ... Busch, D. H. (2013). Disparate individual fates compose robust CD8+ T cell immunity. *Science (New York, N.Y.)*, 340(6132), 630–5. <http://doi.org/10.1126/science.1235454>
- Busch, D. H., & Pamer, E. G. (1999). T Cell Affinity Maturation by Selective Expansion during Infection. *Journal of Experimental Medicine*, 189(4), 701–710. <http://doi.org/10.1084/jem.189.4.701>
- Busch, D. H., Pilip, I. M., Vijn, S., & Pamer, E. G. (1998). Coordinate regulation of complex T cell populations responding to bacterial infection. *Immunity*, 8(3), 353–362. [http://doi.org/10.1016/S1074-7613\(00\)80540-3](http://doi.org/10.1016/S1074-7613(00)80540-3)
- Charles A Janeway, J., Travers, P., Walport, M., & Shlomchik, M. J. (2001). The complement system and innate immunity. Garland Science.
- Chung, D. J., Rossi, M., Romano, E., Ghith, J., Yuan, J., Munn, D. H., & Young, J. W. (2009). Indoleamine 2,3-dioxygenase – expressing mature human monocyte-derived dendritic cells

- expand potent autologous regulatory T cells. *Blood*, *114*(3), 1–4. <http://doi.org/10.1182/blood-2008-11-191197>.The
- Clynes, R. a, Towers, T. L., Presta, L. G., & Ravetch, J. V. (2000). Inhibitory Fc receptors modulate in vivo cytotoxicity against tumor targets. *Nature Medicine*, *6*(4), 443–446. <http://doi.org/10.1038/74704>
- Cohen, J. L., Trenado, A., Vasey, D., Klatzmann, D., & Salomon, B. L. (2002). CD4(+)CD25(+) immunoregulatory T Cells: new therapeutics for graft-versus-host disease. *The Journal of Experimental Medicine*, *196*(3), 401–406. <http://doi.org/10.1084/jem.20020090>
- Curti, A., Trabanelli, S., Salvestrini, V., Baccarani, M., & Lemoli, R. M. (2009). Review article The role of indoleamine 2, 3-dioxygenase in the induction of immune tolerance : focus on hematology. *Hematology*, *113*(11), 2394–2401. <http://doi.org/10.1182/blood-2008-07-144485>.
- Di Ianni, M., Del Papa, B., Cecchini, D., Bonifacio, E., Moretti, L., Zei, T., ... Tabilio, a. (2009). Immunomagnetic isolation of CD4+CD25+FoxP3+ natural T regulatory lymphocytes for clinical applications. *Clinical and Experimental Immunology*, *156*(2), 246–53. <http://doi.org/10.1111/j.1365-2249.2009.03901.x>
- Di Ianni, M., Falzetti, F., Carotti, A., Terenzi, A., Castellino, F., Bonifacio, E., ... Martelli, M. F. (2011). Tregs prevent GVHD and promote immune reconstitution in HLA-haploidentical transplantation. *Blood*, *117*(14), 3921–8. <http://doi.org/10.1182/blood-2010-10-311894>
- Edinger, M., & Hoffmann, P. (2011). Regulatory T cells in stem cell transplantation: strategies and first clinical experiences. *Current Opinion in Immunology*, *23*(5), 679–84. <http://doi.org/10.1016/j.coi.2011.06.006>
- Edinger, M., Hoffmann, P., Ermann, J., Drago, K., Fathman, C. G., Strober, S., & Negrin, R. S. (2003). CD4+CD25+ regulatory T cells preserve graft-versus-tumor activity while inhibiting graft-versus-host disease after bone marrow transplantation. *Nature Medicine*, *9*(9), 1144–50. <http://doi.org/10.1038/nm915>
- Engelhardt, B. G., & Crowe, J. E. (2010). Homing in on Acute Graft vs. Host Disease: Tissue-Specific T Regulatory and Th17 Cells. In *Current topics in microbiology and immunology* (pp. 121–146). http://doi.org/10.1007/82_2010_24
- Ermann, J., Hoffmann, P., Edinger, M., Dutt, S., Blankenberg, F. G., Higgins, J. P., ... Strober, S. (2005). Only the CD62L + subpopulation of CD4 +CD25 + regulatory T cells protects from lethal acute GVHD. *Blood*, *105*(5), 2220–2226. <http://doi.org/10.1182/blood-2004-05-2044>
- Fanger, M. W., Shen, L., Graziano, R. F., & Guyre, P. M. (1989). Cytotoxicity mediated by human Fc

receptors for IgG. *Immunology Today*, 10(3), 92–99. [http://doi.org/10.1016/0167-5699\(89\)90234-X](http://doi.org/10.1016/0167-5699(89)90234-X)

- Filipovich, A. H., Weisdorf, D., Pavletic, S., Socie, G., Wingard, J. R., Lee, S. J., ... Flowers, M. E. D. (2005). National Institutes of Health consensus development project on criteria for clinical trials in chronic graft-versus-host disease: I. Diagnosis and staging working group report. *Biology of Blood and Marrow Transplantation : Journal of the American Society for Blood and Marrow Transplantation*, 11(12), 945–56. <http://doi.org/10.1016/j.bbmt.2005.09.004>
- Fontenot, J. D., Gavin, M. a, & Rudensky, A. Y. (2003). Foxp3 programs the development and function of CD4+CD25+ regulatory T cells. *Nature Immunology*, 4(4), 330–6. <http://doi.org/10.1038/ni904>
- Gavin, M. A., Torgerson, T. R., Houston, E., DeRoos, P., Ho, W. Y., Stray-Pedersen, A., ... Rudensky, A. Y. (2006). Single-cell analysis of normal and FOXP3-mutant human T cells: FOXP3 expression without regulatory T cell development. *Proceedings of the National Academy of Sciences of the United States of America*, 103(17), 6659–64. <http://doi.org/10.1073/pnas.0509484103>
- Gerbitz, A., Schultz, M., Wilke, A., Linde, H., Schölmerich, J., Holler, E., & Dc, W. (2012). Probiotic effects on experimental graft-versus-host disease : let them eat yogurt Brief report Probiotic effects on experimental graft-versus-host disease : let them eat yogurt, 103(11), 4365–4367. <http://doi.org/10.1182/blood-2003-11-3769>
- Ghobrial RR, Boublik M, Winn HJ, A. H. J. (1989). In Vivo Use of Monoclonal Antibodies against Murine T Cell Antigens, 506(3), 486–506.
- Goto, Y., & Hamaguchi, K. (1982a). Unfolding and refolding of the constant fragment of the immunoglobulin light chain. *Journal of Molecular Biology*, 156(4), 891–910. [http://doi.org/10.1016/0022-2836\(82\)90146-2](http://doi.org/10.1016/0022-2836(82)90146-2)
- Goto, Y., & Hamaguchi, K. (1982b). Unfolding and refolding of the reduced constant fragment of the immunoglobulin light chain: Kinetic role of the intrachain disulfide bond. *Journal of Molecular Biology*, 156(4), 911–926. [http://doi.org/10.1016/0022-2836\(82\)90147-4](http://doi.org/10.1016/0022-2836(82)90147-4)
- Goulmy, E., Schipper, R., Pool, J., Blokland, E., Falkenburg, J. H., Vossen, J., ... van Rood, J. J. (1996). Mismatches of minor histocompatibility antigens between HLA-identical donors and recipients and the development of graft-versus-host disease after bone marrow transplantation. *The New England Journal of Medicine*, 334(5), 281–285. <http://doi.org/10.1056/NEJM199602013340501>
- Graef, P., Buchholz, V. R., Stemberger, C., Flossdorf, M., Henkel, L., Schiemann, M., ... Busch, D. H. (2014). Serial Transfer of Single-Cell-Derived Immunocompetence Reveals Stemness of CD8+ Central Memory T Cells. *Immunity*, 41, 116–126. <http://doi.org/10.1016/j.immuni.2014.05.018>

- Gratwohl, A., Hermans, J., Goldman, J., Arcese, W., Carreras, E., Devergie, A., ... Apperley, J. (1998). Risk assessment for patients with chronic myeloid leukaemia before allogeneic blood or marrow transplantation. Chronic Leukemia Working Party of the European Group for Blood and Marrow Transplantation. *Lancet*, 352(9134), 1087–92. Retrieved from <http://www.ncbi.nlm.nih.gov/htbin-post/Entrez/query?db=m&form=6&dopt=r&uid=9798583%5Cnpapers3://publication/uuid/5A12F62F-4B23-4D45-99FD-48E9CE78AEA1>
- Guignet, E. G., Hovius, R., & Vogel, H. (2004). Reversible site-selective labeling of membrane proteins in live cells. *Nature Biotechnology*, 22(4), 440–444. <http://doi.org/10.1038/nbt954>
- Haase, D., Puan, K. J., Starke, M., Lai, T. S., Soh, M. Y. L., Karunanithi, I., ... Rotzschke, O. (2015). Large-scale Isolation of Highly Pure “Untouched” Regulatory T Cells in a GMP Environment for Adoptive Cell Therapy. *Journal of Immunotherapy (Hagerstown, Md. : 1997)*, 38(6), 250–258. <http://doi.org/10.1097/CJI.0000000000000083>
- Hansen, J. A., Clift, R. A., Thomas, E. D., Buckner, C. D., Storb, R., & Giblett, E. R. (1980). Transplantation of Marrow from an Unrelated Donor to a Patient with Acute Leukemia. *New England Journal of Medicine*, 303(10), 565–567. <http://doi.org/10.1056/NEJM198009043031007>
- Henig, I., & Zuckerman, T. (2014). Hematopoietic stem cell transplantation-50 years of evolution and future perspectives. *Rambam Maimonides Medical Journal*, 5(4), e0028. <http://doi.org/10.5041/RMMJ.10162>
- Highfill, S. L., Rodriguez, P. C., Zhou, Q., Goetz, C. a, Koehn, B. H., Veenstra, R., ... Blazar, B. R. (2010). Bone marrow myeloid-derived suppressor cells (MDSC) inhibit graft-versus-host (GVHD) disease via an arginase-1 dependent mechanism that is upregulated by IL-13. *Blood*, 116(25), 612–626. <http://doi.org/10.1182/blood-2010-06-287839>
- Hippen, K. L., Merkel, S. C., Schirm, D. K., Sieben, C. M., Sumstad, D., Kadidlo, D. M., ... Blazar, B. R. (2011). Massive ex vivo expansion of human natural regulatory T cells (T(regs)) with minimal loss of in vivo functional activity. *Sci. Transl. Med.*, 3(83), 83ra41. <http://doi.org/10.1126/scitranslmed.3001809>
- Hoffmann, P., Boeld, T. J., Eder, R., Albrecht, J., Doser, K., Piseshka, B., ... Edinger, M. (2006). Isolation of CD4+CD25+ regulatory T cells for clinical trials. *Biology of Blood and Marrow Transplantation : Journal of the American Society for Blood and Marrow Transplantation*, 12(3), 267–74. <http://doi.org/10.1016/j.bbmt.2006.01.005>
- Hoffmann, P., Eder, R., Boeld, T. J., Doser, K., Piseshka, B., Andreesen, R., & Edinger, M. (2006). Only the CD45RA+ subpopulation of CD4+CD25high T cells gives rise to homogeneous regulatory T-cell lines upon in vitro expansion. *Blood*, 108(13), 4260–7.

<http://doi.org/10.1182/blood-2006-06-027409>

- Hoffmann, P., Ermann, J., Edinger, M., Fathman, C. G., & Strober, S. (2002). Donor-type CD4+CD25+ Regulatory T Cells Suppress Lethal Acute Graft-Versus-Host Disease after Allogeneic Bone Marrow Transplantation. *Journal of Experimental Medicine*, 196(3), 389–399. <http://doi.org/10.1084/jem.20020399>
- Hoffmann, P., Ermann, J., Edinger, M., Fathman, C. G., & Strober, S. (2002). Donor-type CD4+CD25+ Regulatory T Cells Suppress Lethal Acute Graft-Versus-Host Disease after Allogeneic Bone Marrow Transplantation. *Journal of Experimental Medicine*, 196(3), 389–399. <http://doi.org/10.1084/jem.20020399>
- Huss, D. J., Pellerin, A. F., Collette, B. P., Kannan, A. K., Peng, L., Datta, A., ... Fontenot, J. D. (2016). Anti-CD25 monoclonal antibody Fc variants differentially impact Treg cells and immune homeostasis¹. *Immunology*, n/a-n/a. <http://doi.org/10.1111/imm.12609>
- Jankovic, D., Ganesan, J., Bscheider, M., Stickel, N., Weber, F. C., Guarda, G., ... Zeiser, R. (2013). The Nlrp3 inflammasome regulates acute graft-versus-host disease. *The Journal of Experimental Medicine*, 210(10), 1899–910. <http://doi.org/10.1084/jem.20130084>
- Jones, S. C., Murphy, G. F., & Korngold, R. (2003). Post-hematopoietic cell transplantation control of graft-versus-host disease by donor CD425 T cells to allow an effective graft-versus-leukemia response. *Biology of Blood and Marrow Transplantation : Journal of the American Society for Blood and Marrow Transplantation*, 9(4), 243–56. <http://doi.org/10.1053/bbmt.2003.50027>
- Josefowicz, S. Z., Lu, L.-F., & Rudensky, A. Y. (2012). Regulatory T Cells: Mechanisms of Differentiation and Function. *Annual Review of Immunology*, 30, 531–564. <http://doi.org/10.1146/annurev.immunol.25.022106.141623>
- Kleinewietfeld, M., Starke, M., Mitri, D. Di, Borsellino, G., Battistini, L., Rötschke, O., & Falk, K. (2009). CD49d provides access to “untouched” human Foxp3+ Treg free of contaminating effector cells. *Blood*, 113(4), 827–836. <http://doi.org/10.1182/blood-2008-04-150524>
- Knabel, M., Franz, T. J., Schiemann, M., Wulf, A., Villmow, B., Schmidt, B., ... Busch, D. H. (2002). Reversible MHC multimer staining for functional isolation of T-cell populations and effective adoptive transfer. *Nature Medicine*, 8(6), 631–637. <http://doi.org/10.1038/nm0602-631>
- Kolb, H.-J. (2008). Graft-versus-leukemia effects of transplantation and donor lymphocytes. *Blood*, 112(12), 4371–4383. <http://doi.org/10.1182/blood-2008-03-077974>
- Korngold, R., & Sprent, J. (1987). LETHAL GRAFT-VERSUS-HOST DISEASE ACROSS MINOR HISTOCOMPATIBILITY BARRIERS IN MICE VARIABLE CAPACITY OF L3T4 + T CELLS

TO CAUSE The transfer of unprimed T cells to lethally irradiated allogeneic mice expressing multiple minor histocompatibility (H)' an, *165*(June), 1552–1564.

- Koyama, M., Kuns, R. D., Olver, S. D., Raffelt, N. C., Wilson, Y. A., Don, A. L. J., ... Hill, G. R. (2012). Recipient nonhematopoietic antigen-presenting cells are sufficient to induce lethal acute graft-versus-host disease. *Nature Medicine*, *18*(1), 135–42. <http://doi.org/10.1038/nm.2597>
- Lahl, K., Loddenkemper, C., Drouin, C., Freyer, J., Arnason, J., Eberl, G., ... Sparwasser, T. (2007). Selective depletion of Foxp3⁺ regulatory T cells induces a scurfy-like disease. *The Journal of Experimental Medicine*, *204*(1), 57–63. <http://doi.org/10.1084/jem.20061852>
- Larsen, M. E., Kornblit, B., Larsen, M. V., Masmus, T. N., Nielsen, M., Thiim, M., ... Vindelov, L. (2010). Degree of predicted minor histocompatibility antigen mismatch correlates with poorer clinical outcomes in nonmyeloablative allogeneic hematopoietic cell transplantation. *Biology of Blood and Marrow Transplantation*, *16*(10), 1370–1381. <http://doi.org/10.1016/j.bbmt.2010.03.022>
- Lechner, M. G., Liebertz, D. J., & Epstein, A. L. (2010). Characterization of cytokine-induced myeloid-derived suppressor cells from normal human peripheral blood mononuclear cells. *Journal of Immunology (Baltimore, Md. : 1950)*, *185*(4), 2273–2284. <http://doi.org/10.4049/jimmunol.1000901>
- Li, W., Carper, K., Liang, Y., Zheng, X. X., Kuhr, C. S., Reyes, J. D., ... Perkins, J. D. (2006). Anti-CD25 mAb Administration Prevents Spontaneous Liver Transplant Tolerance. *Transplantation Proceedings*, *38*(10), 3207–3208. <http://doi.org/10.1016/j.transproceed.2006.10.094>
- Malek, T. R. (2008). The biology of interleukin-2. *Annual Review of Immunology*, *26*, 453–79. <http://doi.org/10.1146/annurev.immunol.26.021607.090357>
- Mathé, G., Amiel, J. L., Schwarzenberg, L., Catran, A., & Schneider, M. (1965). Adoptive Immunotherapy of Acute Leukemia : Experimental and Clinical Results Adoptive Immunotherapy of Acute Leukemia : Experimental eradicate, 1525–1531.
- Mazurier, F., Fontanellas, A., Salesse, S., Taine, L., Landriau, S., Moreau-Gaudry, F., ... Verneuil, H. De. (1999). A Novel Immunodeficient Mouse Model-RAG2 gamma Cytokine Receptor Chain Double Mutants-Requiring Exogenous Cytokine Administration for Human Hematopoietic Stem Cell Engraftment Common. *Journal of Interferon & Cytokine Research*, *19*(5), 533–541. <http://doi.org/10.1089/107999099313983>
- McDonald, G. B. (2016). How I treat acute graft-versus-host disease of the gastrointestinal tract and the liver. *Blood*, *127*(December 2015), 1–30. <http://doi.org/10.1182/blood-2015-10-612747>

- Miller, J. S., Cooley, S., Parham, P., Farag, S. S., Verneris, M. R., McQueen, K. L., ... Weisdorf, D. J. (2007). Missing KIR ligands are associated with less relapse and increased graft-versus-host disease (GVHD) following unrelated donor allogeneic HCT. *Blood*, *109*(11), 5058–5061. <http://doi.org/10.1182/blood-2007-01-065383>
- Miyara, M., Yoshioka, Y., Kitoh, A., Shima, T., Wing, K., Niwa, A., ... Sakaguchi, S. (2009). Functional delineation and differentiation dynamics of human CD4+ T cells expressing the FoxP3 transcription factor. *Immunity*, *30*(6), 899–911. <http://doi.org/10.1016/j.immuni.2009.03.019>
- Mohr, F. (2012). *Generation and characterization of murine Fab-Streptamers for cell separation*. TU München.
- Morales-Tirado, V., Luszczek, W., van der Merwe, M., & Pillai, A. (2011). Regulatory immunotherapy in bone marrow transplantation. *TheScientificWorldJournal*, *11*, 2620–34. <http://doi.org/10.1100/2011/768948>
- Moreau, J. L., Nabholz, M., Diamantstein, T., Malek, T., Shevach, E., & Thèze, J. (1987). Monoclonal antibodies identify three epitope clusters on the mouse p55 subunit of the interleukin 2 receptor: Relationship to the interleukin 2-binding site. *European Journal of Immunology*, *17*, 929–935. <http://doi.org/10.1002/eji.1830170706>
- Morgan, M. E., Van Bilsen, J. H. M., Bakker, A. M., Heemskerk, B., Schilham, M. W., Hartgers, F. C., ... Toes, R. E. M. (2005). Expression of FOXP3 mRNA is not confined to CD4 +CD25 + T regulatory cells in humans. *Human Immunology*, *66*(1), 13–20. <http://doi.org/10.1016/j.humimm.2004.05.016>
- Müller, A. M., & Henschler, R. (2016). Hematopoietic Stem Cells in Regenerative Medicine : Astray or on the Path ?, 247–254. <http://doi.org/10.1159/000447748>
- Murphy, M., Jason-Moller, L., Bruno, J., Murphy, M., Jason-Moller, L., & Bruno, J. (2006). Using Biacore to Measure the Binding Kinetics of an Antibody-Antigen Interaction. In *Current Protocols in Protein Science* (p. 19.14.1-19.14.17). Hoboken, NJ, USA: John Wiley & Sons, Inc. <http://doi.org/10.1002/0471142301.ps1914s45>
- Nauerth, M., Stemberger, C., Mohr, F., Weißbrich, B., Schiemann, M., Germeroth, L., & Busch, D. H. (2016). Flow cytometry-based TCR-ligand Koff-rate assay for fast avidity screening of even very small antigen-specific T cell populations ex vivo. *Cytometry Part A*, (4). <http://doi.org/10.1002/cyto.a.22933>
- Nauerth, M., Weißbrich, B., Knall, R., Franz, T., Dössinger, G., Bet, J., ... Busch, D. H. (2013). TCR-ligand koff rate correlates with the protective capacity of antigen-specific CD8+ T cells for adoptive transfer. *Science Translational Medicine*, *5*, 192ra87.

<http://doi.org/10.1126/scitranslmed.3005958>

- Nestel, F. P., Price, K. S., Seemayer, T. A., & Lapp, W. S. (1992). Macrophage priming and lipopolysaccharide-triggered release of tumor necrosis factor alpha during graft-versus-host disease. *The Journal of Experimental Medicine*, *175*(2), 405–13. <http://doi.org/10.2214/ajr.155.4.2119110>
- Neudorfer, J., Schmidt, B., Huster, K. M., Anderl, F., Schiemann, M., Holzapfel, G., ... Bernhard, H. (2007). Reversible HLA multimers (Streptamers) for the isolation of human cytotoxic T lymphocytes functionally active against tumor- and virus-derived antigens. *Journal of Immunological Methods*, *320*(1–2), 119–131. <http://doi.org/10.1016/j.jim.2007.01.001>
- Nielsen, S. U., Routledge, E. G., Clark, M., Bindon, C., Dyer, M., Dyer, M., ... Hardy, R. (2002). Human T cells resistant to complement lysis by bivalent antibody can be efficiently lysed by dimers of monovalent antibody. *Blood*, *100*(12), 4067–73. <http://doi.org/10.1182/blood-2002-03-0731>
- Nikolaus, M. J. (2016). *Entwicklung reversibler Fab-Multimere zur Gewinnung und funktionellen Charakterisierung muriner regulatorischer T-Zellen*. Technische Universität München.
- Olson, J. A., Leveson-Gower, D. B., Gill, S., Baker, J., Beilhack, A., & Negrin, R. S. (2010). NK cells mediate reduction of GVHD by inhibiting activated, alloreactive T cells while retaining GVT effects. *Blood*, *115*(21), 4293–4301. <http://doi.org/10.1182/blood-2009-05-222190>
- Pandiyan, P., Zheng, L., Ishihara, S., Reed, J., & Lenardo, M. J. (2007). CD4⁺CD25⁺Foxp3⁺ regulatory T cells induce cytokine deprivation-mediated apoptosis of effector CD4⁺ T cells. *Nature Immunology*, *8*(12), 1353–62. <http://doi.org/10.1038/ni1536>
- Pasquini, M. C., Wang, Z., Horowitz, M. M., & Gale, R. P. (2010). 2010 report from the Center for International Blood and Marrow Transplant Research (CIBMTR): current uses and outcomes of hematopoietic cell transplants for blood and bone marrow disorders. *Clinical Transplants*, 87–105. Retrieved from <http://www.ncbi.nlm.nih.gov/pubmed/21696033>
- Pierson, W., Cauwe, B., Policheni, A., Schlenner, S. M., Franckaert, D., Berges, J., ... Liston, A. (2013). Antiapoptotic Mcl-1 is critical for the survival and niche-filling capacity of Foxp3⁺ regulatory T cells. *Nature Immunology*, *14*(9), 959–65. <http://doi.org/10.1038/ni.2649>
- Plebani, A., Avanzini, M. A., Massa, M., & Ugazio, A. G. (1984). An avidin-biotin ELISA for the measurement of serum and secretory IgD. *Journal of Immunological Methods*, *71*(2), 133–40. Retrieved from <http://www.ncbi.nlm.nih.gov/pubmed/6376634>
- Polchert, D., Sobinsky, J., Douglas, G. W., Kidd, M., Moadsiri, A., Genrich, K., ... Smith, B. (2011). Prevention of Graft Versus Host Disease, *38*(6), 1745–1755.

<http://doi.org/10.1002/eji.200738129>.IFN-

- Porter, D., & Levine, J. E. (2006). Graft-Versus-Host Disease and Graft-Versus-Leukemia After Donor Leukocyte Infusion. *Seminars in Hematology*, 43(1), 53–61. <http://doi.org/10.1053/j.seminhematol.2005.09.005>
- Powrie, F., Leach, M. W., Mauze, S., Caddle, L. B., & Coffman, R. L. (1993). Phenotypically distinct subsets of CD4+ T cells induce or protect from chronic intestinal inflammation in C. B-17 scid mice. *International Immunology*, 5(11), 1461–71. Retrieved from <http://www.ncbi.nlm.nih.gov/pubmed/7903159>
- Qian, L., Wu, Z., & Shen, J. (2013). Advances in the treatment of acute graft-versus-host disease. *Journal of Cellular and Molecular Medicine*, 17(8), 966–975. <http://doi.org/10.1111/jcmm.12093>
- Qin, H. Y., Mukherjee, R., Lee-Chan, E., Ewen, C., Bleackley, R. C., & Singh, B. (2006). A novel mechanism of regulatory T cell-mediated down-regulation of autoimmunity. *International Immunology*, 18(7), 1001–1015. <http://doi.org/10.1093/intimm/dx1035>
- Rashid, a, Auchincloss, H., & Sharon, J. (1992). Comparison of GK1.5 and chimeric rat/mouse GK1.5 anti-CD4 antibodies for prolongation of skin allograft survival and suppression of alloantibody production in mice. *Journal of Immunology (Baltimore, Md. : 1950)*, 148(5), 1382–1388.
- Rubtsov, Y. P., Niec, R. E., Josefowicz, S., Li, L., Darce, J., Mathis, D., ... Rudensky, A. Y. (2010). Stability of the regulatory T cell lineage in vivo. *Science (New York, N.Y.)*, 329(5999), 1667–71. <http://doi.org/10.1126/science.1191996>
- Rusckowski, M., Fogarasi, M., Fritz, B., & Hnatowich, D. J. (1997). Effect of endogenous biotin on the applications of streptavidin and biotin in mice. *Nuclear Medicine and Biology*, 24(3), 263–8. Retrieved from <http://www.ncbi.nlm.nih.gov/pubmed/9228661>
- Sakaguchi, S. (2004). Naturally arising CD4+ regulatory t cells for immunologic self-tolerance and negative control of immune responses. *Annual Review of Immunology*, 22, 531–562. <http://doi.org/10.1146/annurev.immunol.21.120601.141122>
- Sakaguchi, S., Sakaguchi, N., Asano, M., Itoh, M., & Toda, M. (1995). Immunologic self-tolerance maintained by activated T cells expressing IL-2 receptor alpha-chains (CD25). Breakdown of a single mechanism of self-tolerance causes various autoimmune diseases. *Journal of Immunology (Baltimore, Md. : 1950)*, 155(3), 1151–64. <http://doi.org/10.4049/jimmunol.1201644>
- Sakaguchi, S., Vignali, D. a a, Rudensky, A. Y., Niec, R. E., & Waldmann, H. (2013). The plasticity and stability of regulatory T cells. *Nature Reviews. Immunology*, 13(6), 461–467. <http://doi.org/10.1038/nri3464>

- Schroeder, M. a, & DiPersio, J. F. (2011). Mouse models of graft-versus-host disease: advances and limitations. *Disease Models & Mechanisms*, 4(3), 318–33. <http://doi.org/10.1242/dmm.006668>
- Seidel, U. J. E., Schlegel, P., & Lang, P. (2013). Natural killer cell mediated antibody-dependent cellular cytotoxicity in tumor immunotherapy with therapeutic antibodies. *Frontiers in Immunology*, 4(MAR), 1–8. <http://doi.org/10.3389/fimmu.2013.00076>
- Setiady, Y. Y., Coccia, J. a, & Park, P. U. (2010). In vivo depletion of CD4+FOXP3+ Treg cells by the PC61 anti-CD25 monoclonal antibody is mediated by FcγRIII+ phagocytes. *European Journal of Immunology*, 40(3), 780–6. <http://doi.org/10.1002/eji.200939613>
- Sharma, M. D., Hou, D. Y., Liu, Y., Koni, P. A., Metz, R., Chandler, P., ... Munn, D. H. (2009). Indoleamine 2,3-dioxygenase controls conversion of Foxp3+ Tregs to TH17-like cells in tumor-draining lymph nodes. *Blood*, 113(24), 6102–6111. <http://doi.org/10.1182/blood-2008-12-195354>
- Shimabukuro-Vornhagen, a, Hallek, M., Storb, R., & Bergwelt-Baildon, M. (2009). The role of B cells in the pathogenesis of graft-versus-host disease. *Blood*, 114(24), 4919–4927. <http://doi.org/10.1182/blood-2008-10-161638>.
- Shin, H.-J., Baker, J., Leveson-Gower, D. B., Smith, A. T., Segal, E. I., & Negrin, R. S. (2011). Rapamycin and IL-2 reduce lethal acute graft-versus-host disease associated with increased expansion of donor type CD4+CD25+Foxp3+ regulatory T cells. *Blood*, 118(8), 2342–2350. <http://doi.org/10.1182/blood-2010-10-313684>
- Shlomchik, W. D. (2007). Graft-versus-host disease. *Nature Reviews. Immunology*, 7(5), 340–52. <http://doi.org/10.1038/nri2000>
- Shlomchik, W. D., Couzens, M. S., Tang, C. B., McNiff, J., Robert, M. E., Liu, J., ... Emerson, S. G. (1999). Prevention of Graft Versus Host Disease by Inactivation of Host. *Science*, 285(July), 412–415. <http://doi.org/10.1126/science.285.5426.412>
- Shohei Hori, Takashi Nomura, S. S. (2002). Control of Regulatory T Cell Development by the Transcription Factor Foxp3. *Science*, 299(2003), 1057–1061. <http://doi.org/10.1126/science.1079490>
- Singer, B. D., King, L. S., & D'Alessio, F. R. (2014). Regulatory T Cells as Immunotherapy. *Frontiers in Immunology*, 5(FEB), 1–10. <http://doi.org/10.3389/fimmu.2014.00046>
- Stemberger, C., Dreher, S., Tschulik, C., Piossek, C., Bet, J., Yamamoto, T. N., ... Busch, D. H. (2012). Novel serial positive enrichment technology enables clinical multiparameter cell sorting. *PLoS One*, 7(4), e35798. <http://doi.org/10.1371/journal.pone.0035798>
- Stemberger, C., Huster, K. M., Koffler, M., Anderl, F., Schiemann, M., Wagner, H., & Busch, D. H.

- (2007). A single naive CD8+ T cell precursor can develop into diverse effector and memory subsets. *Immunity*, 27(6), 985–97. <http://doi.org/10.1016/j.immuni.2007.10.012>
- Storb, R., Epstein, R. B., Graham, T. C., & Thomas, E. D. (1970). Methotrexate regimens for control of graft-versus-host disease in dogs with allogeneic marrow grafts. *Transplantation*, 9(3), 240–6. Retrieved from <http://www.ncbi.nlm.nih.gov/pubmed/4392379>
- Sudres, M., Norol, F., Trenado, a, Grégoire, S., Charlotte, F., Levacher, B., ... Cohen, J. L. (2006). Bone marrow mesenchymal stem cells suppress lymphocyte proliferation in vitro but fail to prevent graft-versus-host disease in mice. *Journal of Immunology (Baltimore, Md : 1950)*, 176(12), 7761–7767. <http://doi.org/10.4049/jimmunol.176.12.7761>
- Sun, J., Dotti, G., Huye, L. E., Foster, A. E., Savoldo, B., Gramatges, M. M., ... Rooney, C. M. (2010). T Cells Expressing Constitutively Active Akt Resist Multiple Tumor-associated Inhibitory Mechanisms. *Molecular Therapy*, 18(11), 2006–2017. <http://doi.org/10.1038/mt.2010.185>
- Tai, X., Erman, B., Alag, A., Mu, J., Kimura, M., Katz, G., ... Singer, A. (2013). Foxp3 Transcription Factor Is Proapoptotic and Lethal to Developing Regulatory T Cells unless Counterbalanced by Cytokine Survival Signals. *Immunity*, 38(6), 1116–1128. <http://doi.org/10.1016/j.immuni.2013.02.022>
- Takahashi, T., Kuniyasu, Y., Toda, M., Sakaguchi, N., Itoh, M., Iwata, M., ... Sakaguchi, S. (1998). Immunologic self-tolerance maintained by CD25+CD4+ naturally anergic and suppressive T cells: induction of autoimmune disease by breaking their anergic/suppressive state. *International Immunology*, 10(12), 1969–1980. <http://doi.org/10.1093/intimm/10.12.1969>
- Tang, Q., & Bluestone, J. A. (2008). The Foxp3+ regulatory T cell: a jack of all trades, master of regulation. *Nature Immunology*, 9(3), 239–44. <http://doi.org/10.1038/ni1572>
- Tang, Q., & Bluestone, J. A. (2013). Regulatory T-Cell Therapy in Transplantation: Moving to the Clinic. *Cold Spring Harbor Perspectives in Medicine*, 3(11), a015552–a015552. <http://doi.org/10.1101/cshperspect.a015552>
- Taylor, P. a., Lees, C. J., & Blazar, B. R. (2002). The infusion of ex vivo activated and expanded CD4+CD25+ immune regulatory cells inhibits graft-versus-host disease lethality. *Blood*, 99(10), 3493–3499. <http://doi.org/10.1182/blood.V99.10.3493>
- Teillaud, J.-L. (2012). Antibody-dependent Cellular Cytotoxicity (ADCC). *ELS*, 1–8. <http://doi.org/10.1002/9780470015902.a0000498.pub2>
- Thepot, S., Zhou, J., Perrot, A., Robin, M., Xhaard, A., de Latour, R. P., ... Socié, G. (2010). The graft-versus-leukemia effect is mainly restricted to NIH-defined chronic graft-versus-host disease after

- reduced intensity conditioning before allogeneic stem cell transplantation. *Leukemia*, 24(11), 1852–1858. <http://doi.org/10.1038/leu.2010.187>
- Thomas, E. D., Buckner, C. D., Banaji, M., Clift, R. A., Fefer, A., Flournoy, N., ... Weiden, P. L. (1977). One hundred patients with acute leukemia treated by chemotherapy, total body irradiation, and allogeneic marrow transplantation. *Blood*, 49(4), 511–33. Retrieved from <http://www.ncbi.nlm.nih.gov/pubmed/14751>
- Thomas, E. D., Buckner, C. D., Clift, R. A., Fefer, A., Johnson, F. L., Neiman, P. E., ... Weiden, P. L. (1979). Marrow transplantation for acute nonlymphoblastic leukemia in first remission. *The New England Journal of Medicine*, 301(11), 597–9. <http://doi.org/10.1056/NEJM197909133011109>
- Thomas, E. D., & Ferrebee, J. W. (1962). Transplantation of Marrow and Whole Organs: Experiences and Comments. *Canadian Medical Association Journal*, 86(10), 435–444.
- Thornton, A. M., & Shevach, E. M. (1998). CD4+CD25+ immunoregulatory T cells suppress polyclonal T cell activation in vitro by inhibiting interleukin 2 production. *The Journal of Experimental Medicine*, 188(2), 287–96. Retrieved from <http://www.ncbi.nlm.nih.gov/pubmed/9670041>
- Tomlinson, S. (1993). Complement defense mechanisms. *Current Opinion in Immunology*, 5(1), 83–9. Retrieved from <http://www.ncbi.nlm.nih.gov/pubmed/8452679>
- Toubai, T., Sun, Y., & Reddy, P. (2008). GVHD pathophysiology: is acute different from chronic? *Best Practice and Research: Clinical Haematology*, 21(2), 101–117. <http://doi.org/10.1016/j.beha.2008.02.005>
- Trzonkowski, P., Bieniaszewska, M., Juścińska, J., Dobyszuk, A., Krzystyniak, A., Marek, N., ... Hellmann, A. (2009). First-in-man clinical results of the treatment of patients with graft versus host disease with human ex vivo expanded CD4+CD25+CD127- T regulatory cells. *Clinical Immunology*, 133(1), 22–26. <http://doi.org/10.1016/j.clim.2009.06.001>
- Valenzuela, J. O., Iclozan, C., Hossain, M. S., Prlic, M., Hopewell, E., Bronk, C. C., ... Beg, A. A. (2009). PKC is required for alloreactivity and GVHD but not for immune responses toward leukemia and infection in mice. *Journal of Clinical Investigation*, 119(12), 3774–3786. <http://doi.org/10.1172/JCI39692>
- van Rood, J. J. (1968). The detection of transplantation antigens in leukocytes. *Seminars in Hematology*, 5(2), 187–214. Retrieved from <http://www.ncbi.nlm.nih.gov/pubmed/4871670>
- von Boehmer, H., & Daniel, C. (2012). Therapeutic opportunities for manipulating T(Reg) cells in autoimmunity and cancer. *Nature Reviews. Drug Discovery*, 12(1), 51–63. <http://doi.org/10.1038/nrd3683>

- Voss, S., & Skerra, a. (1997). Mutagenesis of a flexible loop in streptavidin leads to higher affinity for the Strep-tag II peptide and improved performance in recombinant protein purification. *Protein Engineering*, *10*(8), 975–982. <http://doi.org/10.1093/protein/10.8.975>
- Waller, E. K., Rosenthal, H., Jones, T. W., Peel, J., Lonial, S., Langston, A., ... Redei, I. (2011). Larger numbers of CD4 bright dendritic cells in donor bone marrow are associated with increased relapse after allogeneic bone marrow transplantation Larger numbers of CD4 bright dendritic cells in donor bone marrow are associated with increased relapse af. *Trials*, *97*(10), 2948–2956. <http://doi.org/10.1182/blood.V97.10.2948>
- Wang, W., Erbe, A. K., Hank, J. A., Morris, Z. S., & Sondel, P. M. (2015). NK cell-mediated antibody-dependent cellular cytotoxicity in cancer immunotherapy. *Frontiers in Immunology*, *6*(JUL). <http://doi.org/10.3389/fimmu.2015.00368>
- Weisdorf, D. (2007). GVHD the nuts and bolts. *Hematology / the Education Program of the American Society of Hematology. American Society of Hematology. Education Program*, 62–67. <http://doi.org/10.1182/asheducation-2007.1.62>
- Whelan, J. A., Dunbar, P. R., Price, D. A., Purbhoo, M. A., Lechner, F., Ogg, G. S., ... Sewell, A. K. (1999). Specificity of CTL interactions with peptide-MHC class I tetrameric complexes is temperature dependent. *Journal of Immunology (Baltimore, Md. : 1950)*, *163*(8), 4342–8. Retrieved from <http://www.ncbi.nlm.nih.gov/pubmed/10510374>
- Wing, K., & Sakaguchi, S. (2010). Regulatory T cells exert checks and balances on self tolerance and autoimmunity. *Nature Immunology*, *11*(1), 7–13. <http://doi.org/10.1038/ni.1818>
- Wood, K. J., Bushell, A., & Hester, J. (2012). Regulatory immune cells in transplantation. *Nature Reviews Immunology*, *12*(6), 417–430. <http://doi.org/10.1038/nri3227>
- Xu, X. N., Purbhoo, M. A., Chen, N., Mongkolsapaya, J., Cox, J. H., Meier, U. C., ... Screaton, G. R. (2001). A novel approach to antigen-specific deletion of CTL with minimal cellular activation using alpha3 domain mutants of MHC class I/peptide complex. *Immunity*, *14*(5), 591–602. Retrieved from <http://www.ncbi.nlm.nih.gov/pubmed/11371361>
- Yu, P., Constien, R., Dear, N., Katan, M., Hanke, P., Bunney, T. D., ... Mudde, G. C. (2005). Autoimmunity and Inflammation Due to a Gain-of-Function Mutation in Phospholipase C γ 2 that Specifically Increases External Ca $^{2+}$ Entry. *Immunity*, *22*(4), 451–465. <http://doi.org/10.1016/j.immuni.2005.01.018>
- Zaiss, D. M. W., van Loosdregt, J., Gorlani, A., Bekker, C. P. J., Gröne, A., Sibilía, M., ... Sijts, A. J. a M. (2013). Amphiregulin Enhances Regulatory T Cell-Suppressive Function via the Epidermal Growth Factor Receptor. *Immunity*, *38*(2), 275–284. <http://doi.org/10.1016/j.immuni.2012.09.023>

- Zanin-Zhorov, A., Ding, Y., Kumari, S., Attur, M., Hippen, K. L., Brown, M., ... Dustin, M. L. (2010). Protein kinase C-theta mediates negative feedback on regulatory T cell function. *Science (New York, N.Y.)*, 328(5976), 372–6. <http://doi.org/10.1126/science.1186068>
- Zheng, H., Matte-Martone, C., Jain, D., McNiff, J., & Shlomchik, W. D. (2009). Central memory CD8+ T cells induce graft-versus-host disease and mediate graft-versus-leukemia. *Journal of Immunology (Baltimore, Md. : 1950)*, 182(10), 5938–5948. <http://doi.org/10.4049/jimmunol.0802212>
- Zheng, H., Matte-martone, C., Li, H., Anderson, B. E., Venketesan, S., Tan, H. S., ... Shlomchik, W. D. (2008). Effector memory CD4+ T cells mediate graft-versus-leukemia without inducing graft-versus-host disease. *Blood*, 111(4), 2476–2484. <http://doi.org/10.1182/blood-2007-08-109678>.The